EXPLORING THE UTILIZATION OF *CRITHIDIA FASCICULATA* AS A MODEL ORGANISM TO STUDY PATHOGENIC KINETOPLASMIDS

Wakisa Kipandula

A Thesis Submitted for the Degree of MPhil
at the
University of St Andrews

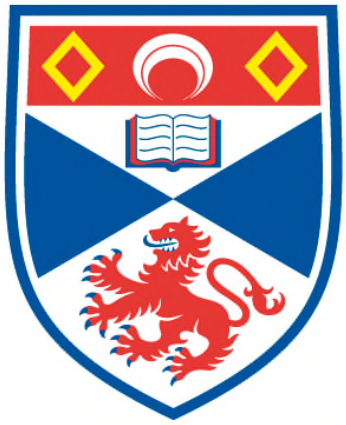

2017

Exploring the utilization of *Crithidia fasciculata* as a model organism to study pathogenic kinetoplastids

Wakisa Kipandula

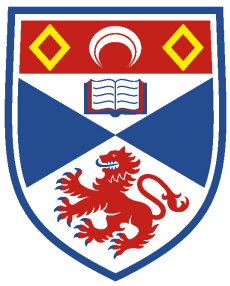

University of
St Andrews

This thesis is submitted in partial fulfilment for the degree of MPhil at the University of St Andrews

Date of Submission

May 2017

Abstract

This study aimed to explore the utilization of *C. fasciculata* as a convenient model organism to study the cell biology and drug discovery vehicle of the pathogenic kinetoplastids. We specifically aimed to: (i) develop and validate aprotein A-TEV-protein C (PTP) tagged protein expression system for *C. fasciculata*, (ii) develop a Resazurin-reduction viability assay with *C. fasciculata* and use this for subsequent screening for anti-crithidial compounds from the GSK open access pathogen boxes, and (iii) to study the effects of ionizing gamma radiation on *C. fasciculata*.

We report the construction of plasmid pNUS-PTPcH, which can be utilised to express PTP tagged kinetoplastids proteins in *C. fasciculata* for subsequent purification. As a proof of concept, we have shown that *C. fasciculata* can be efficiently transfected with this plasmid and facilitate the isolation of two protein complexes: replication factor C (RFC) and the exosome. We have demonstrated that the expressed PTP tagged-replication factor C subunit 3 (PTP-RFC3) co-purifies with RFC1, RFC2, RFC4, RFC5 and RAD17, and that the PTP tagged exosome subunit RRP4 co-purifies with RRP6, EAP1, RRP45, RRP40, RRP41B, CSL4, EAP2, RRP41A and EAP4. In addition, this thesis reports the development of a resazurin-reduction cell viability assay in *C. fasciculata* and reveals attractive core chemical scaffolds present in more than one of the open access GSK pathogen boxes, which will be followed up against the actual pathogenic kinetoplastids. Furthermore, this study has demonstrated that compared to cultured forms of *T. cruzi* which undergo growth arrest for 96 hours after exposure to 500 Gy of gamma radiation, *C. fasciculata* is able to recover and resume normal growth within 24 hours after being subjected to doses as high as 1000Gy.

The constructed plasmid, the identified chemical scaffolds and the observed responses of *C. fasciculata* to gamma irradiation will help facilitate further studies aimed to discover novel drugs for kinetoplastid diseases.

Declaration

I, Wakisa Kipandula, hereby certify that this thesis, which is approximately 30,000 words in length, has been written by me, and that it is the record of work carried out by me, with the exception of a single plasmid consruction carried out by Dr Stuart MacNeill, and that it has not been submitted in any previous application for a higher degree.

I was admitted as an MPhil student in November 2014. The work was carried out in University of St Andrews and the University Of Malawi College Of Medicine between 2014 and 2016.

Date: 10th November 2017 Signature of candidate:

We hereby certify that the candidate has fulfilled the conditions of the Resolution and Regulations appropriate for the degree of MPhil in the University of St Andrews and that the candidate is qualified to submit this thesis in application for that degree.

Date Signatures of supervisors:

In submitting this thesis to the University of St Andrews, I understand that I am giving permission for it to be made available for use in accordance with the regulations of the University Library for the time being in force, subject to any copyright vested in the work not being affected thereby. I also understand that the title and the abstract will be published, and that a copy of the work may be made and supplied to any bona fide library or research worker, that my thesis will be electronically accessible for personal or research use unless exempt by award of an embargo as requested below, and that the library has the right to migrate my thesis into new electronic forms as required to ensure continued access to the thesis. I have obtained any third-party copyright permissions that may be required in order to allow such access and migration, or have requested the appropriate embargo below.

The following is an agreed request by candidate and supervisor regarding the electronic publication of this thesis:

(i) Access to printed copy and electronic publication of thesis through the University of St Andrews.

Date: 10th November 2017 Signature of candidate:

Date Signatures of supervisors:

Acknowledgements

I thank my supervisors Dr Stuart MacNeill and Professor Terry Smith for their valuable guidance, support, advice and motivation while working on this highly interesting project. I acknowledge the assistance offered to me by staff and fellow students in the Biomedical Sciences Research Complex, level 3.

Special thanks to Wilberforce Sabiiti, Beatrice Mwagomba, Kondwani Katundu, Daniel Khomba and everybody who made my stay in very cold and boring St Andrews worthwhile. You are such a wonderful people.

I am indebted to E. Tetaud for providing *C. fasciculata* pNus plasmids. This work would not have been possible without generous funding through the Global Health Implementation Programme at the University of St Andrews by the Gloag Foundation and the Western Union Foundation.

It is with immense gratitude that I acknowledge the management of the University Of Malawi College Of Medicine for granting me a study leave. I am grateful to my wife Wezzie for her encouragement and perseverance while I was away. You are such a strong woman.

Last but not least, the one above all of us, the omnipresent God for answering my prayers and for giving me the strength to plod on despite my constitution wanting to give up this work. Thank you so much Dear Lord.

This work is dedicated to my son Andile.

Publications

Some of the results from this thesis have been published in a well-recognised scientific journal as follows.

i. Kipandula W, Smith TK, MacNeill SA. Tandem affinity purification of exosome and replication factor C complexes from the non-human infectious kinetoplastid parasite *Crithidia fasciculata*. Molecular and Biochemical Parasitology 217: 19-22 (2017). Available from, DOI: **10.1016/j.molbiopara.2017.08.004**

Table of contents

List of Abbreviations

°C	Degrees Celsius
3’	3 prime DNA end
5’	5 prime DNA end
AAA+	ATPase associated with a variety of cellular activities
ATP	Adenosine triphosphate
bp	Base pairs
CBP	Calmodulin binding protein
CL	Cutaneous leishmaniasis
CNS	Central nervous system
Csl4	Cep1 Synthetic Lethal
Ctf8	Chromosome transmission fidelity protein 8
Cyp51	Cytochrome 51
Da	Dalton
DCC1	DNA replication and sister chromatid cohesion 1
DMSO	Dimethyl sulfoxide
DNA	Deoxyribonucleic acid
EC_{50}	Effective concentration inhibiting 50% cell proliferation
EDTA	Ethylenediamine tetra-acetic acid
EGTA	Ethylene glycol-bis (2-aminoethylether)-N,N,N',N'-tetraacetic acid
Elg1	Enhanced level of genomic instability 1
FDA	Food and drug administration
g	Gram
GE	Gut epithelium
GSK	Glaxo Smith Kline
GSPS	Glutathionylspermidine synthetase
Gys	Grays
HAT	Human African trypanosomiasis
Hr	Hour
HTS	High throughput screening
ID	Identity
IFN	Interfelon
IgG	Immunoglobulin G
IG-PGKAB	Intergenic-phosphoglycerate kinase genes A and B
IL-2	Interleukin-2
IR	Ionising radiation
KAP1	Kruppel-Associated protein 1
kb	Kilobase
kDa	Kilodalton
kDNA	Kinetoplast DNA
l	Litre

LB	Luria Bertani medium
M	Molar
MALDI	Matrix-Assisted Laser Desorption/Ionisation
mg	Milligram
ml	Millilitre
ML	Mucosal leishmaniasis
mM	Millimolar
MMV	Medicines for Malaria Venture
MRC-5	Medical Research Council cell strain 5
mtDNA	Mitochondrial DNA
Mw	Molecular weight
NAD	Nicotinamide adenine
NADPH	Nicotinamide adenine dinucleotide phosphate
NCBI	National Center for Biotechnogy Information
nDNA	Nuclear DNA
NECT	Nifurtimox-eflornithine combination therapy
nm	Nanometre
NTD	Neglected tropical disease
ORF	Open reading frame
PAP	Peroxidase Anti-peroxodase
PBS	Phosphate buffered saline
PBS-T	PBS-Tween
PCNA	Proliferating cell nuclear antigen
PCR	Polymerase chain reaction
PDPs	product development partnerships
pIC_{50}	- log of 50% inhibitory concentration
Pol	Polymerase
PPP	Public-private partnerships
PTP	Protein A-TEV-Protein C
RFC	Replication factor C
RLC	RFC-like complexes
RNS	Reactive nitrogen species
ROS	Reactive oxygen species
rpm	Revolutions per minute
rRNA	ribosomal RNA
RRP4	Ribosomal RNA processing 4
SAR	Structure activity relationship
SB	Sample buffer for protein gel electrophoresis
SDS	Sodium dodecyl sulfate
SE	Standard error
Sno RNA	Small nucleolar RNA
TAP	Tandem affinity purification
TE	Tris EDTA
TEV	Tobacco etch virus

Tris	2-Amino-2-hydroxymethyl-propane-1, 3-diol Tris (hydroxymethyl) aminomethane
tRNA	Transfer RNA
TSB	Transformation storage buffer
UTR	Untranslated regions
UV	Ultraviolet
V	Volt
VL	Visceral leishmaniasis
VSG	Variant surface glycoprotein
wt	Wild-type
µg	Microgram
µl	Microlitre
µm	Micrometre

1. Chapter 1: Background introduction

1.1 Introduction

Kinetoplastids comprise of a group of flagellated protozoans that cause fatal diseases in humans and other mammals. They are characterised by the presence of a DNA-containing region, known as a "kinetoplast," in their single large mitochondrion (Stuart et al., 2008). Common human diseases that are caused by these kinetoplastids include; human African trypanosomiasis (HAT), also known as African sleeping sickness, which is caused by two of the three subspecies of *Trypanosoma brucei* (*rhodesience and gambiense*), human American trypanosomiasis also known as Chagas disease, which is caused by *Trypanosoma cruzi*; and various forms of leishmaniasis which are caused by different species of *Leishmania* (Burri and Brun, 2003). *T. brucei*, *T. cruzi* and *Leishmania* species are together further grouped into the Trypanosomatidae, commonly referred to as the '*TriTryps'*. It is estimated that about a half a billion-people living in tropical and subtropical areas of the world are at risk of contracting the diseases caused by the *TriTryps,* with more than 20 million individuals infected with the pathogens that cause them resulting in extensive suffering and more than 100,000 deaths per year (Stuart et al., 2008).

The cellular biology of the various kinetoplastids is very similar. For example, they are all motile protozoans with a single flagellum that originates near their large single mitochondrion and emanates from their flagellar pocket in the cell membrane, the only place where endo- and exocytosis also takes place. Their peroxisomes are modified to perform glycolysis, and thus referred to as glycosomes. Their plasma membrane is underlain with a corset of microtubules and their cell surface is highly decorated with species-specific molecules that are critical for their survival. They typically grow asexually although sexual recombination has been observed in *T. brucei*, *T. cruzi*, and in some *Leishmania* species. Nevertheless, they divide by binary fission, during which their nucleus does not undergo membrane dissolution or chromosome condensation (Stuart et al., 2008). Kinetoplastids have a unique genome organisation, which consists of unidirectional large gene clusters, which are transcribed polycistronically (Teixeira et al., 2011). They possess distinct genetic processes including RNA polymerase I-mediated transcription and trans-splicing of the immature RNA, which is followed by the addition of a 5' mini-exon and 5'-polyadenylation to form mature RNA transcripts (Hajduk and Ochsenreiter, 2010). Although the kinetoplastids share such many similarities, they cause very distinctive forms of disease as shown in **Table 1**.

	Sleeping sickness	Chagas disease	Leishmaniasis
Stages	Early (hemolymphatic) stage, late (CNS) stage	Acute phase, indeterminant phase, chronic phase (cardiac and digestive forms)	VL, CL
Causative agent	*T.b. gambiense*, *T.b. rhodesiense*	*T. cruzi*	~21 *Leishmania* spp. e.g., *L. donovani* (VL), *L. braziliensis*, *L. major* (CL)
Host cell	Extracellular, in blood, lymph, cerebral spinal fluid, and intercellular spaces	Intracellular, in cytoplasm of heart, smooth muscle, gut, CNS, and adipose tissue cells	Intracellular, in phagolysosomes of macrophages
Vectors	Tsetse flies (~20 *Glossina* spp.) (*palpalis* group, *T.b. gambiense*; *morsitans* group, *T.b. rhodesiense*)	Reduviid bugs (~12/~138 *Triatominae* spp.) (*Triatoma*, *Rhodnius*, and *Panstrongylus* spp.)	Phebotomine sandflies (~70 *Phlebotomus* spp. in Old World, *Lutzomyia* spp. in New World)
Mode of transmission	Infected fly bite, congenital (rare), blood transfusion (rare)	Contamination by feces of infected bugs (e.g., at bite site, in mucous membranes, in food or drink),blood transfusion, congenital, organ transplantation (rare)	Infected fly bite
Geographic distribution	Sub-Saharan Africa (~20 countries)	South and Central America (19 countries)	South and Central America, Europe, Africa, Asia (88 endemic countries)
Population at risk	50 million	100 million	350 million
Infected	70,000–80,000	8–11 million	12 million
Deaths/year	~30,000	14,000	51,000 (VL)

Table 1. Details of some kinetoplastid diseases. The data was copied from Maudlin et al. (2004) and Lane et al. (1993). Non-standard abbreviations: CL (Cutaneous leishmaniasis), ML (Mucosal leishmaniasis) and VL (Visceral leishmaniasis).

The general life cycles of kinetoplastids vary according to the invertebrate vector that is involved in the transmission. As described by Bartholomeu et al. (2014), *Leishmania* species multiply as promastigotes in the sand fly's mid-gut. These parasites get injected into the human host as the fly is taking a blood meal and consequently get engulfed by macrophages. Inside the microphages, the parasites develop and proliferate as amastigotes and infect other surrounding cells after cell lysis **(Fig 1a)**.

Trypanosoma cruzi parasites proliferate as epimastigotes in the revuviid bug's mid-gut and spread to colonise the bug's intestines. In the intestines, the parasite develops into infective metacyclic promastigotes forms get excreted alongside the bug's faeces **(Fig. 1b)**. *T. cruzi* parasites target any host cell with a nuclear through recruitment of lysosomal or simply invagination the cell's plasma membrane (Bartholomeu et al., 2014). They then proliferate into amastigotes and trypomastigotes in the cytosol and realised by lysis of infected cells, which are taken up by the surrounding cells (Ueno and Wilson, 2012).

Unlike *T. cruzi* and most *Leishmania species*, *T. brucei* parasites proliferate outside the host cells for their entire life cycle (Bartholomeu et al., 2014) **(Fig. 1c)**. The parasites proliferate in tsetse fly intestines as procyclic forms, which develop into infective metacyclic forms in the salivary glands. The metacyclic parasites are injected into the host through saliva when the fly is taking a blood meal and multiply in the host blood as procyclic trypomastigotes. However, since the *T.brucei* parasites cannot invade and hide inside the host cells like *T. cruzi* and *L.major,* the parasite had to adapt to a mechanism, which avoids being attacked by the host immune response. This is achieved by the parasite's cell-surface "Variant surface glycoprotein" (VSG) which undergoes antigenic variation and avoid the parasite's recognition by the host immune system (Horn and McCulloch, 2010). Through this mechanism, the parasites are always one-step ahead of the host immune responses.

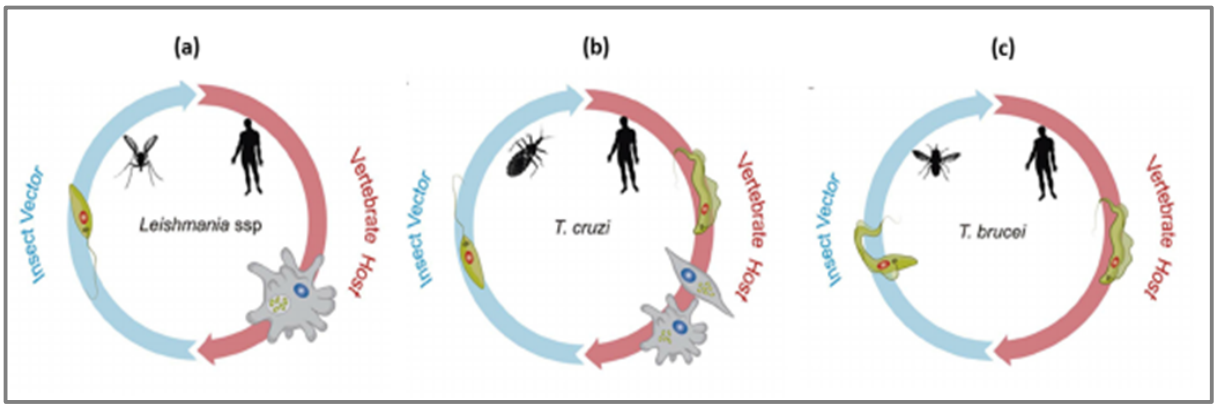

Figure 1. Life cycles of the kinetoplastids**. (a)** L. major multiplies as promastigotes in the mid-gut of a sand fly and are transmitted to the host as metacyclic promastigotes during a blood meal. In the host, the parasites are phagocytosed by macrophages and the metacyclic forms are converted into amastigotes, which multiply numerous times before being released during cell lysis**.** (**b)** T. cruzi epimastigotes in the mid-gut of a bug transform into infective metacyclic trypomastigotes in the bug's rectum and get excreted alongside the bud's faeces to invade the host's nucleated cells. **(c)** T. brucei multiplies as procyclic forms in the intestinal tract of tsetse fly and transformed into infective metacyclic forms in the fly's salivary glands. When taking the blood, the fly injects the parasites into the host blood, which then proliferate as procyclic trypomastigotes (Copied from Bartholomeu et al., 2014).

1.2 Current treatment for disease caused by kinetoplastids

The current HAT treatment is based on five drugs which were developed decades ago, all of which have been reported to possess adverse side effects, challenges in efficacy, administration, and compliance. As recently reviewed by in Field and colleagues (Field et al., 2017), the first stage of HAT caused by *T.b. rhodesiense* and *T.b. gambiense* is treated by suramin and pentamidine, respectively. However, both of these drugs are administered intraparenterally and are associated with toxicities. Melarsoprol is effective against second-stage HAT caused by both *T.b. rhodesiense* and *T.b. gambiense* while eflornithine is only active for second-stage HAT caused by *T.b. gambiense*. The arsenical melarsoprol is administered intravenously for 10 days and is highly toxic causing substantial levels of drug-related mortality due to reactive encephalopathy (Kennedy, 2013). The number of treatment failures after arsenical melarsoprol administration continue to increase due to drug resistance or other unknown factors. The pharmacokinetic studies on melarsoprol led to the treatment regimen being changed to a 10-day course rather than the previous 21- to 35-day course, thus improving patient compliance and reducing hospital costs (Kennedy et al., 2013). Being polyamine biosynthesis inhibitor, eflornithine has been commonly administered for HAT cases caused by infection with *T.b. gambiense,* which are resistant to treatment with melarsoprol (Malvy and Chappuis, 2011). The drug is suitable for second stage of disease

and is not effective against *T.b.rhodesience*. It is usually administered over 14 days as four daily intravenous infusions and has less severe adverse reactions compared to melarsoprol. However, administering 56 intravenous infusions present a logistical drawback especially in resource-limited settings. Nifurtimox-eflornithine combination therapy (NECT) have been shown to be effective in cases of second-stage HAT that are either refractory to treatment with melarsoprol alone or in situations where ornithine is unavailable. NECT has reduced treatment period and less costly than eflornithine monotherapy (Simarro et al, 2012). Moreover, the lack of paediatric formulations for some of the mentioned drugs together with contraindications for pregnant women and those of childbearing age further limit the use of these drugs. Vaccine development for HAT faces the challenge of parasite's antigenic variation whereby the parasites make several antigenic variants by alternate expression and recombination of a repertoire of VSG-encoding genes, allowing them to escape the host immune response (LaGreca and Magez, 2011).

Only two drugs, nifurtimox and benznidazole are currently available for treating Chagas disease. These drugs are orally administered but faces side effects, a long treatment period (>60 days) and variation in sensitives to the parasites (de Castro et al., 2006; Moraes et al., 2014). Both of these drugs are reasonably effective against the acute form of the disease but have poor tolerability and patient compliance (Field et al., 2017). It has been reported elsewhere that once the heart failure develops in chronic Chagas disease, the treatment with benznidazole becomes irrelevant (Wang et al., 2012). Other studies have reported the efficacy of benznidazole as a treatment for adults with Chagas disease who havebeen infected with the parasite for a long time (Viotti et al., 2006 and de Castro et al., 2006). However, the absence of well-structured randomized placebo-controlled studies to assess the specific treatment outcomes in different groups has adversely restricted the use of these drugs. There have been some successes however, with antifungal triazoles and protease inhibitors in experimental models of infection with *T. cruzi* (Doyle et al., 2007).

For visceral leishmaniasis (VL), a liposomal formulation of amphotericin B, AmBisome, was shown to be the most effective and well-tolerated treatment, with a single dose of 5 mg/kg curing 90% of patients (Singh et al., 2012). However, the use of AmBisome as treatment was limited due to the toxicity, requirement for intravenous administration and high costs associated with the drug (Bern et al., 2006; Field et al., 2017). Miltefosine is currently the only oral treatment for VL (Field et al., 2017). However, its clinical use has been limited due to teratogenic effects and increasing reports of treatment failures.

The pentavalent antimonials, sodium stibogluconate and meglumine antimoniate have also been used to treat both VL and CL. Introducing the generic brands of these drugs helped reduce their purchasing costs. However, these drugs are administered parenteral for up to 30 days, they are cytotoxic, and are now becoming obsolete for treatment due to the emergence of drug-resistant parasites (Singh et al., 2012). The emergences of antimonial-resistant parasites lead to the introduction of the antibiotic amphotericin B, which was previously a second-line drug as a first-line drug for treating leishmaniasis in India. The pentavalent antimonials are considered first-line treatment in combination with paromomycin in Africa (Field et al., 2017).

An aminoglycoside Paromomycin has also been reported as a very effective drug in treating leishmaniasis in India (Sundar et al., 2007). Despite havingefficacy essentially equivalent to that of amphotericin B, Paromomycin is associated with ototoxicity and is intramuscularly administered with pain at site of injection (Field et al., 2017).

1.3 Challenges to research on pathogenic kinetoplastids

Although diseases caused by the kinetoplastids continue to disable and kill hundreds of thousands of people in underdeveloped tropical regions, efforts towards identifying effective treatment options continue to receive less attention. The pharmaceutical industry and Western governments have shown little or no interest in supporting research aimed at developing new drugs for kinetoplastid diseases. Perharps this might be because studies on these neglected tropical diseases are associated with little or no prospect of generating significant short- or long-term financial gain. Another possible reason to the slow pace of research on kinetoplastids might be that many fundamental aspects of trypanosome biology have not been studied in depth. Research on pathogenic kinetoplastidshas been mostly hindered by the need to handle these organisms safely in a laboratory, requiring dedicated containment facilities. However, these facilities are very expensive to build, maintain and equip, as experimental apparatus cannot be moved in and out of the containment without rigorous decontamination. In addition, the expensive serum-containing media and difficulties in cultivating these parasites in high yields for different protocols, renders research on kinetoplastids almost impractical and unattractive especially to researchers dwelling in resource limited countries where the kinetoplastid diseases are endemic.

1.4 *C. fasciculata* as a model organism to study kinetoplastid biology

Protists of the genus *Crithidia* (Kinetoplastida: Trypanosomatidae) are flagellate parasites that only infect insects. The genus *Crithidia* contains a number of species with a wide host specificity that are able to parasitize a variety of species grouped into the orders Diptera, Hemiptera and Himenoptera. The host specificity of these organisms depends on the species of the parasite. In particularly, C. *fasciculata* successfully infects many species of mosquitoes (Wallace, 1966).

Crithidia parasites exist in many life cycle forms but only two forms are clearly distinguished; the Choanomastigotes and the Amastigotes. Choanoamastigotes are free-swimming stumpy cells that are round in their posterior part and truncated in the apical pole by the funnel-shaped flagellar pocket close to the kinetoplast, which is slightly anterior to the nucleus. Amastigotes are non-motile round cells with a flagellum non-emerging from the cellular body. Although they are extracellular, *Crithidia* are morphologically similar to amastigotes of the genus *Leishmania* (Olsen, 1974). The development of *C. fasciculata* starts in the gut of the culicid, which becomes infected by ingestion of amastigotes voided with faeces of other hosts. In the gut, amastigotes differentiate into choanomastigotes, ensuring proper colonization of the gut. Choanomastigotes later differentiate back into non-motile round amastigotes, which are attached to the gut epithelium by hemidesmosomes frequently leading to damage (Schaub, 1994). Infected adult mosquitoes contaminate aquatic environments with amastigotes as well as flowers when they feed on nectar, thus providing chances for transmission of the parasite. Amastigotes are released within the faeces or the entire body of the dead insect. Eventually, the larval and pupal instars of mosquitoes get infected in the aquatic habitat and finally amastigotes are transmitted to the adult mosquito through the metamorphosing gut leading to completion of the life cycle as shown in **Fig 2.**

Since *C. fasciculata* has such a monogenetic life cycle involving the extracellular choanomastigote and amastigote stages, they do not infect mammals. This comparison with other species of the same family developing digenetic life cycles responsible for leishmaniasis and trypanosomiasis is of outstanding interest in kinetoplastid research.

Unlike trypanosomes and leishmanial species, *C. fasciculata* is easy to culture in large amounts (>100g wet weight) using inexpensive complex media or fully defined serum-free media (Tetaud et al., 2002). These organisms have been used as feeder cells in the monoxenic culture of Entamoeba histolytica and Malaria parasites (Diamond, 1903).

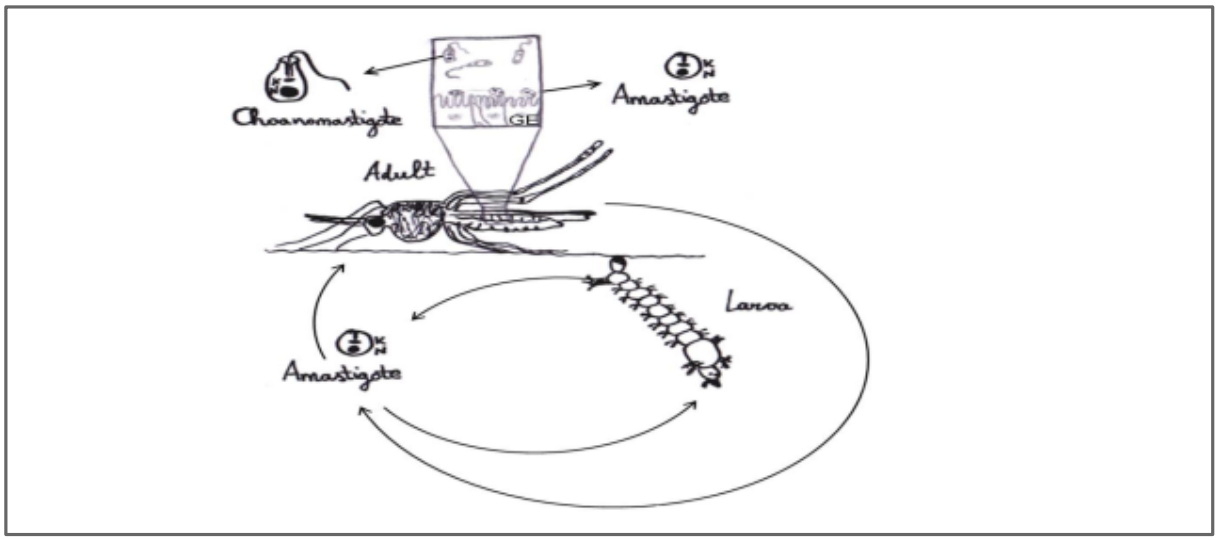

Figure 2. The life cycle of *C. fasciculata.* Amastigotes attached to the culicid gut epithelium are voided in faeces and disseminated in the environment. Eventually, the larval and pupal instars of mosquitoes get infected in the aquatic habitat and finally amastigotes are transmitted to the adult mosquito through the metamorphosing gut. Choanomastigotes are the motile stage that allows the colonization of the gut of the host. GE: gut epithelium. (Copied from Olsen, 1974)

In addition, *C. fasciculata* parasites are easily amendable to molecular genetics and biochemical analysis and their evolutionary proximity to the pathogenic kinetoplastids makes them a very interesting model organism to study biochemical, cellular, and genetic processes unique to kinetoplastids.

The complete genome sequence of *C. fasciculate* has been determined and is publically available at (http://www.ncbi.nlm.nih.gov/nuccore/440789264) to facilitate genome studies of these organisms. Some examples of genetic, biochemical and cellular processes in which *C. fasciculata* has been utilised as a model organisms to study trypanosomes and leishmania species are summarised in a **Table 2**.

Genetic/Biochemical/cellular process studied	Ref.
Effect of tunicamycin on the glucose uptake, growth, and cellular adhesion	Rojas et al., 2014
Inactivation oftopoisomerase I by Fenton systems	Podesta et al., 2003
Identification and characterization of a kinetoplast-specific DNA ligase	Sinha et al., 2004
The replication of kinetoplast DNA	Liu et al., 2005
Trypanothione synthesis	Comini et al., 2005
Trypanosomatid flagellum biogenesis	Sahin et al., 2004
Pharmacodynamic screening-medicinal plants	Tasanor et al., 2006
Application of magnetically induced hyperthermia as a potential therapy against parasitic infections	Grazu et al., 2012
kinetoplast DNA organization- The KAP1 protein	Lukes et al., 2001
Lipoarabinogalactan structures	Schneider et al.,1996
Mitochondrial DNA repair- Mitochondrial DNA Polymerase β	Saxowsky et al., 2002
Genetic manipulation	Hughes and Simpson, 1986
Expression vector	Tetaud et al., 2001

Table 2. Use of C. *fasciculata* to study various biological processes. Studies highlighting genetic, biochemical and cellular processes in which *C. fasciculata* has been utilised as a model organism to study trypanosomatids cellular and molecular biology.

1.5 Aims of the study

The main aim of this study was to explore the utilization of *C. fasciculata* as a convenient model organism to study the cell biology and drug discovery vehicle of the pathogenic kinetoplastids.

We specifically aimed to;

i. Develop and validate an expression vector that can be used to express and isolate PTP tagged kinetoplastid proteins in *C. fasciculate* parasites.
ii. Develop a Resazurin-reduction cell viability assay with *C. fasciculata* and utilise the developed assay to screen for anti-Crithidial compounds from the Open access chemical boxes.
iii. Investigate the effects of gamma irradiation on the *C. fasciculata* parasite's cell growth, metabolic viability, motility and morphology.

2. Chapter 2: Developing and validating an expression vector for subsequent isolation of PTP tagged kinetoplastids proteins in *C. fasciculata.*

2.1 Introduction

2.1.1 Kinetoplastids proteins expression systems

In search for new effective drugs against kinetoplastid diseases, potential drug targets need to be identified, characterised and validated. Recent advancements in transformation, protein expression, isolation and purification procedures have been a major technical breakthrough in identification and characterization of novel proteins as drug targets.

Highly efficient expression of proteins remain an important alternative to the isolation of protein from native sources and is especially useful when the native protein is normally produced in limited amounts or by sources that are impossible, expensive and/or dangerous to obtain or propagate. In the last few years, gene-transfer systems have been developed specifically for pathogenic and medically important kinetoplastids; *Leishmania* spp, *T.brucei* and *T. cruzi.* The parasites transformation is usually facilitated by integration, which occurs exclusively by homologous recombination, or by episomal shuttle vectors. Moreover, various kinetoplatids proteins expression systems are currently available to facilitate relevant studies. These included; the pTEX vector for rapid expression of proteins in both *T. cruzi* and *Leishmania* (Coburn et al., 1991 and Martinez-Calvillo et al., 1997, respectively). Attempts to transform *C. fasciculata* and *T.brucei* with pTEX vector however, have been unsuccessful (Coburn et al., 1991). The pX vector, which has been used for stable transformation of *Leishmania major* and have been successfully applied in studying the parasite's surface antigen genes (LeBowitz et al., 1990). Of recent is the Lexsy, which has been widely used in expressing proteins in non-human pathogenic *Leishmania tarentolae* parasites of gecko. The Lexsy system allows not only easy handling like *E. coli* and yeast, but also full eukaryotic protein folding and the mammalian-type posttranslational modifications of target proteins. The pTSO-HYG4 vectors in *T. brucei*, which utilize the PARP promoter and is able to replicate extrachromosomally with the aid of minicircle origin of replication have been reported (Sommer et al., 1996). Other *T.brucei* expression systems include the TetR and the bacteriophage T7RNAP, which can allow transgenes to be highly transcribed and expressed in *T.brucei* (Wirtz et al., 1999). Mammalian and protozoan signal peptides have also observed to function in *T. cruzi* to target proteins to different cellular compartments (Garg et

al., 1997). In addition, bioactive cytokines (IL-2 and IFN-gamma) have been produced in both *T. cruzi* and *Leishmania* (Tobin et al., 1993), suggesting that mammalian signal peptides are recognized and processed by these protozoans. Vectors bearing an rRNA promoter have been constructed by Biebinger and colleague (Biebinger and Clayton, 1996), for expressing foreign genes in *C.fasciculata*.

More recently, the pNUS vectors have been constructed to express biologically active proteins in *Crithidia* and *L. amazonensis* (Tetaud et al., 2002). Although a number of expression systems have proven useful for production of various heterologous proteins, none of these systems is universally applicable for the production of all proteins. A protein expression system that provides for the efficient expression and isolation of correctly post-translationally modified heterologous proteins in a non-pathogenic host would therefore constitute a highly desired advance in the art.

2.1.2 Multi protein complexes

Most biological processes in a cell are carried out by proteins and by their ability to form multi-protein complexes at an appropriate time. Individual proteins may participate in the formation of a variety of different protein complexes (Gavin et al., 2006). Proteins that are in the same complex can differ in specific function, but they function in the same overall process and hence have a related general function (Panigrahi et al., 2008). Indeed, this protein interaction can regulate proteins activities through either post-translational modification or conformational-transformation.

Studies of individual proteins in a multi-protein complex assembly can provide clear information of their specific functions in the complex (Cusick et al., 2005). The interactions of proteins in a complex to control various significant biological processes for cell viability should therefore not be overlooked as a focus of potential drug targets.

2.1.2.1 The replication factor C protein complex

Eukaryotic replication factor C (RFC) complex previously known as a clamp loader is a heteropentamer consisting of five essential subunits referred to as RFC1 through RFC5(Bowman et al.,2004). With the exception of the large RFC1 subunit (approximately 128 kDa in humans), the RFC 2, 3, 4 and 5 subunits are approximately 38–41 kDa each (Yao and O'Donnell, 2012). The five subunits contain a region of homology with one another (Erzberger and Berger, 2006). This region of homology defines a large family of proteins

referred to as AAA+ proteins. The AAA+ homologous region folds into two domains that bind ATP: the larger N-terminal domain contains the P-loop and DEAD box ATP site motifs, while the smaller C-terminal domain is outside the AAA+ homology region and is mostly composed of α-helix. The C terminal domain mediates a strong inter-subunit interaction that holds the pentamer tight (Bowman et al., 2004). The five RFC components are organised in a circular form (**Fig.3a**). The C-terminal domains define a nearly planar circle referred to as a "collar domain" as shown in **Fig 3a**. One component of RFC is shown (**Fig. 3c)**, to illustrate the three domains structure of clamp loader subunits. By convention, clamp loaders are viewed from the "side" as C-terminal domain on the top, and the N terminal AAA+ domains on the bottom. Proceeding counterclockwise around the circle from the subunit at the far right, the subunit positions are read as A- E subunits or simply RFC1-RFC5 **(Fig. 3b and c)**. The collar C-terminal domain forms a tightly closed circle with no gap and holds the complex together. In all eukaryotesclamp loaders, a gap exists in between the AAA+ domains of subunits RFC1 and RFC5 as shown in **Fig. 3a and c**. This is so because RFC1 has a C-terminal region that extends across the gap and protrudes down toward the N-terminal face of the clamp loader and it interacts directly with the Proliferating Cell Nuclear Antigen (PCNA) and with DNA **(Fig. 3c)** (Bowman et al., 2004).

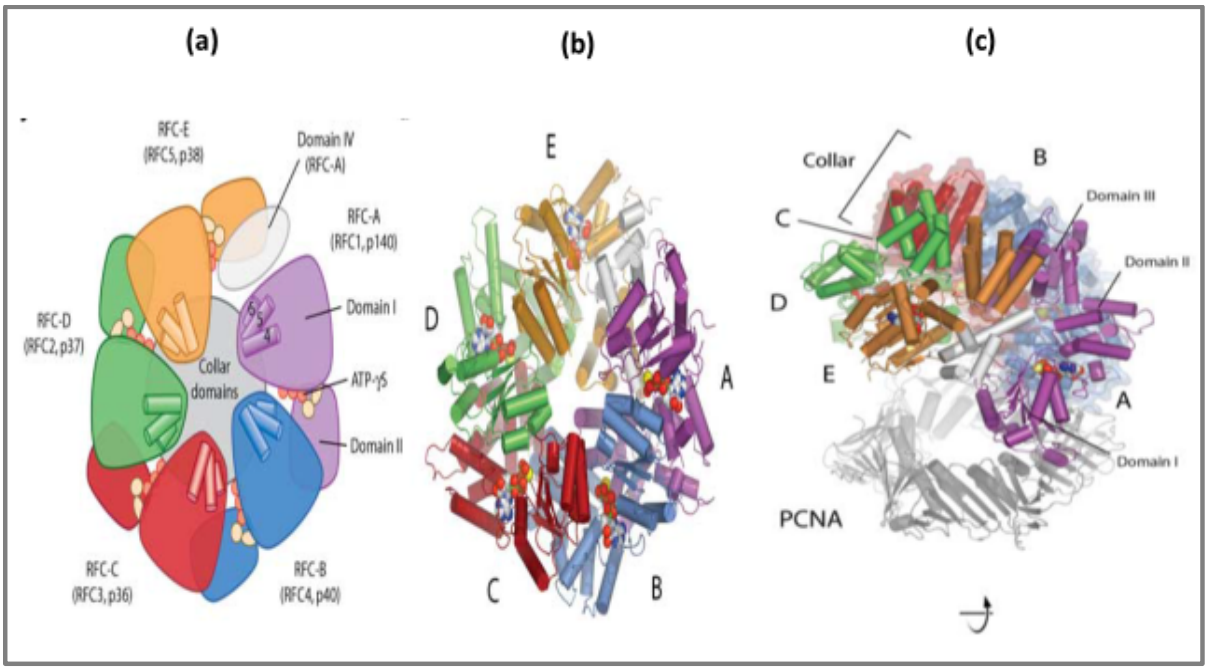

Figure 3. Architecture of the RFC complex: The five subunits of the RFC complex are referred to as RFC-A, RFC-B, RFC-C, RFC-D and RFC-E, respectively, moving in a right-handed sense around the assembly, with the thumb pointing towards the collar (**a** and **b**). The three domains of RFC and the extensions of C-terminal domain that interact with PCNA (**c**). The yeast and human nomenclature for each subunit is shown in parentheses (copied from Bowman et al., 2004).

The RFC complex functions are universally conserved in all eukaryotic organisms. As clamp loaders, RFC complexes catalyses the process of loading the PCNA on to the 3` ends of nascent DNA strands. As described by Hedglin and his colleagues (Hedglin et al., 2013), the complex utilizes the ATP and act as a protein topoisomerase to open the ring of PCNA so that it can encircle the DNA. The ATP hydrolysis causes release of RFC, with concomitant clamp loading onto DNA thus permitting highly processive DNA replication (**Fig. 4)**

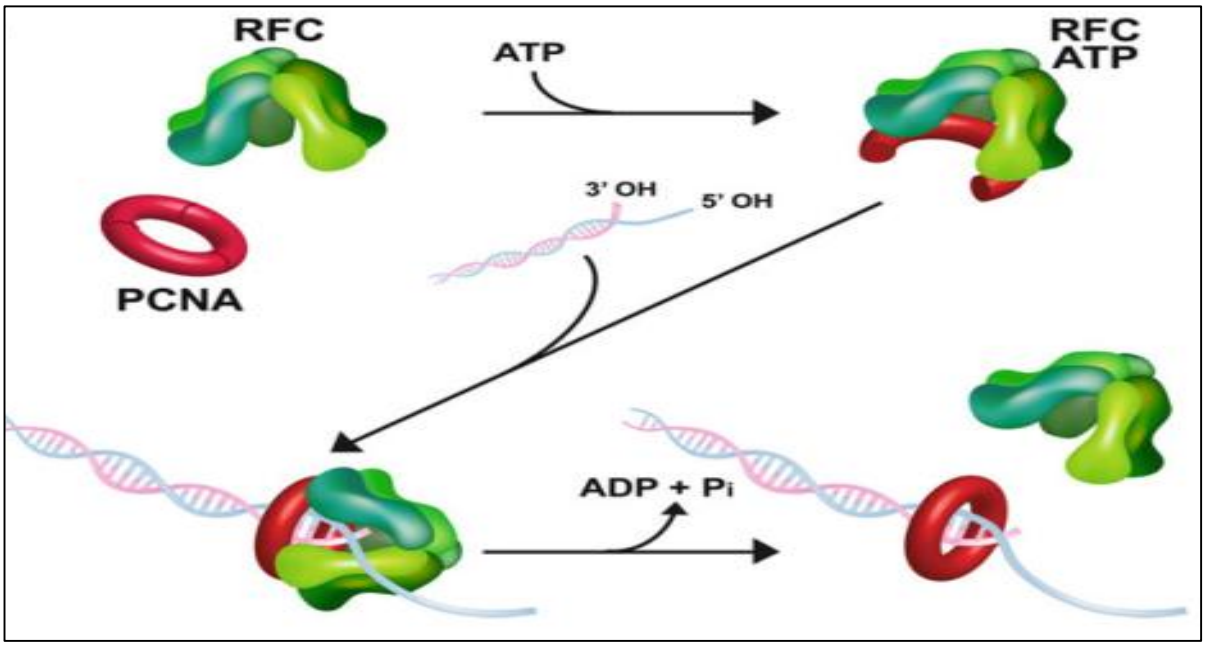

Figure 4. Schematic model of eukaryotic RFC complex as clamp loader. ATP binding to RFC enables RFC to bind and open PCNA. RFC places PCNA onto DNA and then hydrolyses ATP to eject itself out of the PCNA-DNA complex (copied from Hedglinet al., 2013).

The RFC complex have also been reported for switching DNA polymerase enzymes from DNA Pol α to Pol δ during initiation of leading strand DNA replication in the Simian virus 40 origins of replication and as well as synthesizing of Okazaki fragments during lagging strand DNA replication (Yao and O'Donnell, 2012). As a structure specific DNA binding protein, RFC complex is a primer recognition factor for DNA polymerases especially δ and ε, and function as accessory proteins for these enzymes (Bowman et al., 2004). The complex binds primers synthesized by Pol α-primase blocking them for further elongation and increasing their affinity to Pol δ.

Other studies have reported the requirement of RFC complex in DNA repair mechanisms and in replication checkpoints in yeast cells (Schmidt et al., 2001; Chen et al., 2009). When there is no DNA replication due to DNA damage, checkpoint regulatory networks are induced by RFC complex, which avoid the cells to enter in mitosis (so cells accumulate in the interphase) until the DNA damage is restored(Chen et al., 2009).

Alternative forms of RFC protein complexes or RFC-like complexes (RLC) have been purified in various organisms such as yeast, plants and mammals. Each RLC is made up of the four small subunits of the RFC (RFC2-5), but with a specific large subunit of that complex (**Fig. 5)**. One such RLC is Elg1-RFC complex in yeast and humans in which Elg1 replaces RFC1 **(Fig.5a**) (Kim and MacNeill, 2003). Cells with Elg1-RLC deletions had chromosomal instabilities and showed slow S-phase progression suggesting the role of Elg1-RFC in genome stability.

A second form of RFC is Rad24–RLC in which the RFC1 subunit is replaced by Rad24 (known as Rad17 in humans) resulting in the formation of the pentameric Rad24–RLC **(Fig.5b**), that specifically loads the heterotrimeric Rad9–Rad1–Hus1 (9-1-1) clamp complex onto DNA (Majka and Burgers, 2003). In addition, the 9-1-1 complex comprises of other proteins such as Ddc1 and Mec 3 (Kim and MacNeill, 2003). The 9-1-1 clamp complex activates the DNA damage checkpoints (G1, G2 and in the intra-S phases) to ensure that cell cycle progression is halted until repair is complete (Eichinger and Jentsch, 2011).

The third form of alternative RFC in eukaryotes is the Ctf18-Dcc1-Ctf8/ Ctf18-RLC complex (**Fig.5c**). Similar to the other two forms, the RFC1 subunit is replaced by Ctf18 to form the heteroheptameric Ctf18–RLC complex. The Ctf18 subunit is known to interact strongly with two other subunits; the Dcc1, and Ctf8. The Ctf18, Dcc1, and Ctf8 together form a complex (Ctf18-Dcc1-Ctf8) with the four small subunits of RFC (Mayer et al., 2001). Unlike other RLC, the Ctf18-RLC complex is known to play crucial role in chromosome cohesion, the process by which newly replicated sister chromatids remain physically associated until mitotic anaphase (Lengronne et al., 2006). Apart from helping the replicated chromosomes stay together until mitosis, the Ctf18-RFC complex also enhances genome stability in yeast (Ansbach et al., 2008; Gellon et al., 2011). This is achieved by its ability to help the DNA replication machinery move through triplet repeats and able to repair any resulting DNA damage.

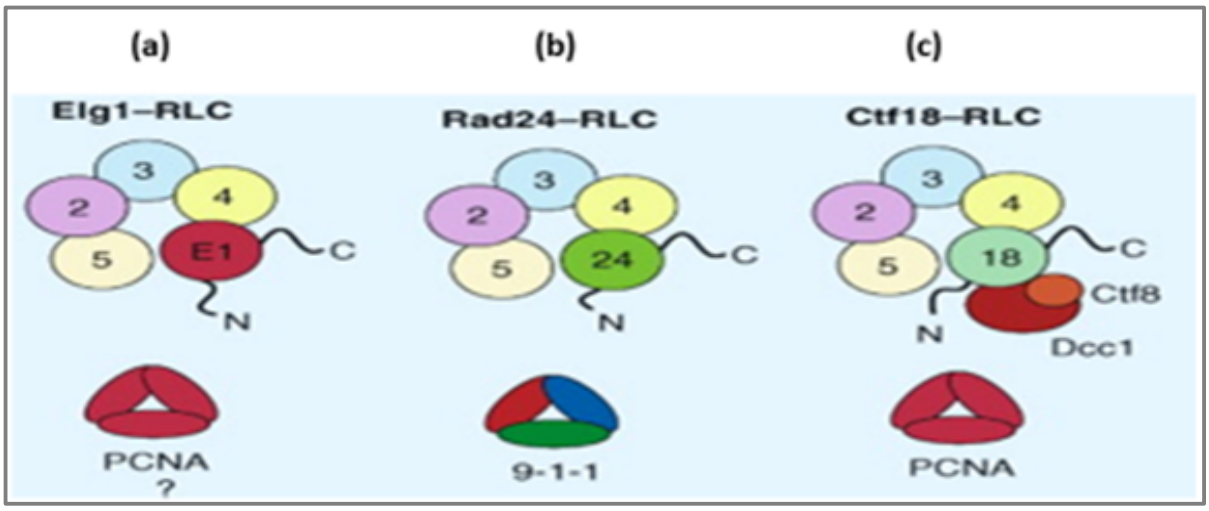

Figure 5. Schematic representation of the three RLCs in eukaryotes with their cognate sliding clamps. The complexes are defined by their large subunits, as the four small RFC subunits designated 2–5 are common to all. Note that the large subunits possess extended amino- and carboxy-terminal regions. **(a**) Elg1-RLC where RFC1 is replaced by Elg1**,(b)** Rad24-RLC in which RFC1 is replaced by Rad 24 (Rad17) and **(c)** Ctf18-RLC in which RFC1 is replaced by Ctf18 but has two additional non-RFC subunits Ctf8 and Dcc1 (Copied fromKim and MacNeill, 2003).

2.1.2.2 The RNA exosome protein complex

As described by Makino and Conti, the core of eukaryotic exosome complex is made up of six RNase PHlike subunits, which assemble into a ring-like structure and three additional subunits composed of S1/KH domains (so-called cap proteins), forming a coaxial ring (Makino and Conti, 2013). At the base of the complex are the six RNase PH-like proteins (**Fig. 6**): RRP41, RRP42, RRP43, RRP45, RRP46, and Mtr3, forming a core ring structure and central channel of the complex. On top of the complex are the three catalytic "cap" subunits; RRP4, RRP40, and Csl4, which have the S1-RNA binding domain (SI) and the K-homology (KH) domain. Apart from the nine core exosome components, two extra subunits--RRP6 and RRP44/Dis3 have been reported in yeast (Lorentzen et al., 2008a). The RRP44/Dis3 is a hydrolytic processive exoribonuclease subunit and is not available in the archaeal organisms (Navarro et al., 2008). If RRP44/Dis3 is associated with humans or trypanosome exosomes, the interaction is weak because it has never been purified in these organisms (Chen et al., 2001; Estevez et al., 2001; Estevez et al., 2003).

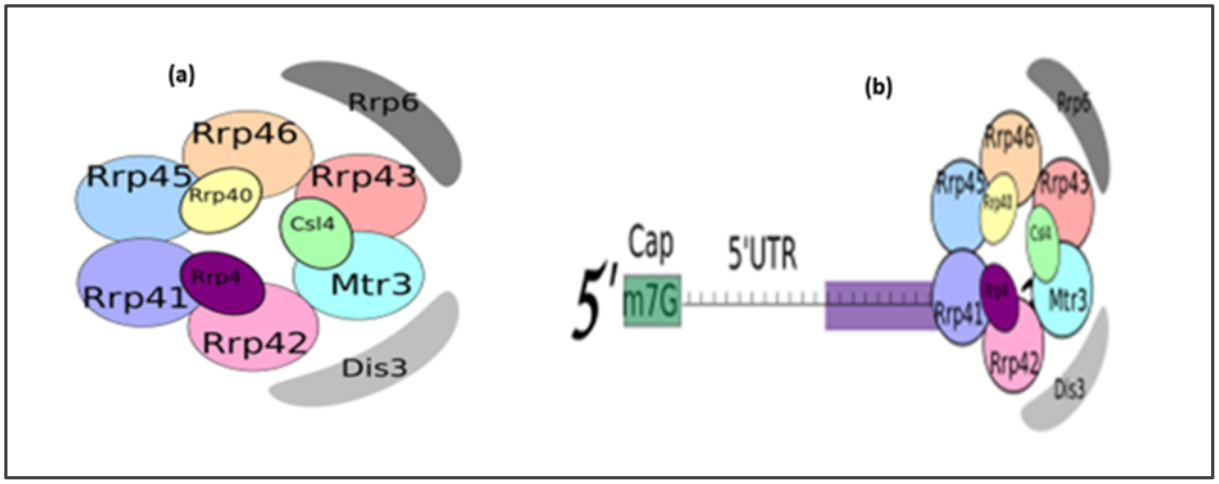

Figure 6. (**a**) A simplified architecture of *Saccharomyces cerevisiae* exosome complex and (**b**) its model interaction with the mRNA fragment (Copied from Navarro et al., 2008).

The exosome complex plays a very significant role in RNA metabolism processes. In the nucleus, the exosome complex regulates messenger RNA numbers during their turnover processes and participates in various RNA maturation processes (Makino and Conti, 2013). The complex degrades the RNA maturation by-products such as 5' External Transcribed Sequences and functions in RNA quality control processes by destroying aberrant products of rRNA, tRNA,snRNA and snoRNA in the nucleus (**Fig. 7b**) (Tomeckiet al., 2010). In cytoplasm, the complex participates in RNA surveillance systems ("non-stop decay", which degrades mRNA with a no stop codon, "nonsense-mediated decay", which degrades products possessing immature stop codons and the "no-go decay", which degrades RNA within stalled ribosomes). The exosome complex has also reported to degrade the 5′ intermediate segments from the RNA interference processes in the both nucleus and cytoplasm (Tomeckiet al., 2010).

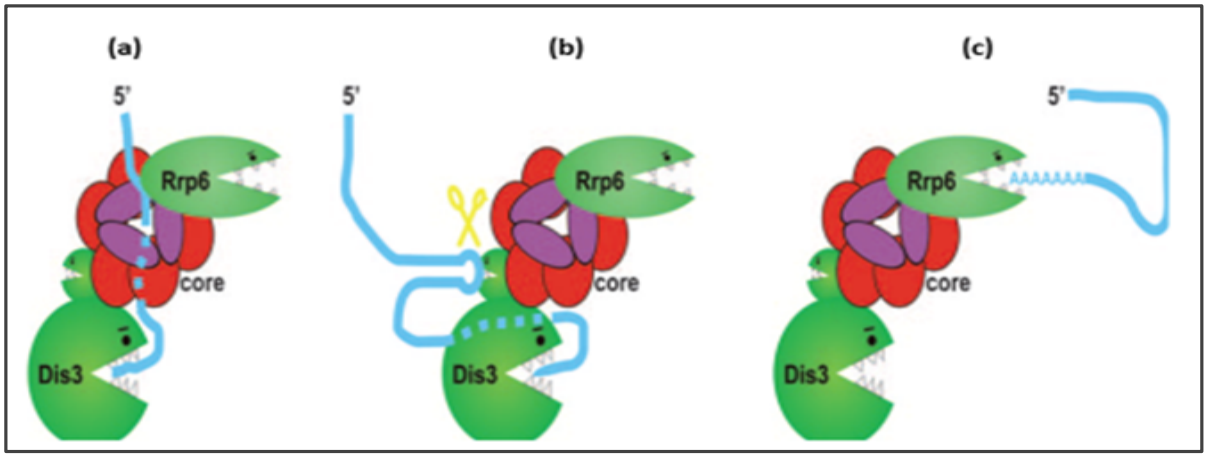

Figure 7. Schematic examples of eukaryotic exosome complex catalytic activities. **(a)** Single stranded substrates with enough long single stranded overhangs are recognised by the trimetric cap of RNA-binding proteins and passes through the central channel of the complex before accessing the RRP44/Dis3-exoribonuclease active site. **(b)** RNA substrates with secondary structures but of no 3' single stranded extensions of enough length to pass through the central channel, access the RRP44/Dis3 exoribonuclease active site directly after being recognized by the OB-fold RNA-binding domains. The PIN domain can endonucleolytically cleavage (yellow scissor) single stranded loops of the secondary structure to assist in 3'-5' exoribonucleolytic degradation by RNB domain catalytic activity. **(c)** In the nucleus, transcripts polyadenylated by the TRAMP are trimmed by RRP6 without passing the central channel and later get degraded (Copied fromTomeckiet al., 2010)

2.1.3 Overview of protein complexes purification methods

Although several biochemical studies have identified proteins likely to play a role in the establishment and maintenance of the pathogenic kinetoplastids's life cycle, specific functions of these proteins has remain unknown in several cases. The process of isolating and identifying protein complexes is very useful when the purpose is to gain more understanding on the specific functions of individual proteins in the complex as well as to determine their importance at a molecular level. Complete genome sequencing of various microorganisms has created a chance to analyse roles of various proteins encoded in their genes. More knowledge on various cellular processes can be acquired through analysing, characterizing and identifying interactions, which exist among proteins in the complex (Schwikowski et al., 2001).

The two-hybrid systems were commonly used identity components of specific protein complexes. However, these were time consuming, labour intensive and limited to a small-scale protein analysis. Moreover, the two-hybrid systems have low rates of true positives and

true negatives results. More effective and reliable strategies of studying protein-protein interactions have been highly needed.

With the development of the Tandem affinity purification (TAP) coupled to Mass spectrometry over the past decades, many proteins complexes have been isolated and the interacting partners identified. As long as a specific protein complex of interest is effectively and adequately isolated, proteins within the complex can be recognised and characterised by TAP-mass spectrometry. Enhanced by the available databases of complete genomic sequences of various organisms, though initially designed for yeast cells, this approach has been widely employed in various organisms (Puig et al., 2001) to facilitate the identification and characterisation of their respective proteins.

As suggested by Schimanski et al (2005), TAP-mass spectrometry limitations are observed in the protein isolation process rather than in the process of identifying them. This is mostly because an individual protein may possess different characteristics from other associated proteins in the complex. More recently, the tagging of protein of interest with either peptides or protein domains has seemed to be a promising strategy of bypassing this limitation during purification process.

The conventional TAP methods required the fusing of a C-terminal TAP tag to a protein of interest. The TAP tag composed of two IgG binding units of protein A of *S.aureus* (ProtA) and a Calmodulin binding domain (CBP) with a cleavage site for a Tobacco etch virus (TEV) protease inserted between them (Rigaut et al., 1999). Apart from a C-terminal TAP tag, there is an N-terminal TAP tag, which is a reverse orientation of the C-terminal TAP tag (**Fig. 8a**). Two TAP steps are required to purify the cell extracts of the tagged protein of interest after transformation as shown (**Fig.8b**).

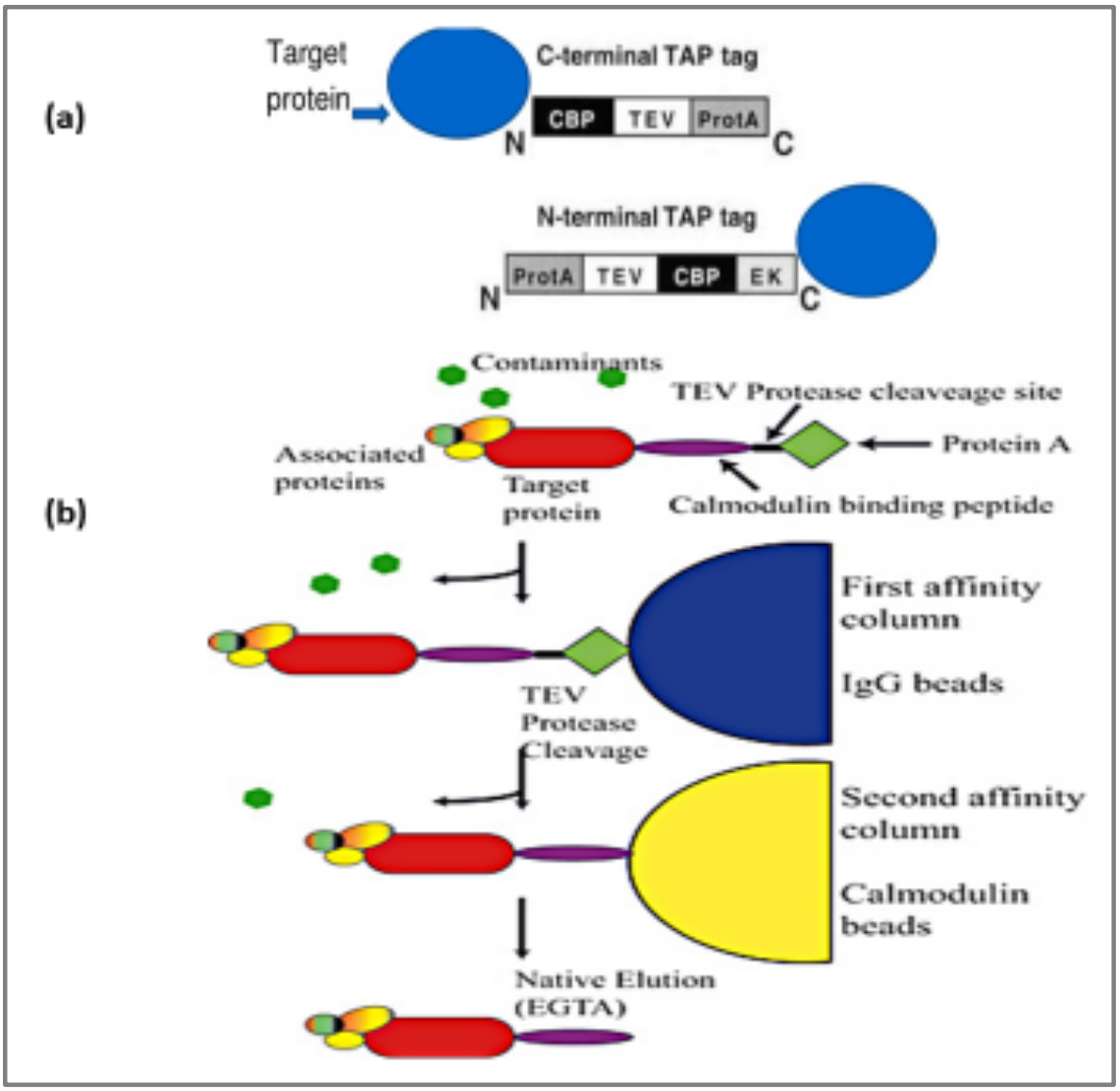

Figure8. A schematic representation of TAP tagging and an outline of the purification procedure. (**a**)Representations of a C- and N-terminal TAP showing orientation of Protein A domains and CBP. (**b**) The TAP purification procedure. In the first step, the protein complex containing the tagged protein of interest binds to IgG matrix by the ProtA fraction. The protein complex is then eluted using TEV protease under native conditions. In the second step, the elution fraction of the first purification step is incubated with beads coated by calmodulin in the presence of calcium. Subsequently, contaminants and the remainder of TEV protease used in the first step are eliminated through washing. Finally, the protein of interest in a complex is obtained by elution using EGTA. (Copied from Rigaut et al., 1999).

Compared to the traditional protein purification methods, the TAP method has been observed to be a very effective tool for isolating pure proteins in adequate quantities from a small volume of cell culture and under native conditions to retain their functions (Rigaut et al. (1999). However, although this has been the case, the TAP tool has been unsuccessful in various cicumstances. For instance, Gavin and his collegues reported the failure of the method to identify and isolate the tagged and associated proteins in yeast (Gavin et al., (2001). The failure was claimed to be due to the TAP tag which interfered with the function of the protein, its location and as well as complex formation.

Recently, several new TAP tags combinations have been developed to overcome the limitations of the conventional TAP tags, including PTP (for ProtC-TEV-ProtA) where CBP is replaced by protein C epitope (ProtC) (**Fig. 9b**), reducing the overall size of the tag from 184 to 169 amino acids and the molecular mass from 20.6 to 18.9 kDa. After TEV protease cleavage, 44 and 29 amino acids accounting for 5.1 and 3.4 kDa, respectively, remain on TAP- and PTP tagged proteins. ProtC is derived from human protein C, a vitamin K-dependent plasma zymogen specifically expressed in hepatocytes. The monoclonal antibody HPC4 recognizes this epitope with high affinity and, as a unique property, has a calcium-binding site that needs to be occupied for its interaction with ProtC.

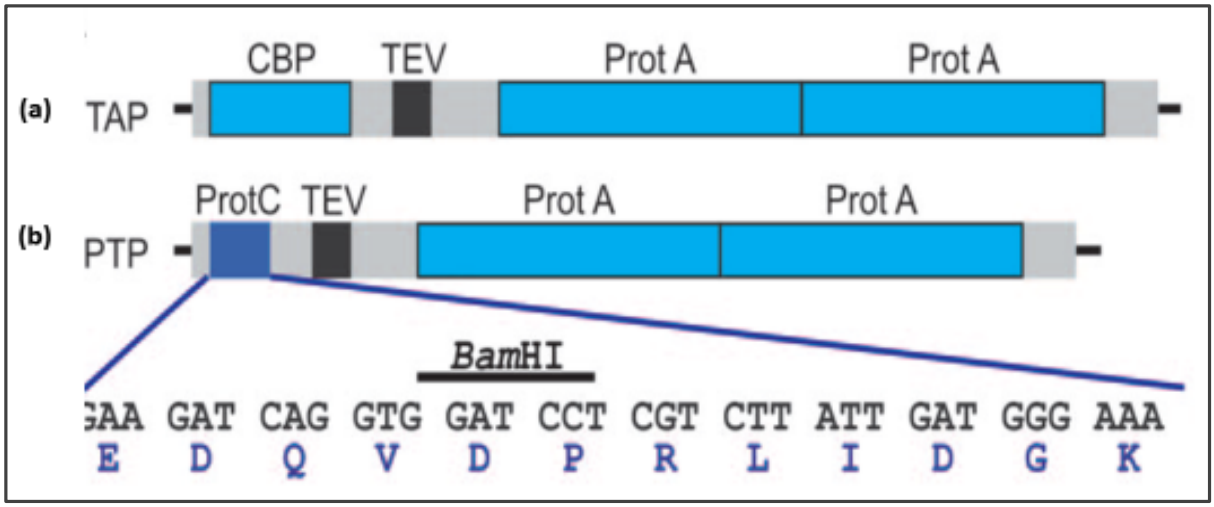

Figure 9. A schematic representation of TAP and PTP tag. (**a**) TAP tag showing Protein A domains, TEV and CBP. (**b**) PTP tag where CBP is replaced by Prot C (Copied from Schimanski et al., 2005).

2.2 Materials and methods

2.2.1 Organisms and reagents

The *C. fasciculata* promastigotes clone HS6 were grown at 27°C with gentle agitation in serum-free defined media as described in **Appendix 1**). The media pH was adjusted to 8.0 with either NaOH or HCl before haemin (10μg/ml) was added. The parasites' genomic DNA was extracted according to DNA extraction procedure described by Bernards et al (1981) as described in **Appendix 2**. Conventional DNA manipulation procedures were conducted using DH5α competent *E.coli* cells. All chemicals and reagents used were of the highest grade and were purchased from Sigma-Aldrich or Thermo Fisher Scientific. DNA manipulation enzymes were purchased from either New England Biolabs, Thermo Fisher Scientific or Promega.

2.2.2 General Molecular biology techniques

2.2.2.1 Designing primers and amplifying ORFs of target proteins

Reverse and forward primers were designed to amplify the entire ORFs of our target subunits (RFC3 and RRP4) from the *C. fasciculata* genomic DNA. Briefly, 10 random bases (GGTGGTGGTG) and 21 consecutive bases of the target gene sequence after a start codon were added upstream and downstream *Nde*I sequence (CATATG) respectively, to create a 5' *Nde*I (forward) primers. The 3'*Not*I (Reverse) primers were also designed by adding 10 random bases (GGTGGTGGTG) and 24 consecutive bases of the target gene sequence before a stop codon (in reverse complement) upstream and downstream the *Not*I sequence (GCGGCCGCC), respectively. Oligonucleotides were then ordered from Integrated DNA Technologies. All primers had melting temperatures (T_m) between 65°C and 74°C, the GC content between 40 and 60%, with balanced distribution of GC-rich and AT-rich domains without secondary structures and had no recognisable intra-primer homology or inter-primer homology. The designed primers are shown in **Appendix 3.** A conventional PCR was used to amplify the ORFs of the target protein subunits (RFC3 and RRP4) using Q5 High-Fidelity DNA polymerase following the manufacturer's instructions with slight modifications as described in **Appendix 4a.**

2.2.2.2 Agarose-gel electrophoresis

The purified DNA products were mixed with 10x loading dye and loaded onto a 1% agarose gel (1% agarose in 1x TAE and 0.001% ethidium bromide) alongside 0.5 μg of a 1 kb DNA

ladder (Fermentas). Gels were run at 120 V for 45 minutes and the DNA was visualised using a UV transilluminator (Syngene U Genius).

2.2.2.3 Preparative restriction digest and Ligations for cloning

Prior to cloning, the vector pNUS-PTPcH and inserts (RFC3 and RRP4) were digested in 60µl reactions with restriction enzymes *NotI* and *NdeI* (NEB) for 3 hours at 37°C and dephosphorylated during the last 60 minutes with Antarctic phosphatase (NEB) according to the manufacture's instruction. The DNA fragments were gel purified using Thermo Scientific DNA purification kit following the manufacture's instruction. 10% of the eluted volume was resolved in a 1% agarose gel containing 0.001% ethidium bromide to confirm the presence and size of the fragments before ligations. For each ligation reaction, 50ng of the gel-purified vectors were combined with 3-fold molar excess of the insert (calculated using NEBioCalculator) and the final volume adjusted to 10µl with distilled sterile water. 10µl of 2x Quick ligation buffer followed by a 1µl of the Quick T4 DNA ligase was then added and mixed thoroughly and briefly centrifuged before incubation at room temperature (25°C) for 20 minutes. The ligation products were directly used for *E.coli* transformation. Protocols and recipes for preparative restriction digests, diagnostic digests, ligations and agarose electrophoresis are described in **Appendix 5.**

2.2.2.4 *E.coli* transformation and Isolation of plasmid DNA

Conventional TSB transformation procedures were used as previously described in Inoue et al. (1990). Briefly, 20ml of LB medium was inoculated with 100µl of the over night grown *E.coli* DH5α cells and incubated at 37°C for 4 hours in a shaker incubator. Cell culture (optical density ~0.5) was then spun down at 3,000 rpm for 10 minutes to pellet cells. The pelleted cells were suspended in 1 ml of TSB (See recipe in **Appendix 6**) and thawed on ice for 30 minutes to make them competent. For each transformation reaction, 100 µl of the competent cells were transferred to a chilled microcentrifuge tube on ice. To this, 10µl of the plasmid DNA was added and the mixture kept on ice for 30 minutes. After 30 minutes incubation on ice, 200µl of LB media was added and the mixture was later incubated at 37°C with shaking for 1 hour. Later, 150 µl of cells were plated on LB plates containing 100µg/ml ampicillin using glass beads and incubated over night at 37°C.

2.2.2.5 Colony PCR for transformations and restriction digest

Transformed cells were analysed by a standard PCR technique by determining the presence of the insert DNA in the plasmid construct using MyTaqRedDNA polymerase following a

protocol described in **Appendix 4b.** Briefly, a final reaction mixture (20µl) contained 5µl volume of cells (from 100µl colony suspension) to provide DNA template during initial PCR heating step, 5µl of the insert specific primers (4µM each) and 10µl MyTaqRed Mix. The presence of a PCR amplicon and size of the product were determined by 1% agarose gel electrophoresis. A miniprep culture was prepared by inoculating a 50µl of correct transformed cells colony suspension in 5ml of LB media containing ampicillin (100µg/ml) for isolation and incubated overnight in a shaker incubator. The Plasmid DNA was purified using a Thermo scientific Miniprep kit following manufactures instructions. A portion of the eluted volume containing plasmids DNA were digested in 20µl reactions with *Nde*I and *Not*I enzymes according to manufactures instruction and as described in **Appendix 5**, to screen and confirm if the plasmids contained the correct inserts. The purified plasmids at a concentration of 1.2µg DNA in 60µl dH_2O and the associated primers (50µl of 3.2 µM) were then sent for sequencing at Dundee sequencing services centre to verify the fidelity of cloning process.

2.2.3 Construction of the expression vector (pNUS-PTPcH)

The expression vector pNUS-PTPcH was constructed by S. MacNeill (personal communication). Briefly, part of pNUS-SPnHc EcoRI fragment (102 bp) encoding a signal peptide (Tetaud et al., 2001), was removed and replaced with sequences derived by PCR amplification of the PTP tag-encoding region of plasmid pC-PTP from Schimanski and his colleagues (Schimanski *et al*., 2005). The cloned region lacked the *Afl*II*, Eco*RI and *Bam*HI sites internal to the PTP tag sequence that are found in pC-PTP and includes unique restriction sites for *Nde*I, *Xho*I, *Eco*RV and *Not*I upstream of PTP for fusing target sequences. The full sequence of the pNUS-PTPcH vector is shown in **Appendix 6.**

2.2.4 Identification of *C. fasciculata* and *T. brucei* homologous proteins from yeast RFC and exosome complexes

Protein sequences of specific known subunits of yeast *Saccharomyces cerevisiae*'s replication factor C and the exosome complexes were used to BLAST search the TriTrypDB database to identify putative *C. fasciculata* and *T. brucei* homologues. The online BLASTP program was used to determine the percentage identity between the protein sequences.

2.2.5 Cloning of the target subunits

Oligonucleotides (**Appendix 2**) were designed to amplify the entire ORFs of Cf-RFC3 and Cf-RRP4 from the C. *fasciculata* genomic DNA. Using conventional PCR (**Appendix 4a**), fragments of Cf-RFC3 and Cf-RRP4 were cloned in-frame with the PTP tag coding sequence of the constructed pNUSPTPcH vector using *NdeI* and *NotI* restriction enzymes, to create C-terminal PTP-tagged versions pNUS-RFC3-PTPcH and pNUS-RRP4-PTPcH. The TSB transformation method was used to propagate the plasmids into DH5α *E.coli* competent cells and the plasmids DNA was isolated as previously described. To verify the fidelity of the cloning process, the purified plasmid DNA were sequenced using pC-Seq-F and pC-Seq-R (**Appendix 3)** as described in Sanger et al. (1977).

2.2.6 Parasite transfection and generation of cell lines

For a successful transfection, *C. fasciculata* parasites were grown to a log phase at 27°C in a shaker incubator and harvested at a density of ~1 x 10^7 cells/ml by centrifugation at 3000 rpm for 5 minutes. The cell pellet (~2 x 10^7 cells/ml) was suspended in 100µl of human T-cell Nucleofactor solution (Lonza) and transferred to a 0.4 cm cuvette containing 15-60µg of purified pNUS-RFC3-PTP or pNUS-RRP4-PTP supercoiled plasmids DNA. The mixture was then subjected to program X-014 of the Amaxa electroporation system (Burcard et al., 2007). Electroporation cells were left on ice for 5 minutes and transferred into a culture flask containing 5ml of fresh medium and incubated at 27°C to recover. After 24 hours of recovery, the cell culture was supplemented with 5 ml of fresh medium followed by hygromycin final concentration of 25µg/ml. Hygromycin-resistant cell lines were subsequently grown with at least 50 µg/mlof drug and viable clones observed within 5 to 10 days. Resistant cell lines were maintained by supplementing the culture with fresh medium containing the antibiotic.

2.2.7 Expression and PTP purification of the proteins

To confirm if the selected cell lines expressed the PTP fusion proteins, cell lysates were prepared from the parasites and analysed by SDS-PAGE and Western blots. Briefly, a sample volume of 1ml (~1 x 10^7 cells) was harvested by centrifugation at 2000 g for 5 minutes. The cell pellet was heated to boil in 2 X SDS-PAGE sample buffer at 95^{o}C for 5 minutes. The protein extract sample was resolved in a 12 % SDS-PAGE and blotted on a Polyvinylidene difluoride (PVDF) membrane. To detect PTP fusion proteins, blots were incubated with PAP reagent, which contained primary antibodies raised against Protein A epitopes of the PTP tag, diluted 1:2000 using 5% milk-PBS-Tween (0.05%) blocking solution. Blots were developed using Goat-Anti-rabbit IgG (H+L DyLight^{TM} 680) conjugated secondary antibody

(ThermoFisher Scientific) diluted in 1:10000 according to the manufacturer's instructions and scaned on Odyssey scanner using the 700nm channel.

Purification of the target proteins and their interacting partners in the complexes was conducted according to the generic TAP method described inSchimanski et al. (2005) with slight modifications. Recipes for solutions and buffers used in the purification experiments are described in **Appendix 7**. Briefly, a volume of 2.5 litres of culture (~ $2x10^7$ cells/ml) was harvested by centrifugation at 800 g for 10 minutes. The cell pellet was washed three times with 5 ml PBS to a final packed cell volume of approximately 4 ml. The cell extract had a volume of ~6.5 ml and contained 150 mM sucrose, 300 mM potassium chloride, 40 mM potassium L-glutamate, 3 mM$MgCl_2$, 20 mM HEPES-KOH (pH 7.7), 2 mM dithiothreitol, 0.1% Tween 20, and half of a Complete Mini EDTA-free protease inhibitor cocktail tablet (Roche, Indianapolis, IN). Cells were Dounced in continuous strokes for 5 minutes in a cold room using a 7 ml Dounce homogenizer (Sigma-Aldrich) and centrifuged at 20,500 g for 10 minutes at 4°C. For IgG affinity chromatography, the resultant lysate was filtered straight into a 10 ml Poly-prep chromatography column (Bio-Rad, Hercules, CA) containing a volume of 200 µl of PA-150 buffer equilibrated IgG Sepharose beads (GE Healthcare). The top and the bottom of the column were sealed with Parafilm and the column rotated for 2 hours at 4°C allowing the PTP tagged protein to bind to the IgG beads. The beads were later washed 2 x with 10 ml PA-150 before equilibrating the column with 8ml TEV buffer. To TEV cleave the IgG matrix bound proteins, a 20µl of TEV protease was diluted in to 2 mL TEV buffer and added to the column rotating it overnight at 4°C.

The TEV and column dead-volume were eluted by washing the IgG beads with 4 ml of PC-150 buffer. 0.5ml of the remaining Mini EDTA-free protease inhibitor tablet (Roche) and 7.5 µl of 1 M $CaCl_2$ were added to the eluate mixture to avoid any proteolysis in the eluate. The mixture was added to a second equilibrated Poly-prep column containing a volume of 200 µl anti-ProtC affinity matrix beads (Roche) and was rotated for 2 hrs in the cold room to allow the tagged protein to bind to the anti-ProtC affinity matrix. After washing the anti-ProtC affinity matrix beads for 6 times with 10 ml PC-150 buffer, the PTP tagged proteins were eluted with a 1.8 ml EGTA/EDTA buffer at room temperature.

To concentrate the eluted proteins, eluates were bound to a volume of 30 µl of StrataClean resin beads (Stratagene) and pelleted at 5,000 g for 1 minute. The beads were later re-suspended in 20 µl 4XNuPAGE LDS sample buffer and boiled at 95°C to release the proteins. A 20 µl of the sample was loaded onto a NuPAGE 4-12% Bis-Tris pre-cast gel and the

proteins were resolved by SDS-PAGE before stained with SYPRO Ruby stain. The stained gels were visualised using a UV transilluminator.

2.2.8 Mass Spectroscopy analysis

Individual protein bands were excised from the gels and analysed by our in-house Mass Spectroscopy and proteomics facility at the University of St Andrews, Biomedical Sciences Research Complex. Briefly, proteins were digested overnight with trypsin prior to separation by AB Sciex 4800 MALDI (Matrix-Assisted Laser Desorption/Ionisation) TOF/TOF^{TM} analyser (AB Sciex, UK). The obtained data were processed with MASCOT and compared against the *C. fasciculata* or NCBI protein databases to unambiguously identify the proteins.

2.3 Results and Discussion

2.3.1 Identification of *C. fasciculata* and *T.brucei* homologous proteins from yeast RFC and exosome complexes

Protein sequences of specific known subunits of yeast *S. cerevisiae* replication factor C and the exosome complexes were used to BLAST search the TriTryp database to identify putative *C. fasciculata* and *T. brucei* homologues. The *S. cerevisiae* RFC and exosome complexes homologs of *C. fasciculata* and *T. brucei* identified are shown in **Table 3**. The percentage (%) identity between the protein sequences were determined using the NCBI online BLASTP program. The identified homologs were selected based on their maximum identity and E-scores in TriTryp database.

The *C. fasciculata* RFC and exosome subunits shared around 30-55% and 28-56% sequence identity with the yeast counterparts, respectively and also shared 65-73% and 34-60% sequence identity with the *T.brucei* homologs, respectively. As expected, *C. fasciculata* proteins were more homologous to the *T.brucei* than the yeast counterparts. The RFC complex subunits of the *C. fasciculata* and *T.brucei* were more identical compared to the exosomes subunits (average identity of 70% and 45% for RFC subunits and exosome, respectively, between *C. fasciculata* and *T. brucei* homologues). This is not surprising as ribosomal RNA metabolisms in trypanosomes are unique as observed in various studies (Ullu et al., 1996; Hartshorne and Toyofuku 1999; Di Noia et al., 2000).

	S. cerevisiae subunits	*T. brucei* homologs		*C. fasciculata* homologs			
	Name	Name	Gene ID	Gene ID	Mwt (Da)	% Identity (positives %) to *S.cerevisiae*	%Identity(positives %) to *T.brucei*
RFC complex subunits	RFC1	*Tb*RFC1	Tb927.11.5650	CFAC1_210019200	72,644	30 (47)	65 (79)
	RFC2	*Tb*RFC2	Tb927.6.3890	CFAC1_260050500	38,286	44 (66)	69 (83)
	RFC3	*Tb*RFC3	Tb927.9.12300	CFAC1_300082900	39,856	43 (62)	72 (83)
	RFC4	*Tb*RFC4	Tb927.11.9550	CFAC1_230046600	33,546	55 (74)	69 (81)
	RFC5	*Tb*RFC5	Tb927.10.7990	CFAC1_280077100	39,086	39 (61)	73 (86)
Exosome complex subunits	RRP4p	*Tb*RRP4	Tb927.7.4670	CFAC1_110005300	32,088	37 (56)	51 (67)
	RRP6p	*Tb*RRP6	Tb927.4.1630	CFAC1_290060300	80,085	31(48)	51 (65)
	RRP40p	*Tb*RRP40	Tb927.9.7070	CFAC1_030007200	34,302	28 (38)	46 (59)
	RRP41p	*Tb*RRP41A	Tb927.10.7450	CFAC1_280032800	26,798	48(76)	60 (75)
	RRP42p	EAP1	Tb927.1.2580	CFAC1_170027500	43,178	29(61)	41 (53)
	RRP43p	EAP2	Tb927.11.16600	CFAC1_300052700	32,147	26(43)	40 (56)
	RRP45p	*Tb*RRP45	Tb927.6.670	CFAC1_240024400	39,758	31 (49)	46 (62)
	RRP46p	*Tb*RRP41B	Tb927.2.2180	CFAC1_160013900	35,618	22(40)	37(50)
	RRP47	EAP3	Tb927.7.5460	CFAC1_180026700	23,121	27(50)	34 (48)
	Mtr3	EAP4	Tb927.11.11030	CFAC1_280054900	23,286	32 (46)	50 (66)
	CSL4p	*Tb*CSL4	Tb927.5.1200	CFAC1_150031200	27,882	30 (44)	41 (53)

Table 3. *C. fasciculata* and *T.brucei* homologs of *S. cerevisiae*'s RFC and Exosome complex subunits. The yeast *S. cerevisiae* protein sequences were used to BLAST search the TriTrypDB database to identify putative *C. fasciculata* and *T. brucei* homologs. The systematic identities, the molecular masses (Mwt) of the predicted *C. fasciculata* peptides and the percentage of identity are indicated.

2.3.2 Construction of the expression vector

TAP has been used for many years as a rapid and efficient method of isolating epitope-tagged protein complexes from crude extracts under native conditions. Initially established in yeasts, the method is now applied to other organisms such as trypanosomes. However, a number of studies have reported the inefficiencies of the original TAP method, which is based on fusing the proteins of interests to a TAP tag consisting of a duplicate protein A epitope, a tobacco etch virus protease cleavage site, and the calmodulin-binding peptide (CBP) (Schimanski et al., 2005; Drakes et al., 2005; Palfi et al., 2005). In most cases, the protein yield recovery has

been very low, an obstacle which has been mainly attributed to the calmodulin affinity purification step. To overcome this limitation, CBP has recently been replaced with PTP and successful results have been reported (Schimanski et al., 2003; Drakes et al., 2005; Palfi et al., 2005; Schimanski et al., 2005). Recently, series of shuttle vectors have been developed by Tetaud and colleagues to facilitate the expression of histidine tagged proteins in *C. fasciculata* (Tetaud et al., 2002). Extending this work, we modified the initial vector and developed a pNUS-PTPcH vector, which can be utilised to facilitate the expression and isolation of PTP tagged kinetoplastids proteins in these convenient parasites. Briefly, the vector pNUS-PTPcH (**Fig. 10c**) was constructed by S. MacNeill (personal communication), by removing and replacing the EcoRI fragment (102 bp) encoding a signal peptide in pNUS-SPnHc plasmid (**Fig.10a**) (from Tetaud et al., 2002) with sequences derived by PCR amplification of the PTP tag-encoding region of plasmid pC-PTP (**Fig. 10b**) (Schimanski et al., 2005). The cloned region included unique restriction sites for *Nde*I, *Xho*I, *Eco*RV and*Not*I upstream of PTP for fusing target sequences to the tag **(Fig. 10c).**

As in the original vectors, *bonafide* replication and transcription promoters were maintained to facilitate episomal expression of the construct. The 5`- and 3`-untranslated (UTR) sequences in the intergenic region of the *C. fasciculata* phosphoglycerate kinase genes A and B (IG-PGKAB) and the *C. fasciculata* glutathionylspermidine synthetase(GSPS) 3` UTR were also maintained as in Tetaud et al. (2002), to allow expression and maturation of the target genes and the hygromycin resistant gene.

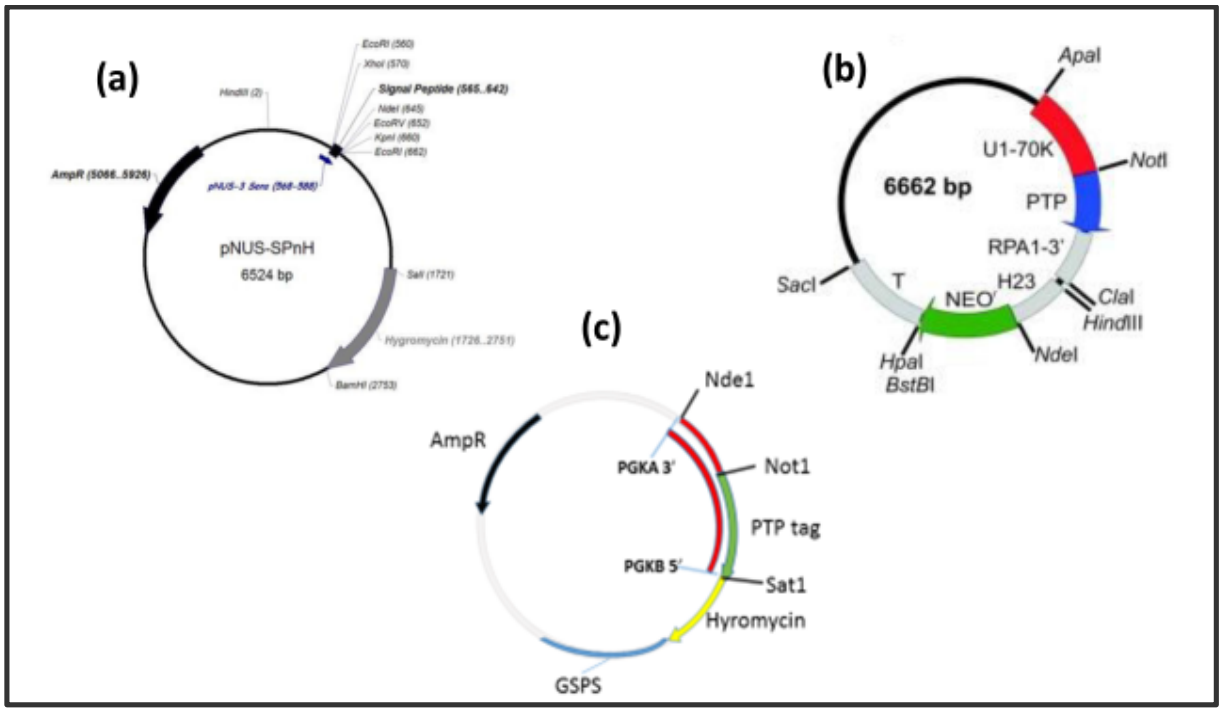

Figure 10. Circular maps of the plasmid constructs. **(a)** The pNUS-SPnH (copied from Tetaud et al.,2002) showing the region encoding signal peptide which was removed and replaced by a PTP tag-encoding sequence from pC-PTP-NEO plasmid **(b)** (Copied from Schimanski et al., 2005). **(c)**The constructed pNUS-PTPcH plasmid showing the IG-PGKAB, GSPS and specific restriction sites *Nde*I and *Not*I for cloning genes of interest.

2.3.3 Cloning of *C. fasciculata* RFC3 and RRP4 subunits in pNUS-PTPcH plasmid and Transfection.

Using PCR, we successfully cloned the ORF of target subunits RFC3 (CFAC1_300082900) and RRP4 (CFAC1_110005300) in frame with the PTP sequence of the constructed pNUS-PTPcH shuttle vector to create C-terminal PTP-tagged versions pNUS-RFC3-PTPcH (**Fig. 11a**) and pNUS-RRP4-PTPcH (**Fig. 11b**). Unlike the RFC complex, exosome complex have previously been TAP isolated using RRP4 subunit as a bait (Estevez et al., 2001). We therefore took advantage of this approach and also PTP tagged RRP4 in our constructs for validation.

C. fasciculata parasites were succesfuly transfected with the constructed plasmids using Amaxa program X-014 (Burcard et al., 2007), where it conferred hygromycin resistance and persisted as circular extrachromosomal DNAs that could be recovered back in *E.coli*.

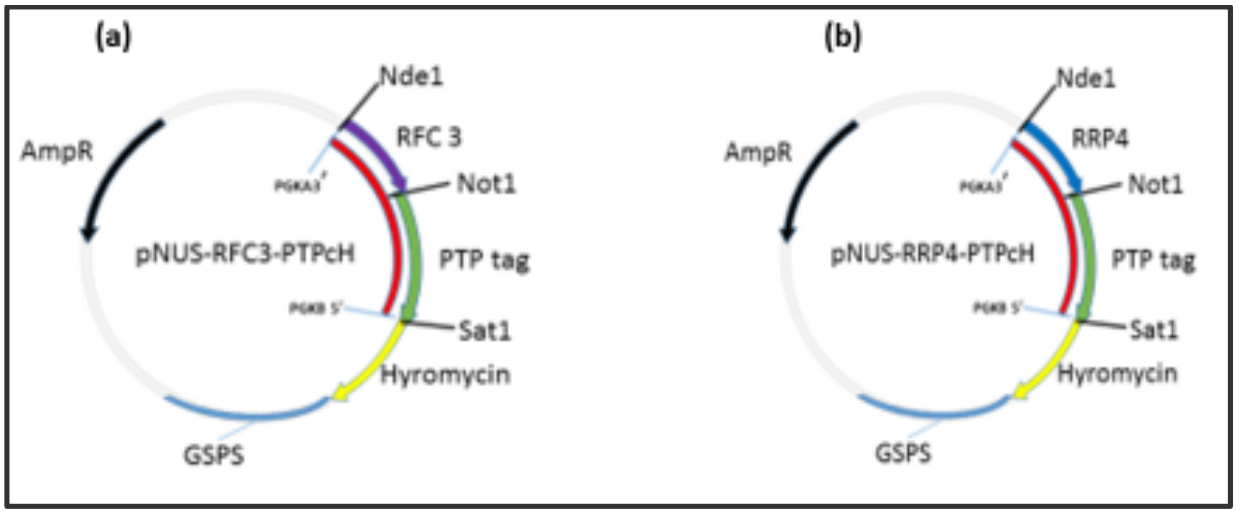

Figure 11. Circular maps of RFC3 and RRP4 tagged versions. **(a)** pNUS-RFC3-PTPcH and **(b)** pNUS-RRP4-PTPcH.In each case, fragments of the target genes, the PTP cassette, the *C. fasciculata* IG-PGKAB gene flank, the resistance marker and the 3`flank GSPS are drawn in different colours.

2.3.4 Expression and PTP purification of the proteins

To validate the pNUS-PTPcH plasmid, we first determined if the cloned genes were expressed in *C. fasciculata* cells. Cell lysates were prepared from the resistant cell lines and analysed by SDS-PAGE and Western blots. The immunoblot revealed two proteins of sizes ~51kDa and ~57kDa that were confirmed with the theoretical masses as PTP-tagged RRP4 and RFC3, respectively (**Fig. 12a**). When the hygromycin concentration was increased from 50µg/ml to 200µg/ml, the expression of the tagged proteins also increased though cells grew more slowly (data not shown), a similar observation to (Tetaud et al., 2002) and others. However, increasing the hygromycin concentration to 200µg/ml did not significantly increase the expression of PTP tag protein from empty pNUS-PTPcH cell lines.

To determine if the tagged proteins and their interacting partners could be isolated from their respective complexes, the two consecutive step TAP method was used as previously described in the methods and the eluted complexes analysed by SDS-PAGE and SYPRO-ruby staining. The specificity of the purification method was monitored by generating a cell line expressing the empty pNUS-PTPcH. In this case, no bands were detected from the cell lysates of cells expressing the empty plasmid (data not shown).

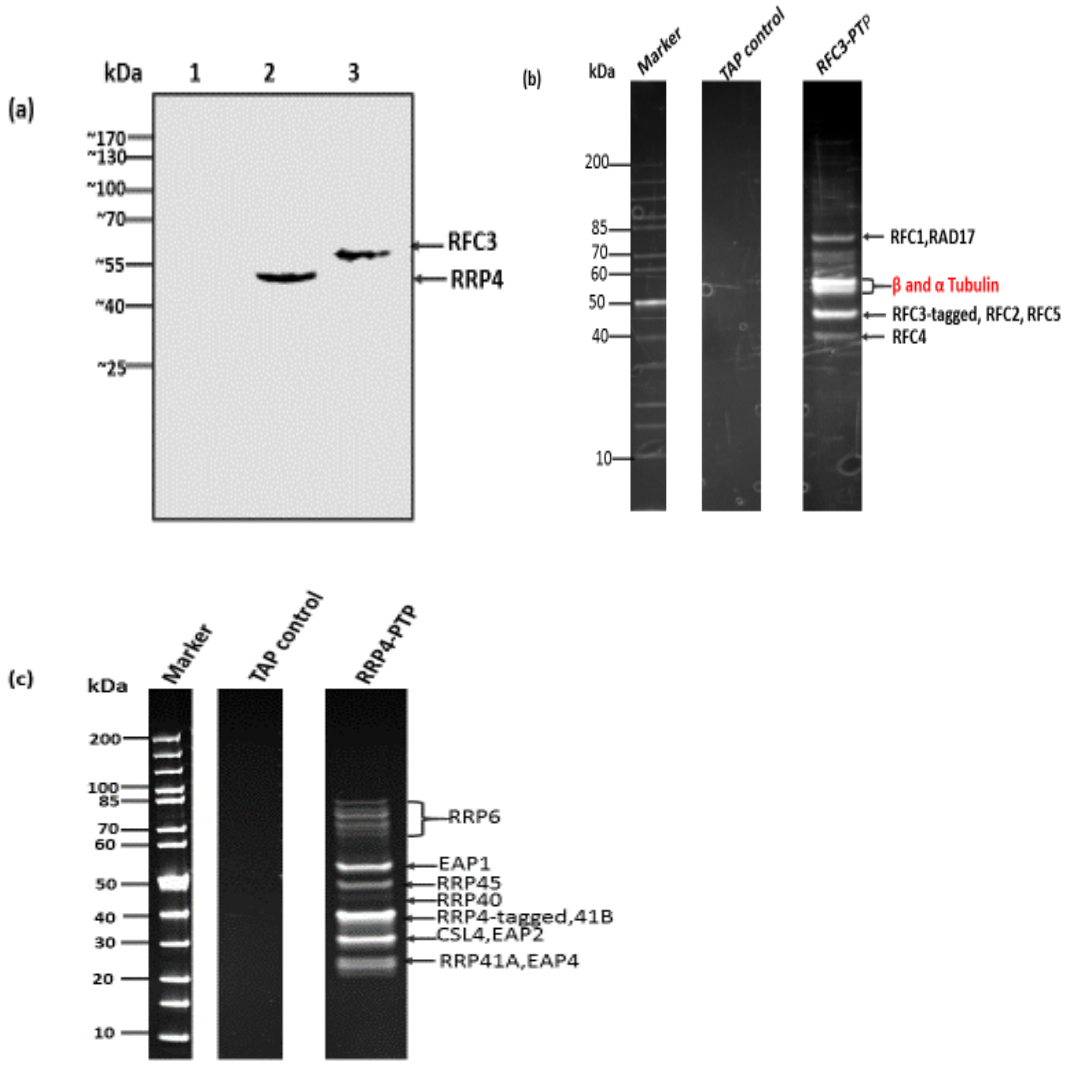

Figure 12. Western blot analysis of *C. fasciculata* expressing the tagged proteins and Sypro Ruby stained SDS-PAGE gels of TAP purified proteins. **(a)** 1 x 10^7 cells/ml were analysed with the PAP reagent directed against the Prot A domains of PTP. Lane 1, *C. fasciculata* WT; Lane 2, *C. fasciculata* expressing pNUS-RRP4-PTP and Lane 3, *C. fasciculata* expressing pNUS-RFC3-PTPcH. Purified components of *C. fasciculata* Replication factor C **(a)** and exosome **(b)** multiprotein complexes, separated by SDS-PAGE and Sypro Ruby stained. The probable identities of subunits as determined by mass spectrometry are indicated. The *C. fasciculata* cell line expressing the empty pNUS-PTPcH was used as our purification specificity control (TAP-control).

Table 4a. Mass spectrometric identification of subunits in pNUS-RFC3-PTPcH pull-down			
Protein	**Gene ID**	**Mascot score**	**Coverage**
RFC1	CFAC1_210019200	586	21%
RFC2	CFAC1_260050500	1144	59%
RFC3	CFAC1_300082900	1507	77%
RFC4	CFAC1_230046600	941	70%
RFC5	CFAC1_280077100	997	52%
Rad17	CFAC1_260035800	174	6%

Table 4b. Mass spectrometric identification of subunits in pNUS-RRP4-PTPcH pull-down			
Protein	**Gene ID**	**Mascot score**	**Coverage**
RRP41A	CFAC1_280032800	988	83%
RRP41B	CFAC1_160013900	326	34%
RRP6	CFAC1_290060300	1943	62%
EAP1	CFAC1_170027500	950	34%
RRP45	CFAC1_240024400	829	31%
RRP40	CFAC1_030007200	1173	70%
RRP4	CFAC1_110005300	1330	48%
CSL4	CFAC1_150031200	573	40%
EAP2	CFAC1_300052700	585	33%
EAP4	CFAC1_280054900	691	40%

Five major polypeptide bands were identified in the pNUS-RFC3-PTP pull downs. Mass spectrometry identification of these polypeptides revealed RFC complex subunits 1-5 (**Fig. 12b**), which were confirmed by comparing their electrophoretic nobilities with the theoretical masses. Details of mass spectroscopy analysis of the identified subunits and associated protein sequences are shown in the **Table 4a** and the associated protein sequences are shown in **Appendix 8a.** Two additional proteins Rad17 and tubulin were also detected. Tubulin is most abundant protein in cells and is not part of the RFC complex. We therefore conclude

that this was most likely a contaminant. RFC1 subunits have been shown to be replaced by Rad17 in fission yeast, which forms a pentameric alternative RFC complex derivative Rad17-RFC (Al-Khodairy et al., 1994 and Griffiths et al., 1995), which plays a role in the DNA-damage replication checkpoint response, specifically by loading the 9-1-1 complex onto the DNA. The co-purification of Rad17 in these experiments may suggest that such alternative complexes exist in kinetoplastids as previously (MacNeill, 2014).

To analyse whether we could express and isolate exosome complex subunits in *C. fasciculata* using the constructed pNUS-PTPcH plasmid, we fused the PTP sequence to the C-terminus of RRP4, which is known to be present in the 11S exosome complex and previously CBP-TAP purified in *T.brucei* parasites. However, unlike the conventional TAP-RRP4 purification in which only four exosome components in *T.brucei* were purified (Estevez et al., 2001), we purified all exosome components in *C. fasciculata* by PTP tagging. Ten subunits were detected after MASCOT peptides mass analysis, which were unambiguously identified as RRP6, EAP1, RRP45, RRP40, RRP4 (Tagged), RRP41B, CSL4, EAP2, RRP41A and EAP4 (**Fig. 12c**). Details of mass spectroscopy analysis of the identified subunits and associated protein sequences are shown in the **Table 4b** and the associated protein sequences are shown in **Appendix 8b.** The observed different sizes of bands corresponding to RRP6 could be due to proteolysis or partial post-translational modification of the protein. We did not find EAP3 subunit in our experiments. Estevez and colleagues also did not TAP purified EAP3 in the cytosolic extracts of *T.brucei* (Estevez et al., 2001). Perhaps this could be due to the weak interaction of EAP3 with the core exosome complex subunits (EAP3 interacts with the core complex through RRP6) or it was degraded. However, the fact that EAP3 has been isolated in *L.tarentolae* (Cristodero et al., 2008), further optimizations on extract preparation, and using antisera to confirm this finding should be considered. For wider applicability, further experiments are needed to determine if the purified components are functional. It will be also worthwhile to find out if *T.brucei* and perhaps *Leishmania* could also be transformed with this particular construct.

Efficient and high-level heterologous expression of proteins is a crucial step in protein from native sources and is especially useful when the native protein is normally produced in limited amounts or by sources, which are impossible, expensive and/or dangerous to obtain or propagate. We are considering optimising our purification experiments with the anticipation to isolate other novel interacting subunits, which will be validated as potential drug targets in other pathogenic kinetoplastids.

To conclude, we report the application of tandem affinity purification to *C. fasciculata* for the first time, demonstrating the effectiveness of the technique by purifying both the intact exosome and replication factor C complexes. Adding tandem affinity purification to the *C. fasciculata* toolbox significantly enhances the utility of this excellent model system. The present protein expression vector can therefore be used in place of or as an adjunct to other protein expression systems for production of proteins needed for the discovery, evaluation, or production of diagnostics, vaccines, therapeutics or medical treatments of kinetoplastid pathogens.

3. Chapter 3: Developing a Resazurin-viability assay in *Crithidia fasciculata* allowing subsequent screening for Anti-Crithidial Compounds from the GSK Open Access Pathogen Boxes

3.1 Introduction

Compounded by massive global food, water shortages and climate change, kinetoplastid diseases continue to have a devastating, long-term impact on both human and animal health and the general welfare in the world, and therefore represent a major global challenge. Although there have been some successes in drug discovery against kinetoplastid diseases for example; the SCYX-7158, Fexinidazole and Diamidine series for HAT (Drugs for Neglected Diseases, 2012b); the K777 and triazoles for treating Chagas disease (Barr et al., 2005; Urbina, 2010); the 8-aminoquinoline NPC1161, bis-quinolines series, DB766, rhodacyanine dyes and amiodarone for Leishmaniasis (Richard and Werbovetz, 2010) and the more recent GNF6702 drug candidate against all the three kinetoplastids (Khare et al., 2016), progress in discovering new and effective drugs against the three pathogenic kinetoplatids has been very slow, mostly due to reasons previously discussed (see Chapter 1). One approach in accelerating the discovery of novel leads for the treatment of pathogenic kinetoplastids has been the use of simple, robust and inexpensive cell-based systems to serve as tools for high throughput screening (HTS) of large sets of chemical libraries.

However, very few reports are available on HTS assays for the kinetoplastids. A non-human infective kinetoplastid parasite *C. fasciculata* could enhance HTS and speed up the process of searching for new drugs to treat the diseases caused by the pathogenic kinetoplastids. As previously discussed, *C. fasciculata* parasites are lower non-humans infective trypanosomatids, which can be handled in a standard laboratory without specific biosafety issues. The parasites can be easily and quickly grown to high densities in less expensive liquid media or fully defined serum-free media and therefore could shortern the long turn around time associated with the pathogenic kinetoplastids screening assays.

In this chapter, we report the development and the application of a resazurin reduction--- *C. fasciculata* cell assay for primary screening and predicting compounds with potential activities against the pathogenic kinetoplastids. In particular, we utilized the developed assay to query the Open Access Chemical boxes for compounds with inhibitory activities against *C. fasciculata* parasites, which will be followed up against the actual pathogenic kinetoplastids.

3.1.1 Open access chemical boxes

Some few decades ago, an innovative collaboration model for research and development for neglected diseases emerged in the form of public-private partnerships (PPPs), which later came to be known as product development partnerships (PDPs). A notable example of such PDPs are the Medicines for Malaria Venture (MMV) and the Glaxo Smith Kline (GSK) Tres Cantos which were formed with the aim of catalysing the discovery, development and the delivery of new medicines against tropical diseases.

Almost seven million compounds have been tested in phenotypic assays against malaria over the last decade, which has resulted in a solid pipeline of new preclinical and clinical candidates (Preston et al., 2016). Moreover, an open science initiative has made many of these structures available online and a collection of 400 key malaria phenotypic 'hits', called the 'Malaria Box', was launched in 2013. Building on this model, in December 2015, MMV took this a stage further with an initiative to stimulate the drug discovery for neglected parasitic diseases by introducing a Pathogen box. The 'Pathogen Box' (www. Pathogen box.org), contains 400 diverse drug-like molecules, which is provided at no cost to research groups. Each of the 400 compounds in the 'Pathogen Box' has confirmed activity against one or more key pathogens that cause some of the most socioeconomically important diseases worldwide such as tuberculosis, malaria, sleeping sickness, leishmaniasis, schistosomiasis, hookworm disease, toxoplasmosis and cryptosporidiosis. All the 400 compounds were tested for cytotoxicity with compounds included in the library being at least 5-fold more selective for the pathogen than its mammalian host.

Between October 2012 and May 2014, a diverse set of 1.8 million compounds were screened by the GSK Tres Cantos against the three pathogenic kinetoplastids i.e. *L. donovani, T. cruzi and T. brucei* (Peña et al., 2016). Secondary confirmatory and orthogonal intracellular anti-parasitic assays were conducted, and the potential for non-specific cytotoxicity determined. From this high through put screening, three anti-kinetoplastid chemical boxes were assembled. The selection of representative chemical boxes for the three kinetoplastids started from the most potent, specific, and non-cytotoxic compounds in the dose–response outputs of each screen after having filtered for lead-like properties as described in Pena et al. (2016). In order to generate representative boxes with high chemical diversity and potency, compounds were clustered initially by similarity using a complete-linkage algorithm (Leach et al., 2007) and a threshold of 0.55. Secondly, they were sorted by decreasing potency (i.e. pIC_{50}). The hypothetical biological target space covered by these

diversity sets was also investigated through bioinformatics methodologies. The analysis suggested that most of the compounds are new chemical entities with potential novel mechanisms of action that have not been previously exploited against these parasites. Clusters of compound were represented by only two members in the final ranked boxes. The final boxes contained 592 compound entries; 192 were active against *L. donovani* (Leish-Box), 222 against *T. cruzi* (Chagas-Box) and 192 against *T. brucei* (HAT-Box). The three anti-kinetoplastid chemical boxes showed little overlap, pointing to specific mechanisms of growth inhibition or structural divergence across molecular targets in each parasite. Three compounds were in both the Leish-Box and Chagas-Box, nine in both the Chagas-Box and HAT-Box and one compound was present in all three chemical boxes (Peña et al., 2016).

Both the Pathogen and the GSK kineto boxes containing compounds are provided free to researchers upon request and the data of all these chemical boxes is publically available with the aim of facilitating and stimulating the drug discovery for these diseases. We therefore took advantage of these boxes to identify compounds with anticrithidial activitivies that will be followed up against the actual pathogenic kinetoplastids.

3.1.2 High throughput phenotypic screening assays

Different assays have been developed and investigated to identify new active starting points for drug development against kinetoplastid pathogens. Most of these assays are based on the selection of compound collections and evaluating them in either target-based or phenotypic (whole cell) screening (Pink et al., 2005). Most of the new drug candidates that were approved by the FDA between 1999 and 2008 were identified through phenotypic screening (37% versus 23% discovered by target-based approaches) (Lee et al., 2012). However, the target-based approaches have out numbered phenotypic screening and the success of phenotypic screening has been underrated.

Unlike target-based screens, which rely upon known therapeutic pathways, phenotypic screening has the advantage of identifying new other targets. A compound may affect two or more proteins or pathways in the organism, which would not be identified in a high-throughput target-based screen. Unfortunately, lack of membrane permeability can lead to inactivity being reported for a particular compound that initially demonstrated target activity when assessed in a phenotypic screen. This can be a double-edged sword as a target specific molecule with inactivity in a phenotypic screen would be lost. However, given the costs and

frequent failure to suitably optimize and progress molecules for drug discovery, this loss is usually considered acceptable in phenotypic screens (Sykes and Avery, 2013).

In the process of searching for new drugs against kinetoplastid diseases in which very few validated targets exist, a non-reductionist approach such as the phenotypic screening therefore holds significant advantages. Phenotypic screening is considered a cost-effective method of identifying activities of unknown compounds and provide a wider view of the antiparasitic activity that can be hitting either single or multiple targets (De Muylder et al., 2011). Reliable and reproducible phenotypic assays are of great benefits to kinetoplastids drug discovery where assay cost becomes an issue because of the low funding schemes dedicated to kinetoplastid diseases research and the lack of interest in these diseases by large pharmaceutical companies. Recent developments in various platforms for phenotypic screening especially the high throughput screening (HTS) assays has opened new doors of investigation and has allowed the evaluation of significantly larger compound collections (10,000 to several million) representative of a much broader chemical diversity such as those provided by the MMV and GSK Tres Cantos. A number of such whole cell phenotypic screening assays have used succesfully in identifying some novel antikinetoplastid candidates for example; the hydrazine CA272 and a quinolone derivative CH872 for leishmaniasis (Siqueira-Neto et al., 2010), azole antifungals---ianoconazole, bifonazole, and oxiconazole nitrate for *T. cruzi*, the five new scaffolds--phenylthiazol-4-ylethylamide, phenoxymethylbenzamide, 6-aryl-3-aminopyrazine-2-carboxamide, pyrido-isoxazol-2-ylanilide and aminoethyl benzoylarylguanidine (Sykes and Avery,2013) and the quinolones (Hiltensperger et al., 2012; Fotie et al., 2010) for *T. brucei*.

3.1.3 Resazurin-reduction cell-based HTS assay

The establishment of a simple *in vitro* cell culture systems for axenic growth of kinetoplastids has led to the exploration of a various whole cell assay formats to serve as tools for HTS, with the aim of assessing large sets of chemical libraries and prioritize those for further synthesis of analogues in hit-to-lead and lead optimisation phases of the drug discovery process (Muskavitch et al., 2008). For evaluating the cell viability following exposure to test compounds, the resazurin (Alamar Blue™) (Räz et al., 1997; Sykes and Avery, 2009) and Cell-Titer-Glo™ luminescent cell viability assay (Mackey et al., 2006) methods have emerged as those most amenable to HTS because of their high signal-to-background ratio and reproducibility. Generally, these assays are performed in "automation-friendly" microtiter plates with either a 96, 384 or 1536 well format.

The resazurin-based assay is preferred due to its simplicity, low cost, lack of radioactive materials and non-toxic and transferability to the field if necessary. It has been extensively used for screening of drug susceptibility in whole cell cultures of trypanosomes and other cell lines for so many years (Bowling et al., 2012; Sykes and Avery, 2009, Räz et al., 1997; Shimony and Jaffe, 2008; Nare et al., 2010), *Leishmania* (Fumarola et al., 2004b) human cells (Ahmed et al., 1994; O'Brien et al., 2000), fungi (Tiballi et al., 1995), bacteria (Baker and Tenover, 1996; Franzblau et al., 1998).

Resazurin is an active ingredient of alamar blue. Resazurin dye is a water-soluble, non-toxic, permeable through cell membranes and is stable in culture medium. It is highly dichromatic based on Kreft's dichromaticity index (Kreft and Kreft, 2009). The dye acts as an intermediate electron acceptor in the electron transport chain without interference of the normal transfer of electrons (Page et al., 1993). The oxidation-reduction potential of resazurin is +380 mV at pH 7.0, 25 °C. It can therefore be reduced by NADPH (E_o = 320 mV), FADH (E_o = 220 mV), FMNH (E_o = 210 mV), NADH (E_o = 320 mV), as well as the cytochromes (E_o = 290 mV to +80 mV) (Rampersad, 2012). Resazurin can be converted from its oxidized, non-fluorescent, blue colour to the reduced, highly fluorescent, pink coloured resorufin that can further be reduced to nonfluorescent uncoloured dihydroresorufin (Page et al., 1993) (**Fig. 13**). Mitochondrial reductases and other enzymes such as the diaphorases (EC 1.8.1.4, dihydrolipoamine dehydrogenase) (Matsumoto et al., 1990), NAD (P) H: quinone oxidoreductase (EC 1.6.99.2) (Belinsky and Jaiswal, 1993) and flavin reductase (EC 1.6.99.1) (Chikuba et al., 1994) located in the cytoplasm and the mitochondria may be able to reduce resazurin. Therefore, resazurin reduction may signify an impairment of cellular metabolism and is not necessarily specific to interruption of electron transport and mitochondrial dysfunction (Mood and Mommsen, 2005). This change from oxidized to reduced state allows flexibility of detection where measurements can be quantitative as colorimetric and/or fluorometric readings (the latter being more sensitive) or qualitative as a visible change in colour indicating presence or absence of viable cells. These properties of resazurin have been exploited to provide a quantitative measurement of parasite proliferation and viability to identify a variety of inhibitor compounds.

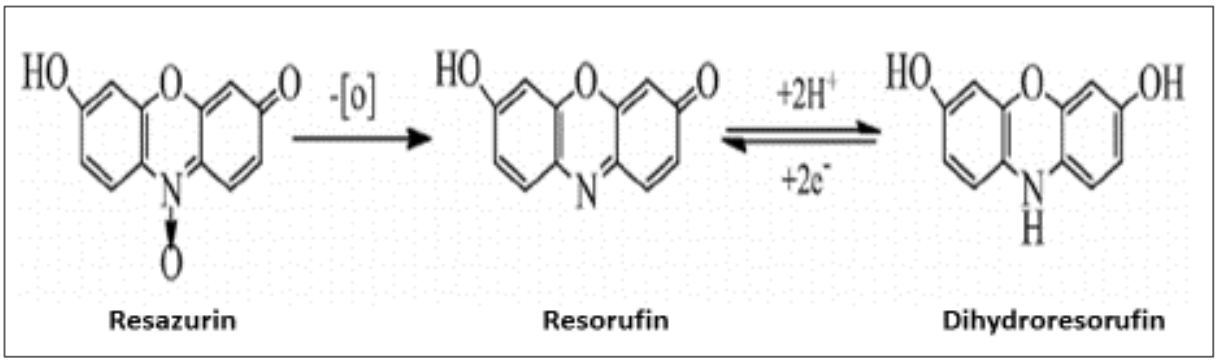

Figure 13. Schematic of Resazurin reduction reaction. Reducing environment in viable cells continuously converts the essentially non-fluorescent resazurin to a highly fluorescent resorufin, increasing the overall fluorescence and colour of the media surrounding cells. The resorufin is further reduced to uncoloured and no fluorescent dihydroresorufin.

Indeed, utilizing these robust and reliable assays with convenient organisms like *C fasciculata* and taking advantage of the available open access chemical boxes in drug discovery screening cascades could play a very crucial role in speeding up the process of searching for new drugs against kinetoplastids.

3.2 Materials and methods

3.2.1 Parasites and cell culture

The *C. fasciculata* promastigotes clone HS6 was used in all assays and parasites were grown at 27^{o}C with a gentle agitation in axenic serum-free defined culture media containing Yeast extract, Tryptone, Sucrose, Triethanolamine, Tween 80 and supplemented with haemin as described in **Appendix 2.** All chemicals and reagents used in the experiments were of highest grade and were purchased from Sigma-Aldrich. The parasites were sub-cultured every 2-3 days to ensure log growth phase for subsequent experiments.

3.2.2 Compounds libraries

Chemical boxes were kindly provided by MMV and GKS Tres cartos following a request. The Pathogen Boxes contained 400 chemicals representing compounds that were active against one or more of 12 distinct pathogens (http://www.pathogenbox.org/about-pathogen-box/supportinginformation). Individual compounds had only been tested to confirm activity against the pathogen for which the compounds were first reported to be active, and have not been tested against the other pathogens represented in the Pathogen Box. All compounds have been tested for cytotoxicity; typically, they were five-fold less potent against a human fibroblast cell line (MRC-5) than the pathogen (www. pathogenbox.org/about-pathogen-box/supporting-information).

The three GKS kineto chemical boxes (Leish-box), (Chagas-box) and HAT box) with each box containing ~200 compounds assembled by Pena and his colleagues (Pena et al., 2016) as previously discussed, were donated by GSK Tres-Cartos. These compounds included details on the pathogen against which the compound was shown activity, their cytotoxicity as well as other useful data such compound ID, batch ID, trivial name, molecular weight, salt, and cLogP. More information about these compounds can also be accessed online via ChEMBL-NTD (https://www.ebi.ac.uk/chemblntd).

Both the MMV and the GSK compounds were supplied in 96-well plates, containing 10 µL of 10 mM dimethyl sulfoxide (DMSO) solution of each compound. Each compound was then diluted with PBS to a working concentration of 2.5 mM (DMSO 25%) working and aliquoted into multiple plates. The compounds were stored at -80°C and thawed at room temperature prior to use. Each of the 400 compounds was screened in quadruplicate at a concentration of 100 µM (DMSO 0.5% final concentration) in 96-well plates.

Subsequent pure compounds were repurchased from Sigma-Aldrich for structure-activity relationships (SARs). Similary, these compounds were prepared in stock concentration of 10 mM with DMSO and screened at 100 µM (DMSO 0.5% final concentration).

The Alamar Blue solution was prepared by dissolving 12.5 mg Resazurin sodium salt (Sigma-Aldrich) in 100 ml of Phosphate Buffered Saline (PBS). The solution was then sterilized by filtration with a 0.22 µm Millipore Express PLUS membrane filter and used immediately. All fluorescence measurements in this study were performed with the Spectra Max Gemini XPS Microplate reader (Gemini XPS, Molecular devices) with excitation wavelength of 530 nm and 560 nm.

3.2.3 Resazurin-reduction *C. fasciculata* cell-based assay optimization

Although resazurin-reduction assay has been extensively used for screening drug susceptibility of various cell types, none has tempted to apply this assay in *Crithidia*. Therefore, a number of conditions such as; the growth kinetics of cells, maximum cell densities, the incubation period, the resazurin concentration and the DMSO concentrations had to be considered and optimised for the resazurin-reduction assay to work as a screening tool in this system.

3.2.3.1 The multiplicative kinetics of *C. fasciculata*

Cell densities of three replicate cultures starting at $1x10^3$, $1x10^4$ and $3x10^4$ cells/ml were microscopically monitored and counted using a haemocytometer at 24 hour intervals, over 5 days. A growth curve was plotted to estimate the doubling time and the maximum number of cells attainable in a 25-cm^2 before stationary phase and possible cell death occur.

3.2.3.2 Determining the effect of incubation period and the volume of resazurin on fluorescence development

In order to determine the fluorescent development at different volumes of the dye and the incubation period, *C. fasciculata* choanoamastigotes ($5x10^4$cells/ml) were incubated in the presence of various resazurin dye volumes (5, 10, 15 and 20 µl) and monitored after every 1 hour for a period of 4 hours. The experiment was performed twice and the results were averaged over eight replicate wells.

3.2.3.3 Determining the relationship between cell density and the Resazurin fluorescence

To determine the relationship between cell density and the fluorescence signal, the parasites in the logarithmic phase of a stock suspension of $80x10^6$cells /ml were serially diluted (100 µl) into 96-well plates followed by addition of 10 µl of resazurin. Plates were incubated at 27°C and fluorescence measured after every 1 hour for a period of 4 hours. The experiment was performed twice and the results were averaged over eight replicate wells.

3.2.3.4 Determining the effect of DMSO concentrations on the assay signal

A 90µl of medium containing *C. fasciculata* choanoamastigotes ($5x10^3$cells/ml) was inoculated into a 96-well plate and incubated for 24-hours. Ten microliters of various (0.5-9% final) concentrations of DMSO diluted in the medium were then added to the plates and further incubated for 24 hours. The experiments were performed twice and the results were averaged over eight replicate wells.

3.2.4 Compound sensitivity assays

3.2.4.1 Primary screening assays

C. fasciculata choanoamastigotes in the log phase of growth were diluted 1:20 in the growth media, and 20µl was counted using a hemocytometer. For anti-crithidial activity, compounds were added to the test plates with medium containing the parasites (density: $5x10^3$cells/ml) to achieve a final compound and DMSO concentration of 100 µM and 0.5%, respectively. The controls on each plate included wells containing growth media--0.5% DMSO without cells (Positive control) and growth media--0.5% DMSO with cells only (Negative control). The activities of test compounds were normalized against controls from the same plate according

to the following formula: Activity (%) = [1 − (F_{Cpd} − F_{Pos}) / (F_{Neg} − F_{Pos})] ×100, where F_{Cpd} corresponds to the emitted fluorescent signal expressed in arbitrary fluorescence units for the test compound; and F_{Neg} and F_{Pos} correspond to the mean fluorescent signal of the negative and the positive control wells, respectively. For estimation of the hit confirmation rate, compounds were considered "confirmed" when the normalized anti-parasitic activity was equal to or greater than 80% (≥80%) at 100 µM concentration.

3.2.4.2 Dose-response assessments of active compounds

Compounds which showed ≥80% inhibition when tested at 100 µM concentration in at least one biological replicate were re-tested in 10-point dose response, two-fold dilution experiments starting at various compound concentrations with the parasites seeding density of $5x10^3$cells/ml. Wells containing the 0.5% DMSO growth media with no cells and 0.5% DMSO growth media with cells but no drug served as 100% inhibition and 100% growth controls, respectively. Pentamidine and suramin were used as reference compounds. A 10 µl of Resazurin® was added after 44 hours incubation and fluorescence development was determined after a total drug exposure time of 48 hours. The obtained fluorescence data was analysed with the graphic data analysis software "GraFit" which calculated EC_{50} values by linear regression from the sigmoidal dose inhibition curves.

Compounds which did and did not yield an EC_{50} value within the confines of the analysis parameters were simply expressed as the "true active" and "false active" compounds, respectively. A few compounds of interests, which had comparably low EC_{50} values were cherry picked from the top ten lists, purchased from commercial sources (Sigma-Aldrich) and screened to finally confirm their activities.

EC_{50} was defined as the amount of a compound required to decrease the *C. fasciculata* viability by 50% compared to those grown in the absence of the test compound. All experiments were performed twice, with each drug concentration in quadruplet. For standardisation, of EC_{50} values were converted to pIC_{50} using a converter found at www.sanjeevslab.org/tools.html. According to the FDA, pIC_{50} is the recommended way of measuring/reporting the effectiveness of a substance in inhibiting a specific biological or biochemical function. The pIC_{50} represents the concentration of a drug that is required for 50% inhibition *in vitro*while EC_{50} mainly represents the plasma concentration required for obtaining 50% of a maximum effect *in vivo.*

3.3 Results and Discussion

3.3.1 Resazurin-reduction *C. fasciculata* cell-based assay optimization

In order to determine the maximum cell numbers that could be used for developing the screening assay, the growth kinetics of *C. fasciculata* parasites growing in our formulated serum free medium was analysed using the growth curve as shown (**Fig.14)**. The parasites grew quite robustly under axenic conditions in *vitro* and reached the stationary phase after 3 days. Similar C. *fasciculata* choanoamastigotes growth kinetics in *in vitro* culture systems have been reported elsewhere (Calderón-Arguedas et al., 2006 and Scolaro et al., 2005). An average generation time was determined according to Popp and Lattorff (2011) equations and gave an estimation of approximately 4.5 hours. The doubling time observed is shorter than the doubling time (6.8 hours) reported for *T. brucei brucei* blood foams when grown in HMI-9 supplemented with 10% fetal calf serum (Skyes and Avery, 2009) and 7 hours for *Leishmania* species (personally communicated by Menzies S, Terry Smith's laboratory).

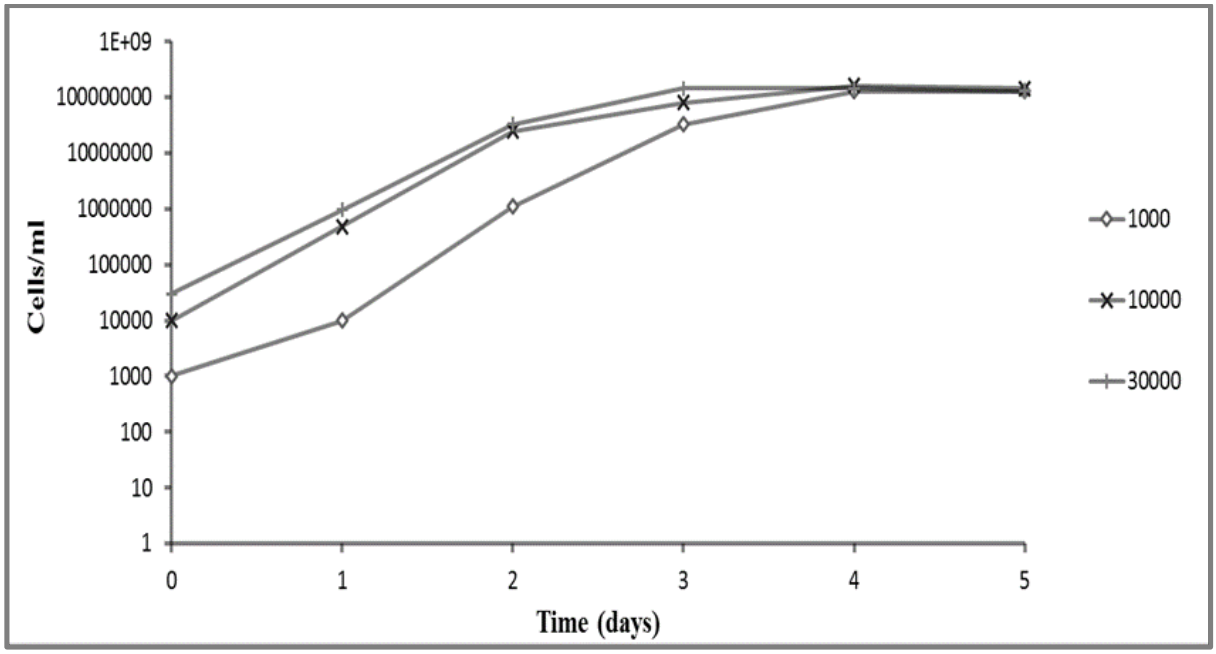

Figure 14. Growth curve of *C. fasciculata* choanoamastigotes. Cultures starting at 1000, 10000 and 30000 cells/ml were microscopically monitored and counted using a haemocytometer at 24 hours intervals for 5 days. Average counts were obtained from two biological replicates and the experiment was repeated twice.

A linear relationship was observed between the incubation time and the fluorescent development of Resazurin reduction (**Figure 15**). However, low dye concentrations gave relatively higher fluorescent signal as compared to high concentrations. Skyes and Avery (2009) and Raz et al. (1997) also observed a similar independent relationship between

resazurin concentration and the fluorescent signal in their assay development. Obviously, this is due to quick reduction of small volumes of the dye by the cells or perhaps high concentrations of resazurin salts had inhibitory effect on cell growth and metabolism. For higher cell inoculums, the fluorescent signal easily reached saturation within some few minutes when a 5% (5 µl) dye concentration was used but we were able to get strong fluorescent signal after 4 hours incubation with a 10% (10 µl) resazurin. We therefore considered using the 10% resazurin as an ideal dye concentration for all of our assays.

The fluorenscence signal correlated with cell numbers (**Fig.16**). However, for high cell densities such as $80x10^6$/ml and $40x10^6$/ml the fluorescence signal reached saturation after 1 hour and 2 hours incubation, respectively. We were able to obtain a very strong signal with $20x10^6$ cells/ml giving the best maximum fluorescence to background signal ratio of 9:1. The reported signal to background ratio (S/B) is much higher than the 3:1 obtained on *T. b. gambiense* and but lower than on *T. b. rhodesience* (15:1) in similar assays (Raz et al., 1997). These differences could be attributed to variations in the dehydrogenase activity responsible for metabolizing resazurin or reduced uptake of the dye substrate among the parasites. Differences in the fluorescence analysers, concentrations of the dye used as well as the composition of media used to culture these parasites could potentially also account for some of the variations observed.

Future studies should however, aim to accurately determine the linearity between the fluorenscence signal and the cell density. For example, carrying out the experiment at much lower parasite density than 80 $x10^6$ cells/ml or perharps using direct transfer (inoculation) of known cell densities (starting at very lower densities) from the culture to the wells according to Sykes and Every (2009) and Raz et al (1997).

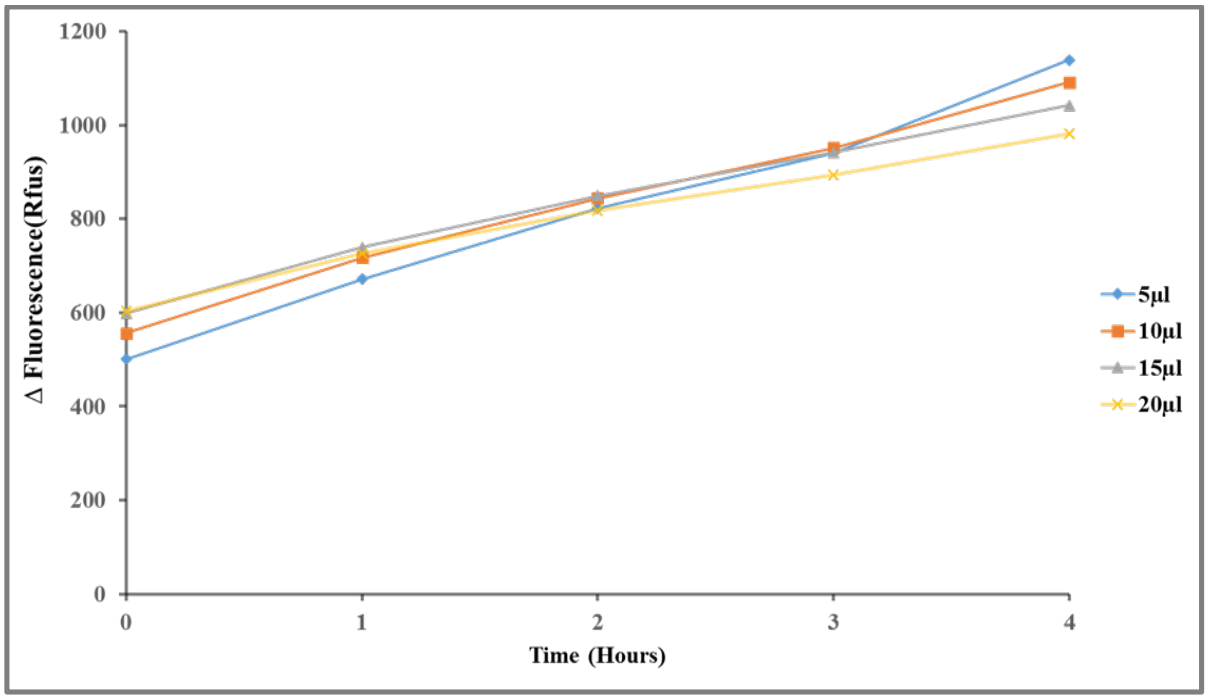

Figure 15. The effect of incubation period and the volume of resazurin on fluorescence development. The fluorescence was monitored by incubating *C. fasciculata* choanoamastigotes ($5x10^4$cells/ml) in the presence of various resazurin volumes (5, 10, 15 and 20 µl) at 1 hour interval for 4 hours period. All experiments were performed twice and average signals plotted.

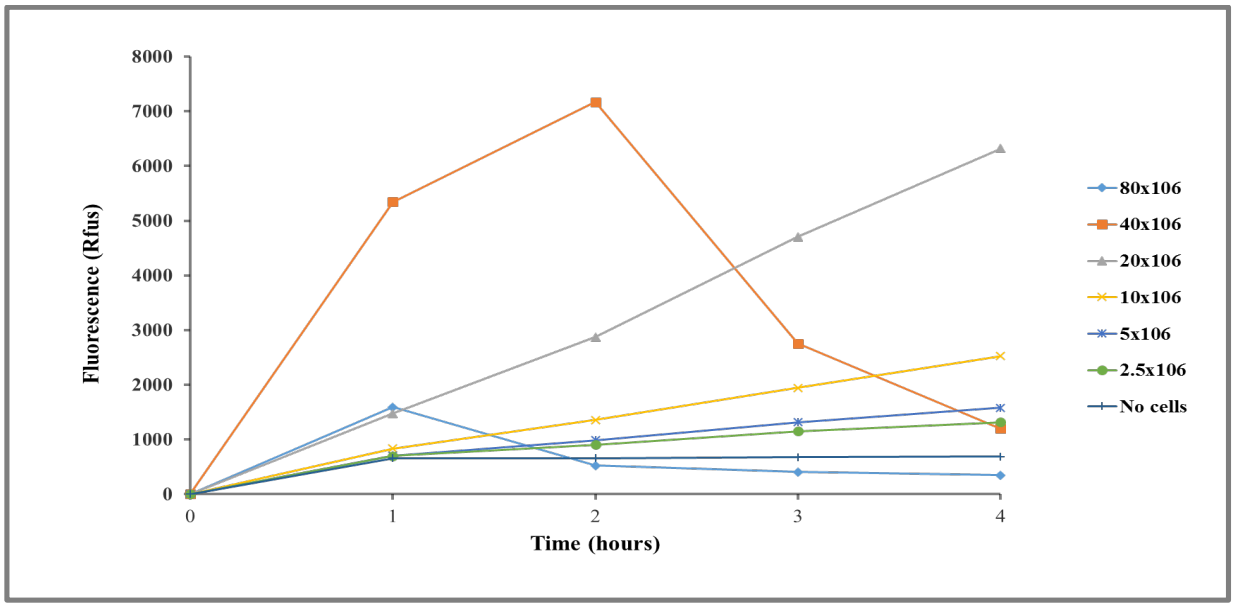

Figure 16. Relationship between the *C. fasciculata* choanoamastigotes density and resazurin fluorescent signal. Serial two-fold dilutions of parasites starting at 80 $x10^6$ cells/ml were prepared in 100 µl followed by addition of resazurin and fluorescence measurement to determine parasite viability. All experiments were performed twice and average signals plotted.

Since compounds library collections were diluted in DMSO, which is known to be toxic to various cells, we exposed the parasites to various DMSO concentrations to determine wether it had any effect on the cells viability. The *C. fasciculata* parasites were able to tolerate maximum DMSO concentrations of up to 0.5% with no significant decrease in fluorescent signal **(Fig. 17)**. This DMSO sensitivity is a bit higher than 0.42% reported for blood forms *T. b. brucei* by Skyes and Avery (2009) but comparably lower than that reported on blood stream forms of *T. brucei* and *T.brucei* congolense (Merschjohann and Steverding, 2006). Since *C. fasciculata* parasites grows almost everywhere including the harsh environments and unprotected from the UV from the sun, we expected the parasites to more resistant to DMSO than the blood stream forms trypanosomes. The fact that the blood stream forms trypanosomes also endure a harsh host immune system should also not be ruled out as a possibility of their advantage to with stand such toxic concentrations of DMSO. Nevertheless, one other possible factor that may have resulted to such different observations of DMSO sensitivities might be due to the nature of the medium used in each of the protocols. Different culture medium may have different constitutes which may positively or negatively react with the DMSO effecting the viability and consequently the doubling times of the parasites. Moreover, the use of water to dilute compounds have been observed to possess significant effects on the cell viability and EC_{50} value of the compounds possibly due to osmotic effect of water on cells and changes in buffering capacity of the medium as reported somewhere (Sykes and Avery, 2009).

After optimizing conditions such as cell concentrations, incubation times, resazurin concentration and the DMSO concentration, the assay performance and its capabilities to discriminate the activities of different compounds was determined by calculating the Z` factor, a statistical parameter for use in evaluation and validation of high throughput screening assays (Zang et al.,1999). Statistically, the assay performed well according to the Z` factor criteria (cut off=0.5, but closest to 1 as possible) by obtaining an average Z` factor of 0.7 (a maximum plating cell density of $5x10^3$cells/ml, 48 hours incubation, 10% v/v resazurin and max 0.5% DMSO). The distribution Z` factor in a total of 100 randomly selected plates (**Fig.18)** also confirmed that the assay was able to discriminate compounds with different levels of inhibition in *C. fasciculata* viability assay during the screening process.

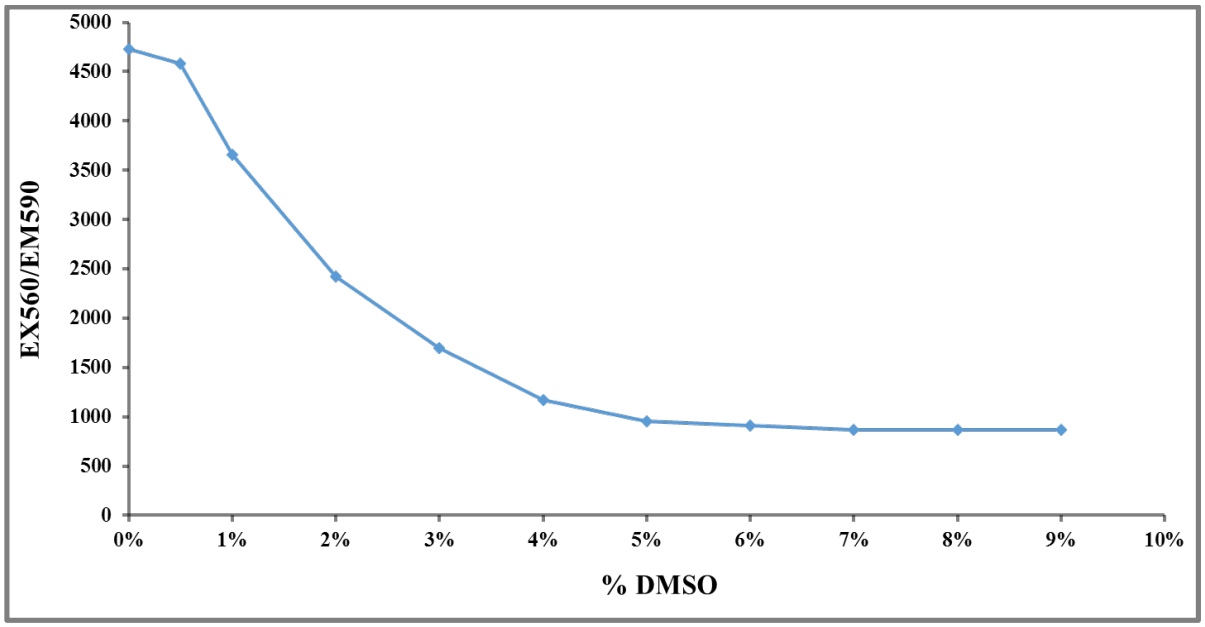

Figure 17. Dimethyl sulfoxide (DMSO) concentration and fluorescent signal. A cell density of $5x10^3$cells/ml was incubated for 48 hr in various DMSO concentrations and resazurin (10%) florescent signal measured. The experiment was performed twice with signal at each DMSO dose averaged from quadruplicate samples

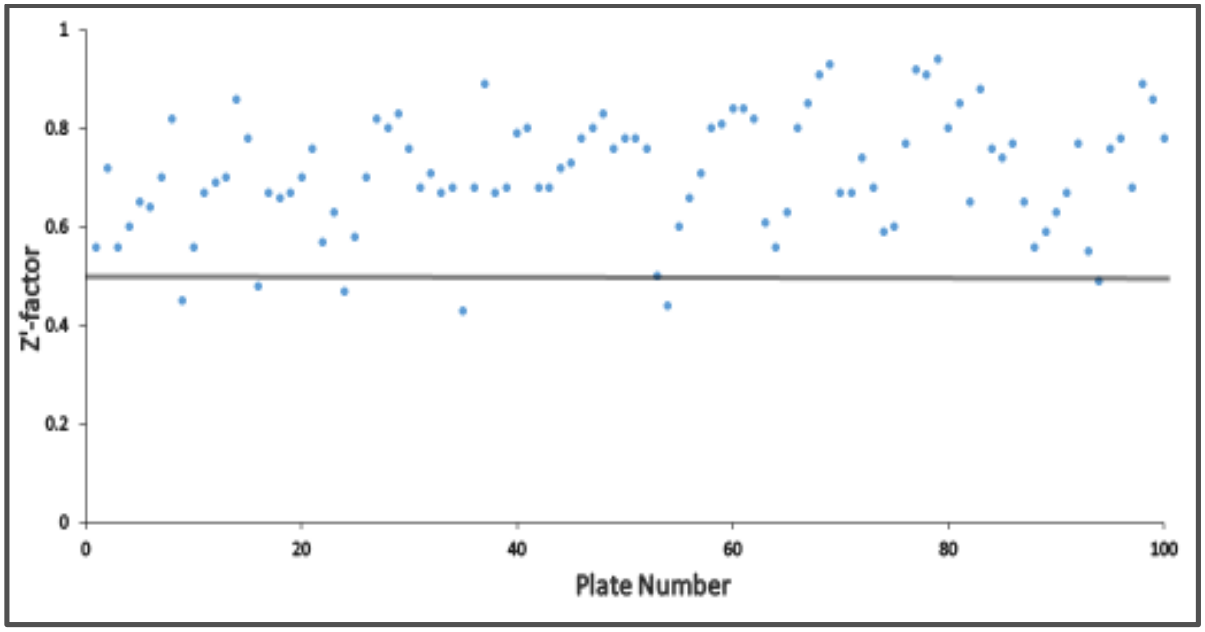

Figure 18. Distribution of Z` factors in a total of 100 plates randomly selected from the MMV (25 plates) and; GSK *T. brucei* (25 plates), *T. cruzi* (25 plates) and *Leishmania* (25 plates) boxes.

3.3.2 Screening GSK pathogen boxes for anti-crithidial compounds with a resazurin-reduction assay.

Utilizing the conditions established during optimization, the Resazurin reduction--*C. fasciculata* assay was used to screen for anti-crithidial compounds in the Open Access Chemical boxes (MMV pathogen box and GKS chemical boxes) to identify a workable number of potential compounds for follow up testing against the actual pathogenic kinetoplastids.

Using an inhibition cut-off of ≥80%, the primary screening of MMV pathogen box led to the identification of 91 (23%) compounds with inhibitory activities against *C. fasciculate* (**Fig. 19**) (**Appendix 9**). The potency of the 91 compounds was further evaluated through dose-response experiments to determine their IC_{50} values. This led into the identification of 72 (79%) true active compounds and 19 false active compounds thus representing 18% hit rate**.**

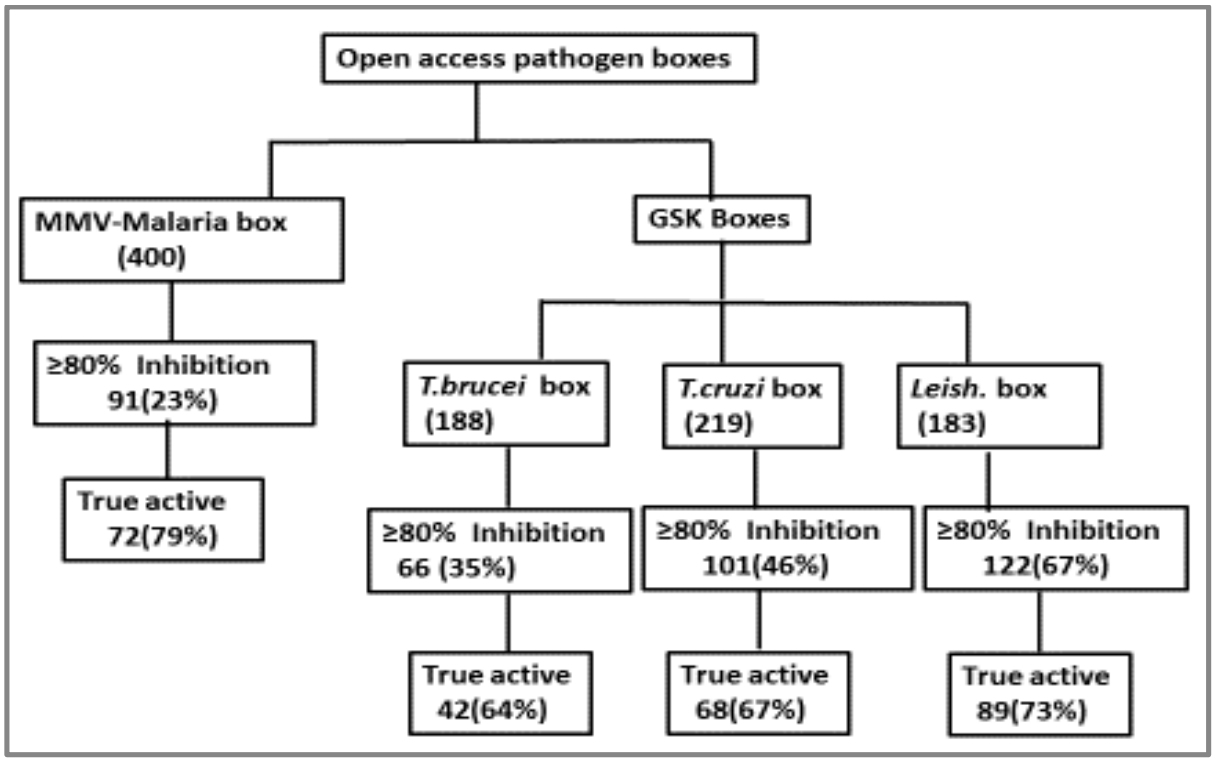

Figure 19. The workflow used to identify and progress hits of the open access pathogen boxes including key criteria considered in the decision-making process. In this case, all the compounds that had inhibition of ≥80% were progressed to dose-response experiments to determine their IC_{50} values. True active compounds are those that had a ≥80% inhibition and showed an IC_{50} in dose-response experiments.

Ten compounds (top ten) were then cherry picked from the **72** true active compounds in the MMV boxes and the profiles of these top ten hits are shown in **Table 5.**
Strikingly, three compounds (**1**, **6** and **9**) shared a pyrimidin-4-amine chemical fragment. Pyrimidin-4-amine derivatives are well-known kinase and cytochrome P450s inhibitors in various organisms (Pena et al., 2016 and Gunatilleke et al., 2012). One compound (**5**) had a quinazoline-2, 4-diamine series well referenced in the literature as inhibitors of folate synthase pathways in *Leishmania, Trypanosoma* and *Plasmodium* (Pez et al., 2003; Khabnadideh et al., 2005; Muller and Hyde, 2013).

From the GSK boxes, the primary screening of a *T. brucei* box identified a total of 66 compounds (35%) with inhibitory activities against *C. fasciculata* (**Appendix 10**), of which only 42 (64%) were true active representing a hit rate of 22%. Screening the *T. cruzi* and *Leishmania* boxes identified 101(46%) and 122(67%) compounds with inhibitory activities against *C. fasciculata* (see **Appendix 11** and **12,** respectively), of which 68 (67%) and 89(73%) were true active, respectively **(Fig. 19)**, representing the hit of 31% and 49% for *T. cruzi* and *Leishmania* box, respectively. The enriched hits rates observed among the GSK boxes suggest the commonality of the targets shared between *C. fasciculata* and the *T. brucei, T. cruzi,* and to the large extent the *leishmania* species. Since all the GSK compounds were previously shown to be active against each of the respective kinetoplastids in vitro (Pena et al., 2016), this might suggest that the hits have favourable properties to reach their active biological targets shared between *C. fasciculata* and the pathogenic kinetoplastids in these assays.

Compound ID		pIC50	cLogP	Compound name	Mwt	Structure of the compound
1	MMV021013	7.4 ± 0.004	3.55	**N-cyclohexyl-6-cyclopropyl-2-(pyridin-2-yl)pyrimidin-4-amine**	294.40	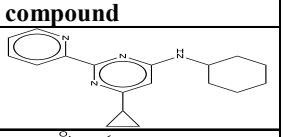
2	MMV272144	7.7 ± 0.03	-0.27	1-(3-methoxyphenyl)-5-(methylsulfonyl)-1*H*-tetrazole	254.27	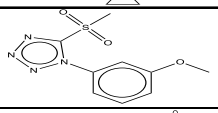
3	MMV688755	8 ± 0.001	2.81	(*S*)-2-nitro-6-((4-(trifluoromethoxy)benzyl)oxy)-6,7-dihydro-5*H*-imidazo[2,1-*b*][1,3]oxazine	359.26	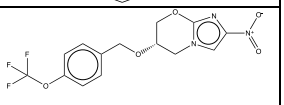
4	MMV689243	8 ± 0.003	4.26	*N*-(4-(trifluoromethyl)phenyl)-*N*-(1-(5-(trifluoromethyl)pyridin-2-yl)piperidin-4-yl)pyridin-3-amine	466.42	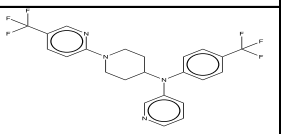
5	MMV675968	8 ± 0.005	2.31	5-chloro-6-(((2,5-dimethoxyphenyl)amino)methyl)quinazoline-2,4-diamine	359.81	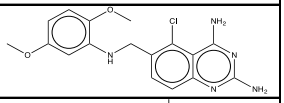
6	MMV658988	6.1± 0.01	3.93	**5-chloro-*N*,6-dimethyl-*N*-phenethyl-2-(pyridin-2-yl)pyrimidin-4-amine**	338.84	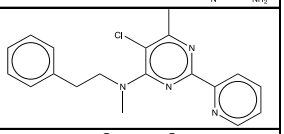
7	MMV553002	6.3 ± 0.1	-0.31	3-((methylsulfonyl)methyl)-2H-benzo[b][1,4]oxazin-2-one	239.25	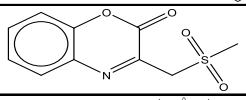
8	MMV688262	7±0.04	5.04	2-methyl-6-nitro-2-((4-(4-(4-(trifluoromethoxy)phenoxy)piperidin-1-yl)phenoxy)methyl)-2,3-dihydroimidazo[2,1-b]oxazole	534.48	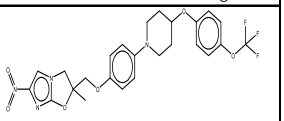
9	MMV688470	6.1±0.02	3.12	**1-(2-(1-(methylsulfonyl)piperidin-4-yl)ethyl)-3-(naphthalen-1-ylmethyl)-1H-pyrazolo[3,4-d]pyrimidin-4-amine**	464.58	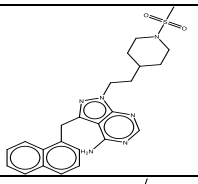
10	MMV676445	6.1±0.01	2.71	2-(((1-propyl-1H-benzo[d]imidazol-2-yl)methyl)amino)phenol	281.35	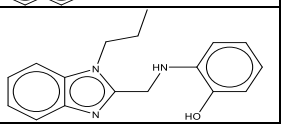

Table 5. Profiles of the top ten hits identified from screening of the MMV pathogen box. Compounds with pyrimidin-4-amine scaffold are highlighted in red.The cytotoxicity of all these compounds are at least 5-fold more selective for the pathogens than their mammalian hosts. The cLogP, cytotoxicity data and other relevant information of these compounds are found at (http://www.pathogenbox.org/about-pathogen-box/supportinginformation).

Ten compounds (top ten) were then cherry picked from the list of the true active compounds in each of the *T. brucei, T. cruzi* and *Leishmania* box and the profiles of the top ten hits are shown in **Table 6, 7 and 8,** respectively**.**

From the *T. brucei* GSK box (**Table 6**), two compounds (**4** and **8**) also had a pyridine-4-amine chemical fragment while three compounds (**1**, **5** and **10**) shared a 5-nitrofuran-2-yl fragment and the other compounds had distinct structures. The nitro-substituted aryl group derivatives are substrates of type I nitroreductases of various parasites which are metabolized into toxic nitrile products harmful to the parasites (Hall et al., 2011). Nevertheless, the 5-nitrofuran-2-yl derivatives also inhibitors of Myco-bacterium tuberculosis H37RV (Doreswamy and Chanabasayya, 2013).

The fact that there are no mammalian homologues to the 5-nitrofuran-2-yl targets place their derivatives as potential drug candidates against various pathogens. The increasing interest in treating kinetoplastids diseases with nitro drugs such as nifurtimox and benznidazole (Patterson and Wyllie, 2014), and the nitro-aromatic chemicals present in these sets calls for further studies on their substrate selectivities.

Compound ID		pIC50	Cytotoxicity	cLogP	Compound name	Mwt	Structure of the compound
1	TCMDC-143074	5.5±0.3	<4.0	3.422	**2-(4-chlorophenyl)-5-(5-nitrofuran-2-yl)-2H-tetrazole**	291.65	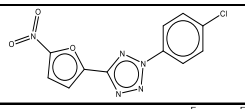
2	TCMDC-143457	5.4±0.01	<4.0	1.21	2-(3-(4-(difluoromethoxy)-3-methoxyphenyl)-1,2,4-oxadiazol-5-yl)acetonitrile	281.221	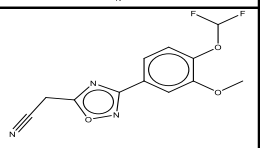
3	TCMDC-143609	5.4±0.2	4.7	1.881	4-bromo-2-nitrobenzonitrile	227.018	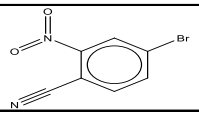
4	TCMDC-143363	5.3±0.03	4.5	2.772	**N-(5-cyclopropyl-1H-pyrazol-3-yl)-6-methyl-2-(pyrrolidin-1-yl)pyrimidin-4-amine**	284.367	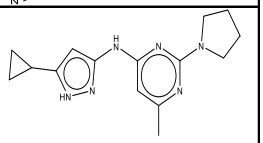
5	TCMDC-143112	5.3±0.1	4.8	2.654	**(2-(diethylamino)thiazol-5-yl)(5-nitrofuran-2-yl)methanone**	295.319	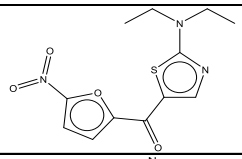
6	TCMDC-143316	5.1±0.5	4.5	3.74	5-methyl-7-(2,4,5-trichlorophenoxy)-[1,2,4]triazolo[1,5-a]pyrimidine	329.575	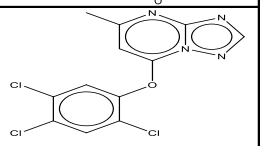
7	TCMDC-143172	5.0±1.0	<4.0	4.29	3-chloro-N-(5-chlorobenzo[d]oxazol-2-yl)benzamide	307.132	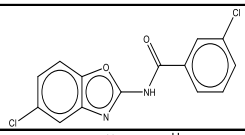
8	TCMDC-143460	5.0±0.7	<4.0	2.383	**N-(4,5-dimethyl-1H-pyrazol-3-yl)-1H-pyrrolo[2,3-b]pyridin-4-amine**	227.265	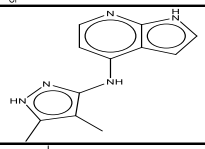
9	TCMDC-143079	5.0±0.04	<4.0	1.358	4-(benzylcarbamoyl)-1,2-phenylene bis(methylcarbamate)	357.361	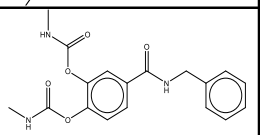
10	TCMDC-143073	5.0±0.3	<4.0	1.212	**3-(5-(5-nitrofuran-2-yl)-2H-tetrazol-2-yl)pyridine**	258.198	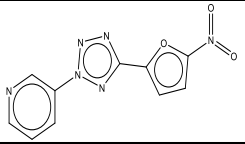

Table 6. Profile of ten top hit compounds identified in the GSK *T.brucei* box. Compounds with pyrimidin-4-amine scaffold are highlighted in red and those with 5-nitrofuran-2-yl scaffold are in blue. Data on cytotoxicity and cLogP and other information about these compounds is found on (https://www.ebi.ac.uk/chemblntd).

No compounds with common scaffolds were identified in the *T. cruzi* box (**Table 7)**. However, of particular interest, we identified one compound (**3**) with a quinolin-8-ol chemical scaffold previously reported for their antifungal properties but of which their mode of action is not yet known (Musiol et al., 2006). We also identified one compound (**8**) in the *T. cruzi* box, which shared a common 2, 2, 2-trifluoroacetate moiety with two compounds (**2** and **10**) in *Leishmania* box (**Tables 7** and **8**).

The *Leishmania* box also revealed two more compounds (**1** and **2**) with pyrimidin-4-amine based structure (**Table 8).** The increased number of active compounds sharing a pyrimidin-4-amine structural class identified in both the MMV and GSK boxes strongly suggest the need for follow up testing of their analogues against the pathogenic kinetoplastids.

Compound ID		pIC50	Cytotoxicity	cLogP	Compound name	Mwt	Structure of the compound
1	TCMDC-143149	5.9±0.05	<4.0	-0.242	5-((allyloxy)methyl)-2-nitro-5,6-dihydrooxazolo[3,2-b][1,2,4]triazole	226.189	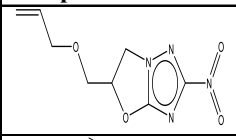
2	TCMDC-143088	5.6±0.1	<4	0.432	1-(1-methyl-3-nitro-1H-1,2,4-triazol-5-yl)piperidine	211.221	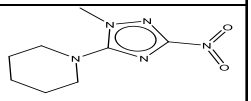
3	TCMDC-143308	5.7±0.01	4.7	2.799	**2-methyl-7-((pyridin-2-ylamino)(pyridin-3-yl)methyl)quinolin-8-ol**	342.394	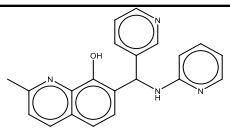
4	TCMDC-143593	5.8±0.03	<4.0	3.005	((1S,2S)-2-((bis(pyridin-3-ylmethyl)amino)methyl)cyclopropyl)(3-methoxyphenyl)methanone	387.474	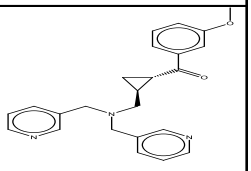
5	TCMDC-143590	5.7±0.07	4.3	3.947	1-(4-(4-bromo-2-chlorophenoxy)butyl)-1H-imidazole oxalate	419.655	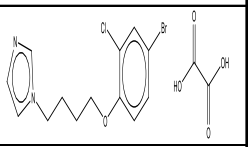
6	TCMDC-143606	5.6±0.01	4.7	2.666	6-ethyl-7-propylpyrido[2,3-d]pyrimidine-2,4-diamine	231.297	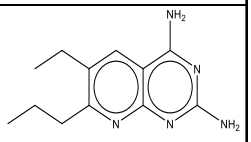
7	TCMDC-143622	6.5±0.02	4.3	4.109	2-(4-(4-((4-chlorophenyl)sulfonyl)piperazin-1-yl)phenoxy)-N,N-dimethylethan-1-amine	423.957	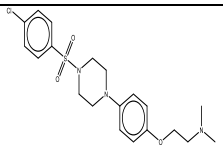
8	TCMDC-143422	6.2±0.05	<4.0	3.173	**(3aS,7aS)-2-(2-fluorophenyl)-5-(pyridin-3-yl)octahydro-1H-pyrrolo[3,4-c]pyridine 2,2,2-trifluoroacetate**	411.393	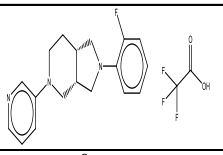
9	TCMDC-143612	6.3±0.03	4.4	1.913	N-(cyclohexylmethyl)-1,2,3-thiadiazole-5-carboxamide	225.311	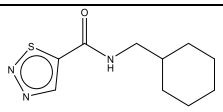
10	TCMDC-143127	5.7±0.01	<4.0	2.525	(2-chloro-4-(pyrrolidin-1-yl)phenyl)(4-methyl-1,4-diazepan-1-yl)methanone	321.845	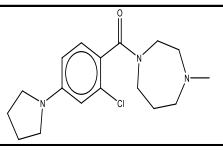

Table 7. Profile of ten top hit compounds identified in the GSK *T. cruzi* box. Compound with quinolin-8-ol and 2, 2, 2-trifluoroacetate scaffolds are highlighted in green and yellow, respectively. Data on cytotoxicity, cLogP and other information about these compounds is found on (https://www.ebi.ac.uk/chemblntd).

Compound ID		pIC50	Cytotoxicity	cLogP	Compound name	Mwt	Compound structure
1	TCMDC-143621	6.9±0.01	4.3	3.7	*N*-(3-methoxyphenyl)-6-methyl-2-(pyridin-2-yl)**pyrimidin-4-amine**	292.343	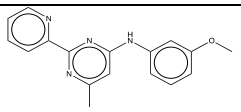
2	TCMDC-143487	6.8±0.003	4.8	3.597	6-cyclopropyl-2-(1-methyl-1*H*-imidazol-2-yl)-*N*-(2methyl benzyl)**pyrimidin-4-amine2,2,2-trifluoroacetate**	433.437	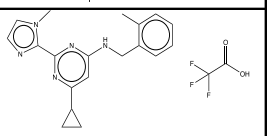
3	TCMDC-143239	6.0±0.2	<4.0	3.648	*N*-(6 ethyl benzo[*d*]thiazol-2-yl)-4 morpholinopicolinamide	368.461	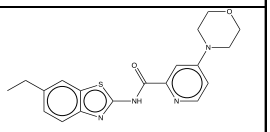
4	TCMDC-143586	6.0±0.02	4.0	3.005	((1*S*,2*S*)-2-((bis(pyridin-2-ylmethyl)amino)methyl)cyclopropyl)(3methoxyphenyl)methanone	387.474	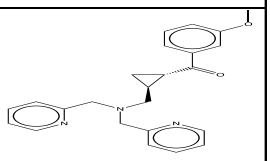
5	TCMDC-143375	5.9±0.1	<4.0	4.188	5-ethyl-*N*-(1-phenyl-1*H*-imidazol-2-yl)thiophene-3-carboxamide	297.381	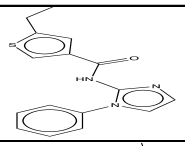
6	TCMDC-143315	5.6±0.06	<4.0	3.07	2-(((1-butyl-1H-tetrazol-5-yl)methyl)thio)-4,6-dimethylnicotinonitrile	302.404	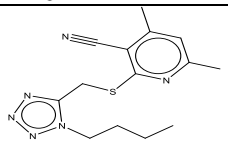
7	TCMDC-143113	5.5±0.2	4.4	3.856	N-(4-(pyridin-2-yl)thiazol-2-yl)-1,2,3,4-tetrahydronaphthalene-2-carboxamide	335.431	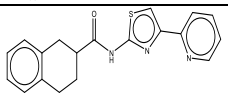
8	TCMDC-143358	5.4±0.01	<4.0	3.349	N-benzyl-2-((1-phenyl-1H-pyrazolo[3,4-b]pyridin-3-yl)oxy)acetamide	358.393	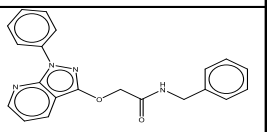
9	TCMDC-143252	5.5±0.5	<4.0	4.289	N-butyl-4-isobutyramido-N-phenylbenzamide	338.443	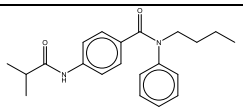
10	TCMDC-143218	5.5±0.3	5.0	1.55	4-(5-amino-3-phenyl-1H-pyrazol-1-yl)-6-(pyridin-2-yl)-1,3,5-triazin-2-amine octakis (**2,2,2-trifluoroacetate**)	1242.549	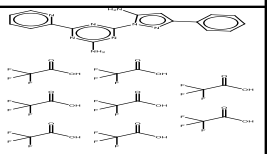

Table 8. Profile of ten top hit compounds identified in the GSK *Leish* box. Compounds with pyrimidin-4-amine and 2, 2, 2-trifluoroacetate scaffolds are highlighted in red and yellow, respectively. Data on cytotoxicity, cLogP and other information about these compounds is found on (https://www.ebi.ac.uk/chemblntd).

A total of eight chemical fragments were chosen from the top ten lists of active compounds from the respective chemical boxes and their near neighbors purchased from commercial sources. These fragments were prioritised based on: (i) existing *in vitro* or *in vivo* data regarding their potency and efficacy in other applications (ii) evaluation of their chemical structure for drug-like potential and metabolic liabilities; and (iii) the availability of near neighbors for SAR studies. The purchased near neighbors were then analysed in dose-response experiments to confirm their potency.

Unfortunately, no significant improvement in the *in vitro* activities was observed in the pure near neighbour compounds of the chosen fragments. This could be possibly due to the general physicochemical properties of these pure compounds. However, compounds **1**, **2** and **4** harbouring an uncumbered 2-pyridinyl moety were observed to be more potent compared to other near neighbors (**Table 9).**

	Name of the compound	**pIC50**	**Mwt**	**Structure**
1	4,5-dichloro-6-methyl-2-(**2-pyridyl**)pyrimidine	5.0±0.6	240.09	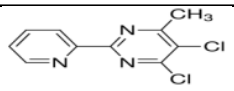
2	2-(**2-pyridinyl**)-6-(trifluoromethyl)-4-pyrimidinol	5.3±1.0	241.17	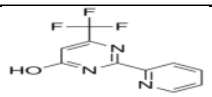
3	2-(4,6-Dimethyl-pyrimidin-2-yl)-5-methyl-2*H*-pyrazol-3-ylamine	4.0±0.2	203.24	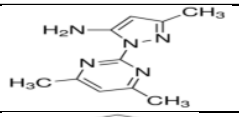
4	5-(isopropylsulfonyl)-2-(**2-pyridyl**)pyrimidin-4-amine	5.4±0.7	278.33	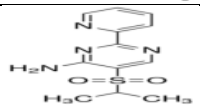
5	Ethyl 4-methyl-1,2,3-thiadiazole-5-carboxylate	4.2±0.7	172.21	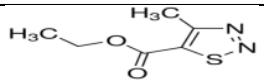
6	1,2,3-thiadiazole-4-carboxylic acid	4.1±1.0	130.12	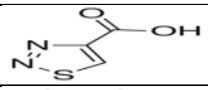
7	Cyclohexanemethyl-amine	4.4±0.4	113.20	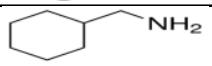
8	N-(cyclohexylmethyl)-4-oxo-4H-chromene-2-carboxamide	3.9±0.6	285.34	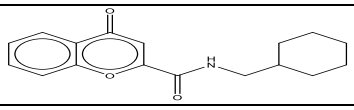

Table 9. Profiles and pIC50s of near neighbour compounds based on the more potent compounds in the top ten lists of the chemical boxes. Compound number 8 (N-(cyclohexylmethyl)-4-oxo-4H-chromene-2-carboxamide) have structural similarity to compound number 7(Cyclohexanemethyl-amine) all of them showing comparably low potency.

The potency of near neighbors harbouring a 2-pyridyl ring provided confidence in the anti-*crithidial* activities of compounds harbouring this moety. Derivatives of 2-pyridyl are well reported as CYP51 inhibitors, previously shown to enhance the anti-*Mycobacterium tuberculosis* and anti-trypanosome activity of 2-aminothiazoles (Meissner et al., 2013 and Kaiser et al., 2015). Nevertheless, two pyridinyl derivatives, (*S*)-(4-chlorophenyl)-1-(4-(4-(trifluoromethyl) phenyl)-piperazin-1-yl) -2-(pyridin-3-yl) ethanone and the *N*-[4-(trifluoromethyl)phenyl]-*N*-[1-[5-(trifluoromethyl)-2-pyridyl]-4-piperi-dyl]pyridin-3-amine have also been identified as promising drug candidates in animal models of Chagas disease(Hargrove et al., 2013).

The reasons to the failure to retain potency observed in the other near neighbors might be because of inefficient pin transfer or perharps due to other physicochemical properties of these pure solid compounds. However, as is crucial for any screening approach, our hit definition was set to identify a workable number of compounds for follow-up, and despite the relatively modest sensitivity of our assay, it enabled the identification of compounds with a high likelihood of confirmed activity when cherry-picked for follow-up testing.

In conclusion, we have developed a simple drug screening system with *C. fasciculata* that can be used to predict compounds with potential activities against the pathogenic kinetoplatids. Using the developed assay, we repurposed the open access chemical boxes for anti-crithidial compounds and we have identified attractive chemical scaffolds, which will be considered in follow up testing against the actual pathogenic kinetoplastids.

The utilization of *C. fasciculata* to predict compounds with potential activities against the pathogenic kinetoplastids could therefore provide a less expensive but easy and faster altenative approach in search of potential drug candidates against these pathogens.

4. Chapter 4: The effects of ionizing gamma radiation on the kinetoplastid *Crithidia fasciculata*

4.1 Introduction

4.1.1 Gamma ionizing irradiation and its effects on cells

Gamma irradiation is described as electromagnetic radiation of short wavelength emitted by radioactive isotopes with unstable nuclei that break up and decay to reach a more stable form. It has been widely used for sterilization of medical devices, food preservation and processing of tissue allografts and blood components avoiding the need for high temperatures that can damage such products (Hansen and Shaffer, 2001; Kainer et al., 2004; Mendonca et al., 2004; Osterholm and Norgan, 2004). For the past few decades, studies on the effects of ionizing irradiation stress have been an important issue in different areas of interest, from environmental safety and industrial monitoring to aerospace and currently in biology.

The absorption of ionizing radiation by living organisms may directly disrupt atomic structures and produce chemical and biological changes in their cells (Azzam et al., 2012). Radiation may also act indirectly through radiolysis of water, thereby generating reactive chemical species that may damage nucleic acids, proteins and lipids (Eric and Amato, 2006) (**Fig. 20**).

The combined direct and indirect effects of radiation may initiate series of biochemical and molecular signalling events that may repair the damage or progress into permanent physiological changes that may consequently lead to cell death (Sharma et al., 2012). The oxidative biochemical changes may continue to arise for days and sometimes months after the initial exposure possibly because of continuous generation of reactive oxygen (ROS) and nitrogen (RNS) species in the cells (Petkau, 1987). Surprisingly, these processes occur not only in the irradiated cells but also in their progeny (Spitz et al., 2004; Kryston et al., 2011; Sharma et al., 2012).

The radiation-induced oxidative stress may spread from targeted cells to non-targeted bystander cells through intercellular communication mechanisms (Azzam et al., 2012; Seymour and Mothersill, 2004; Prise and O'Sullivan 2009) **(Fig. 21)**. The progeny of these bystander cells also experience changes in their oxidative metabolism and may exhibit a wide range of oxidative damages such as protein carboxylation, lipid peroxidation, and enhanced rates of spontaneous gene mutations and neoplastic transformations (Buonanno et al., 2011).

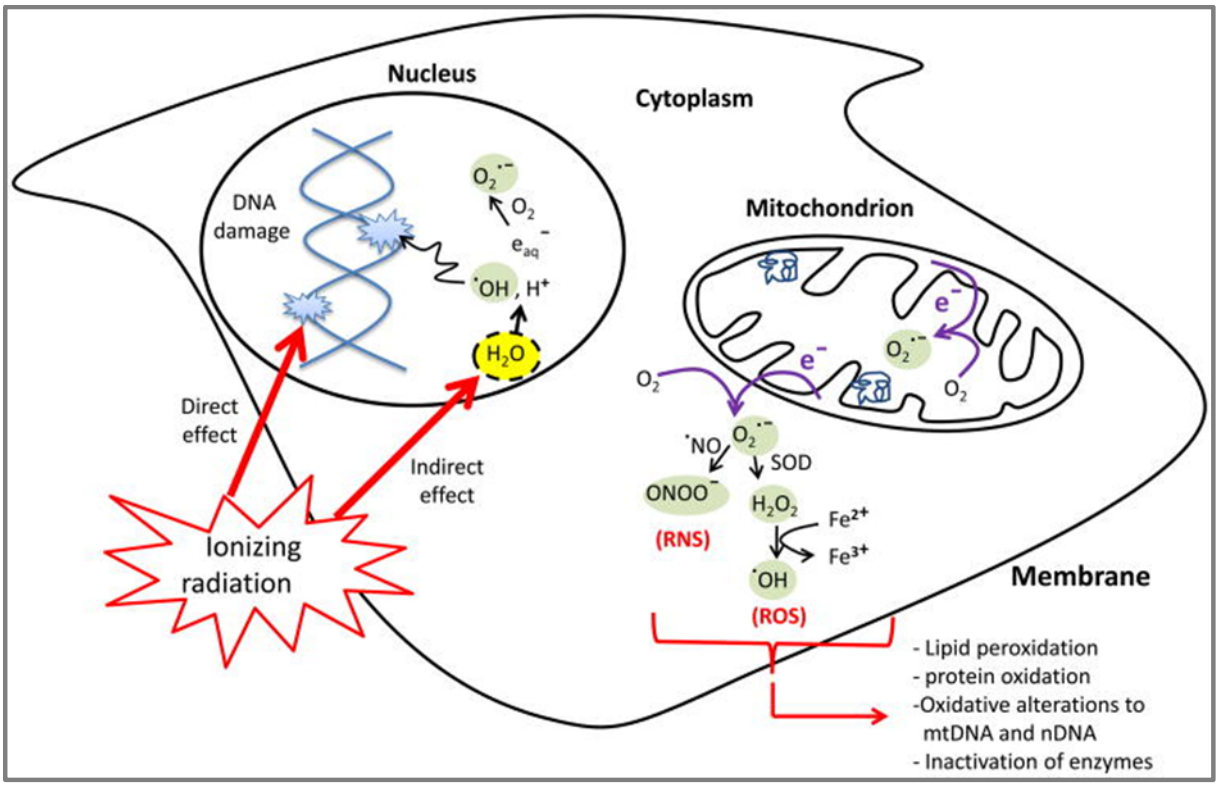

Figure 20. Direct and indirect effects of ionizing gamma radiation on a cell. Absorption of ionizing radiation directly disrupts atomic structures and producesbiochemical changes in the cells. Indirectly, the radiation may generate ROS and RNS through radiolysis of cellular water that contribute to persistent alterations in lipids, proteins, nuclear DNA (nDNA) and mitochondrial DNA (mtDNA) (Copied from Azzam et al., 2012).

In humans, the persistence of such stressful effects in progeny cells has profound implications for long-term health risks such as emergence of a second malignancy after radiotherapy treatments (Cucinotta and Chappell, 2010). Increasing evidence also supports the role of chronic oxidative stress in the progression of degenerative diseases and radiation-induced late tissue injury (Azzam et al., 2012 and Sharma et al., 2012).

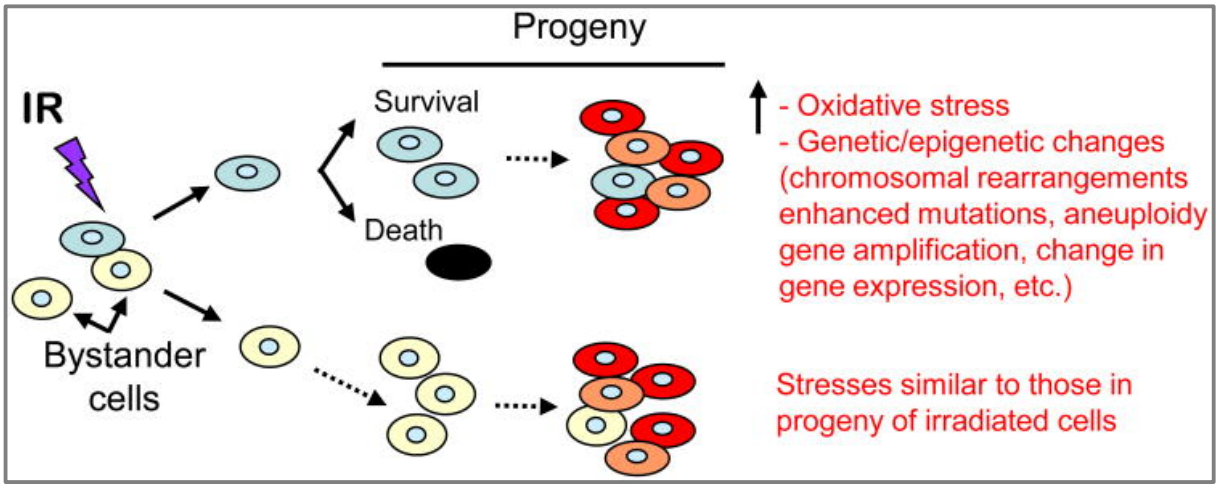

Figure 21. Ionizing radiation (IR) induces targeted and non-targeted (bystander) effects. Communication of stress-inducing molecules from cells exposed to IR propagates stressful effects, including oxidative stress, to the bystander cells and their progeny. The induced effects may be similar in nature to those observed in progeny of irradiated cells.(Copied from Azzam et al., 2012).

Although there are many common mechanisms of response of organism and cells to irradiation and other stresses they encounter, the main difference is the extent of DNA damage (Ravanat et al., 2001). However, these differences are mostly attributed to high dose rates. In cases of low dose radiation, direct effects of irradiation such as clustered DNA damage and DNA double strand breaks are minimal while the indirect DNA damages caused by the induction of ROS and RNS becomes major problem (Ravanat et al., 2001). For high doses, adverse effects accumulate in the cells in a deterministic manner that depends directly on the amount of the dose. However, for low doses the effects are stochastic, non-linear on the amount of the dose, and depend mainly on the efficiency of the stress response's protective mechanisms (Moskalev et al., 2011).

4.1.2 Effects of gamma irradiation stress on Kinetoplastids

Similar to other organisms, the oxidative stress induced by gamma ionizing irradiation has profound effects on kinetoplastids. Single and double-strand breaks and base damage may occur in the kDNA after subjected to a large amount of gamma radiation-induced oxidative stress (Takeda et al., 1986 and Regis-da-Silva et al., 2006). Since kDNA replication always takes place earlier than mitosis, cell reproduction and proliferation is hindered once the DNA is damaged, suggesting that a viable kDNA is needed for cell division (Achim et al., 2002). Nevertheless, the oxidative stress induced by the ionising gamma radiation is observed to alter kinetoplastid gene expression in the first 96 hours after gamma radiation, when DNA repair has already been completed (Grynberg et al., 2012). Among the genes that are highly expressed, categories of members of the retrotransposon hot spot gene family and kDNA are the most up-regulated genes (Grynberg et al., 2012). However, functional gene categories related to basal metabolism, translation and protein degradation processes tend to be repressed during this time. Other researchers have reported the increased expression of Rad51 mRNA in *T. cruzi* after irradiation and have associated it with the resistance to ionising radiation observed in these organisms (Regis-da-Silva et al., 2006).

Apart from the inhibition of proliferation and decrease in the infectivity, gamma irradiation was also been observed to cause fragmentation of chromosomes in *L. major* and consequently produce changes in the karyotypes of these organisms (Seo et al., 1993). The inhibition of proliferation and decrease in the infectivity might be because of destruction of the parasite's chromosomes. Certain doses of gamma irradiation are able to destroy the infectivity of the parasites but not their viability. Mice and chicken-embryos repeatedly inoculated with the irradiated *T. cruzi* parasites could not get infected (Brener, 1962 and Chiari et al., 1968).

Resistance to the ionizing gamma radiation varies within the pathogenic kinetoplastids as between other organisms. Irradiation doses of higher than 1000 Gy have shown to inhibit the mobility and reproductively of culture forms of *T. cruzi* (Silva et al., 1967 and Chiari et al., 1968). Blood forms of *T.brucei gambeinse* are sensitive to gamma radiation doses higher than 120Gy (Halberstaedter, 1938) while *L.major* culture forms can endure gamma radiation doses up to 500 Gy (Seo et al., 1993). It is possible that the mechanisms behind these parasites radiation resistance maybe part of the responses against the stresses the organisms face such as changes in temperature, pH and osmolarity in the insect's saliva and gut (Kollien and

Schaub, 2000). Inaddition, blood digestion by the vector may be sources of heme molecules required for the Fenton's chemical reaction that produce reactive chemical species and consequently causing oxidative stress (Kollien and Schaub, 2000).

Although *C. fasciculata* parasites have been used previously as a model organisms to study kDNA replication and repair mechanisms of the pathogenic kinetoplastids (Saxowsky et al., 2002, Shapiro and Englund, 1995), no any study has investigated the responses of these parasites to gamma irradiation and that it is still unclear to wether the parasites are Trypanosomes or Leishimania—like, in terms of their DNA replication and repair mechanisms after stress. We therefore initiated studies to investigate theresponses of *C. fasciculata* parasites to gamma radiation. We particularly investigated the effect of the irradiation on the cell growth, metabolic viability, motility and morphology as parameters of our investigation. In the long term, this will provide basis in understanding the post-irradiation DNA damage and repair mechanisms in *C. fasciculata* as a model for the corresponding systems in the pathogenic kinetoplastids.

4.2 Experimental procedures

4.2.1 Parasites strain and cell culture

The *C. fasciculata* promastigotes clone HS6 was used in this experiment and maintained in a culture media as previously described in methods section of chapter 2. The parasites were sub-cultured every 2-3 days to ensure log growth phase for subsequent experiments.

4.2.2 Irradiation of parasites

*C.fasciculata*log phase choanoamastigotes in tissue culture plastic flasks were irradiated with ionising gamma rays from a Cobalt-60 irradiator at the University of St-Andrews, School of Medicine Radiation facility. This apparatus has a dose rate of 2.51 Grays per minute (Co-60 half-life is 11.833 years).

4.2.3 Growth experiments

A total of 200ml medium was inoculated with log phase *C. fasciculata* choanoamastigotes to a final density of $2x10^6$ cells/ml. The medium containing cells was then divided into five cell flasks each containing 40 ml. The four flasks were irradiated at room temperature with varying gamma dosages (250, 500, 750 and 1000 Gy); the non-irradiated control flask (0 Gy) was left at room temperature the same length of time as the irradiated flasks. Cells were

counted using a haemocytometer immediately after irradiation and at 24 hours interval for 5 days post-irradiation to generate the growth curve.

4.2.4 Parasites Viability experiments

Two techniques – the Trypan blue exclusion and the Resazurin (Alamar blue) reduction methods were employed to determine the viability cells after exposure to the radiation. For the Trypan blue exclusion test, 100 µl of cells was suspended in an equal volume of 0.4% Trypan blue solution. A 20µl cell suspension was thenloaded into a haemocytometer and examined immediately under a microscope at low magnification. The blue stained cells were counted and compared against the total number of cells counted to determine the structural viability using the equation: % viable cells = [1 – (Number of blue cells counted ÷ Number of total cells counted)] × 100.

For the Alamar blue reduction assay, aliquots of 25% (10 ml) of the medium containing the irradiated cells, control cells (100% viability) and the cell-free medium were inoculated in the 96 well plates (200 µl/well) and incubated at 27^{o}C in a shaker incubator for 68 hours.After 68 hours, 20 µl of Alamar blue (0.125 mg/ml) was added to the wells and the plates further incubated for 4 hours. Fluorescence measurements were performed with the Spectra Max Gemini XPS Microplate reader (Gemini XPS, Molecular devices) at excitation wavelength of 530nm and 590 nm emission wavelength of 530 nm. The experiments were performed in duplicate and the results were averaged over eight replicate wells and normalised using an equation: Activity (%) = $[1 - (F_{Untreated} - F_{Treated}) / (F_{Untreated} - F_{Cell\ free})] \times 100$, where $F_{treated}$ corresponds to the emitted fluorescent signal expressed in arbitrary fluorescence units for the treated; and $F_{Untreated}$ and$F_{Cell\ free}$ correspond to the mean fluorescent signal of the untreated and the cell free wells, respectively.

4.2.5 Parasites motility estimates

A conventional wet mount technique was used to estimate a fraction of the parasites that were motile after exposed to ionising gamma radiation stress. Briefly, a 20 µl of cell suspension was pipetted onto a clean microscope slide and a coverslip gently lowered onto the sample. The slide was immediately examined using a microscope with a 20X objective. At least ten widely spaced fields were examined to provide estimates of percentage motile cells.

4.2.6 Parasites morphology

To assess the parasites morphology after irradiation, cells were stained with Giemsa solution (Sigma-Aldrich) using a standard Giemsa staining protocol and visualised on a microscope. Briefly, slides containing cells were fixed in methanol for 5 minute and stained with Giemsa solution for 30 minutes. The slides were then washed gently with deionised water and air-

dried prior to microscopy. At least 10 widely spaced fields were examined per sample and 5 images were taken for morphology evaluation.

4.3 Results and Discussion

In order to ascertain the response of *C. fasciculata* choanoamastigotes to the ionising gamma radiation, the cells were exposed to varying gamma dosages with all finishing at the same time experimental set-up. The non-irradiated control flaskwas left at room temperature the same time duration as the irradiated flasks to generate the growth curve as shown in **Fig. 22**. A clear correlation was observed between gamma raadiation doses and the decrease in the cell growth. The control non-irradiated cells reached early stationary stage of growth within 48 hours, more quickly than the irradiated cells. Remarkably, we found that a gamma dose of 1000 Gy was able to arrest the growth of *C. fasciculata* the first 24 hour of post-irradiation (**Fig. 22**). Culture forms of *T. cruzi* were observed to endure gamma radiation doses as high as 1000 Gy while their blood stream forms could only tolerate doses not more than 300 Gy (Silva et al., 1967 and Chiari et al., 1968). In contrast, bloodstream forms of *T.brucei gambiense* and cultured forms of *L.major* can only endure gamma doses of up to 120 and 500 Gy (Halberstaedter, 1938 and Seo et al., 1993), respectively. Surprisingly, a gamma ray dose of 500 Gy was able to arrest the growth of *T. cruzi* for 96 hours (Vieiraet al., 2014), longer than what have been currently observed with *C. fasciculata* parasites, which are able to resume normal growth just after 24 hours post-irradiation with as much as 1000 Gy. The *C. fasciculata* postirradiation growth kinetics might therefore be similar to the observed post-irradiation growth kinetics of a radiation resistant bacterium *D. Radiodurans,* which is also able to resume normal growth within 9-24 hours due to its robust DNA repair machinery (Liu et al., 2003). This observation may suggest that *C. fasciculata* parasites posses active post-irradiation recovery machinery compared to *T. cruzi* parasites. One might agree that since *C. fasciculata* parasites grows almost everywhere mostly in the harsh environments and unprotected from the UV from the sun, the parasites have developed rapid recovery mechanisms to cope up with the oxidative stresses in their environments. A comparative and systematic genome-wide investigation of the genes and pathways involved in these unique parasites post-stress recovery mechanisms would therefore be useful for further understanding of how other kinetoplastids respond to and recover from such similar stress.

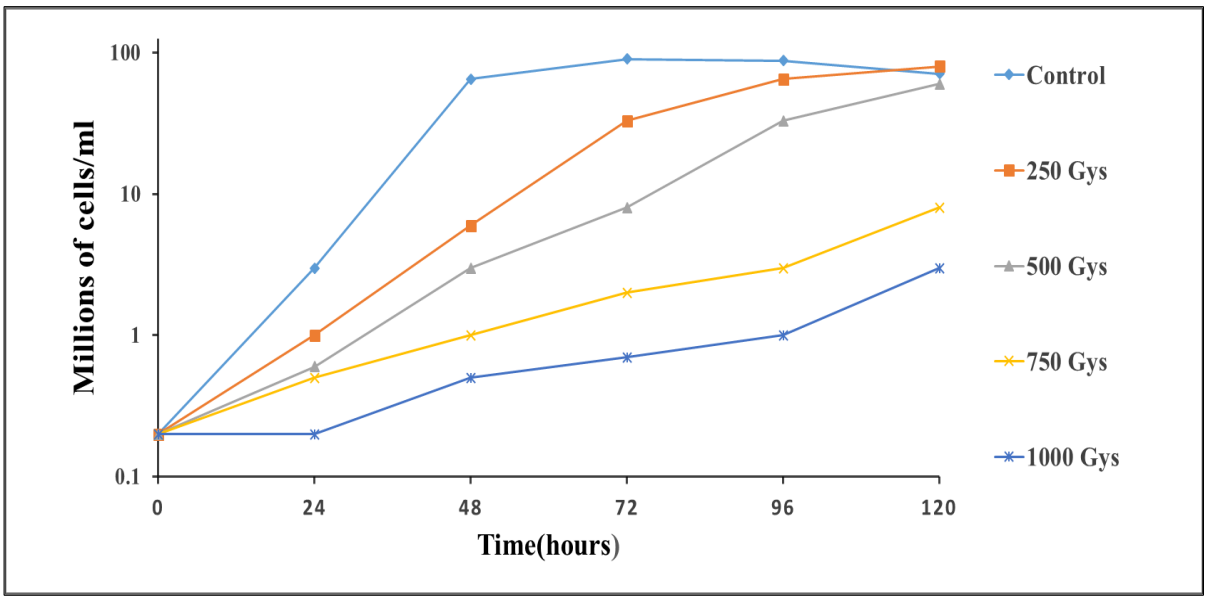

Figure 22. Growth curve of *C. fasciculata* choanoamastigotes after exposed to varying ionising gamma doses. Cultures were microscopically monitored and counted using a haemocytometer at 0 hour post-irradiation and 24 hours intervals for 5 days. Average count was obtained from two measurements per sample.

To determine the viability of the parasites at 0 hours and at 72 hours of post-irradiation, two techniques; the Trypan blue dye exclusion and the Alamar blue (Resazurin) reduction methods were employed, respectively.

The Trypan blue dye exclusion test has been widely used to determine the number of viable cells present in a cell suspension (Strober, 2001). It is based on the assumption that live cells possess intact cell membranes that exclude certain dyes such as Trypan blue whereas dead cells do not. Viable cells therefore, have a clear cytoplasm whereas a non-viable cell has a blue cytoplasm (Strober, 2001). In our experiments, no significant differences in cell viability after exposure to different radiation doses were observed at 0 hours ($p \geq 0.05$) (**Fig. 23a**). This observation is consistent with Emmet. (1950) and Chiari et al. (1968), who reported that some gamma dosages can only destroy the parasites infectivity but not their viability. This may suggest that unlike the DNA, which is a well-known primary target of irradiation damage, cell membranes are perhaps not altered with the gamma radiation induced oxidative stress. However, the decrease in the cell permeability due to the irradiation itself should not be ignored as a possible cause of this observation. Perhaps the irradiation itself rendered cells less permeable to the dye as demonstrated by Khale and his colleagues (Khare et al., 1982),

where the uptake of several amino acids was reduced in *Candida albicans* following exposure to various gamma dosages. The cell viability or rather the cell membrane integrity of post-irradiation when assessed with Trypan blue or any other dye exclusion method should therefore be interpreted with caution unless assessed in parallel with other specific parameters of membrane damage such as sulfhydryl content, potassium ion permeability, sodium ion and many more.

Alamar blue reagent has been widely used over the past 50 years in studies on cell viability and cytotoxicity in a range of biological and environmental systems (Rampersad, 2012). Live cells maintain a reducing environment within the cytosol of the cell. Resazurin, the active ingredient of alamar blue reagent, is a non-toxic, cell permeable compound that is blue in colour and virtually non-fluorescent. Upon entering cells, resazurin is reduced to resorufin, a compound that is red in colour and highly fluorescent. Live cells are able to convert resazurin to resorufin in proportional to the cell density, and thus increasing the overall fluorescence and colour of the media surrounding cells while dead cells. In our experiments, a clear correlation was observed between gamma dosages and the decrease in the cell viability after 72 hours of post-irradiation when assessed with alamar blue reduction assay **(Fig. 23b**). The dose dependent decrease in the viability of C. fasciculata parasites currently observed is consistent with other studies on the pathogenic kinetoplastids (Chiari et al., 1968and Regis-da-Silva et al., 2006).

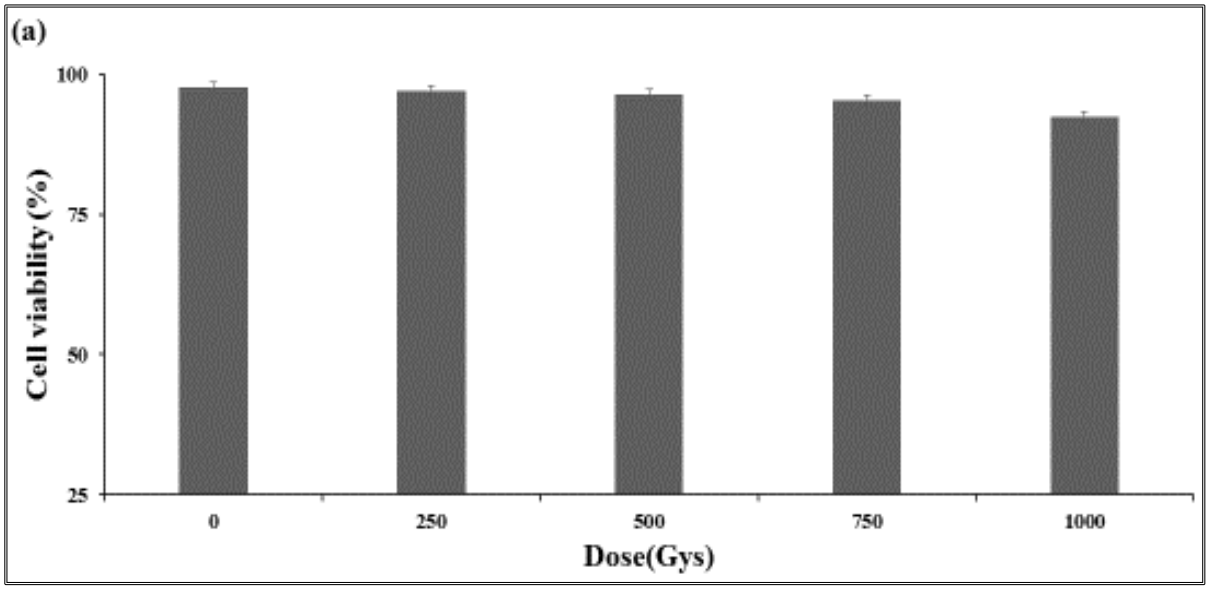

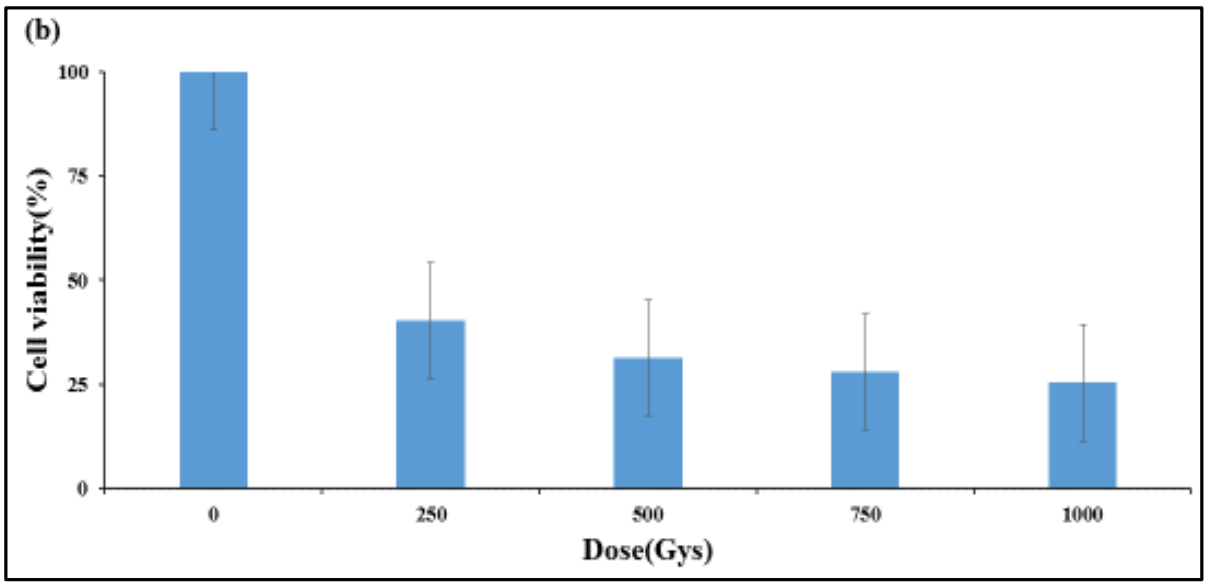

Figure 23. Viability of *C. fasciculata* choanoamastigotes post-irradiation. (**a**) Viability at 0 hours assessed with Trypan blue exclusion test. (**b**) Viability after 72 hours of irradiation assessed with Alamar blue reduction assay. Values represent the mean±SE of two experiments each performed with eight replicate wells.

The motility of the parasites was not significally affected with gamma radiation doses (up to 1000 Gys) **(Fig. 24).** Intriguingly, the parasites were very motile irrespective of their gamma irradiation doses when observed under the microscope immediately after irradiation. However, similar studies on *T. cruzi* have reported that the mobility of the parasites were rapidly affected with gamma dose of 4660 Gys; employing doses of 3500, 2450 and 1550Gys, the mobility could be observed up to 72 hours post-irradiation, after which it gradually decreased (Chiari et al., 1968). We can therefore speculate that doses less than 1550 Gys could perhaps have little or no effect on the motility of either *T. cruzi* or *C.fasciculata*.

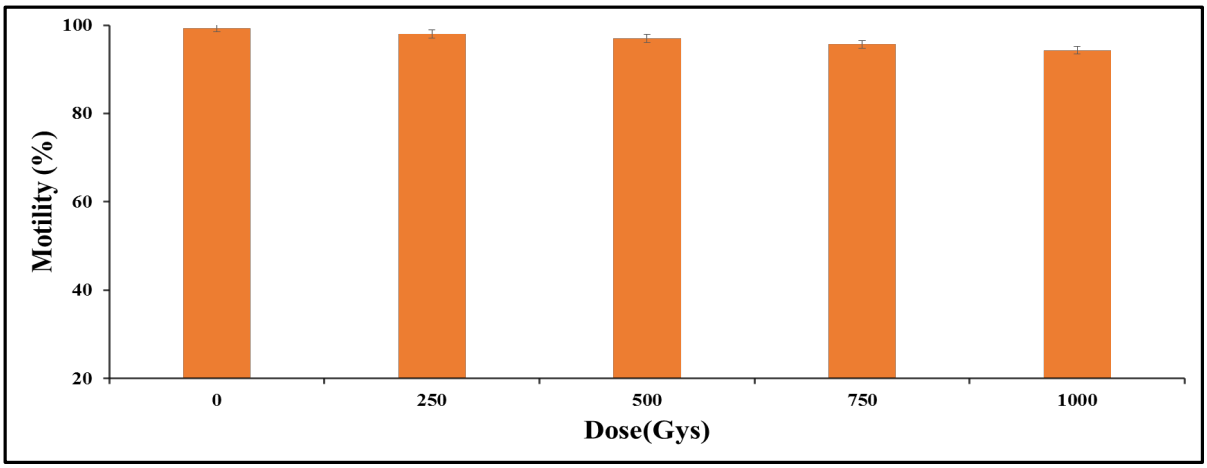

Figure 24. Motility of *C. fasciculata* choanoamastigotes at 0 hours of post-irradiation. A wet mount was prepared for each sample immediately after irradiation to determine cells motility. Motility was calculated as percentages of mobile cells out of all cells counted.Values represent the mean±SE of three counts.

We also did not observed significant morphological changes of the *C. fasciculata* parasites after exposure to gamma doses up to 1000Gy, contraly to *T. cruzi* parasites that are able to maintain their morphologies when exposed to gamma doses not exceeding 600 Gy. However, at 0 hours post-irradition, cells subjected to 250 Gy and 1000Gy were long and slender and stained less dense than the controls (**Fig. 25**). Structures such as the nucleus, kinetoplast and flagillum could be observed after 120 hrs of post-iraditon indicating a recovery. Future studies should aim to use more sensitive stains and powerful tools like electron microscopy to precisely assess morphological changes of individual ultrastructural features of the parasites after irradiation.

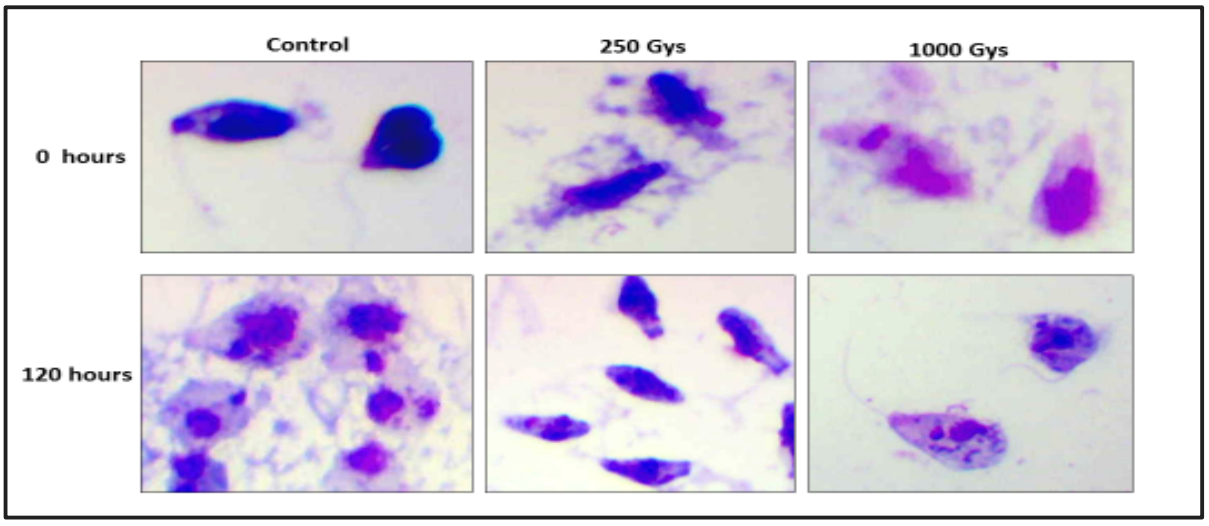

Figure 25. Morphology of *C. fasciculata* at 0 hours and 120 hours of post-irradiation. Cells were stained with 10% Giemsa solution. At least 10 widely spaced fields were examined per sample and 5 images were taken for morphology evaluation.

In general, although it was also not possible to conduct a side-by-side comparative study of the susceptibility of *C. fasciculata* and the pathogenic kinetoplastids to gamma irradition, *C. fasciculata* appears to be more like *T. cruzi* in respect to the resistant to gamma radiation and suggests that these parasites may perharps posses an enhanced postirradiation recovery mechanism as compared to the pathogenic kinetoplastids.

C. fasciculata may therefore be a suitable organism fundamental for studies aimed at understanding the rapid kDNA repair mechanisms and protein expression profiles in the kinetoplastid pathogens when exposed to harmful environments.

5. Chapter 5: General discussion and principal conclusions

5.1 General Discussion

This project aimed at exploring the utilization of *C. fasciculata* as a convenient model organism to study the biology of the pathogenic kinetoplastids and its suitability as a drug discovery vehicle.We specifically aimed to; (i) Develop and validate an expression system that can be used to purify protein complexes from *C.fasciculata*. (ii) Develop *C. fasciculata* as a non-pathogenic compound screening model for kinetoplastid diseases. (iii) Study the effects of ionizing Gamma radiation on the model kinetoplastid *C.fasciculata*.

One may argue on the significance of conducting these studies in *C. fasciculata* parasites, given that many tools are currently available to do such studies directly in trypanosomes or *leishmania* species. Nevertheless, *C. fasciculata* is a monogenic parasite of insects and therefore may not have some important biological pathways found in the digenic kinetoplastid pathogens. For example, the biological payways that help the pathogenic kinetoplastids to survive in stressful environments found in the veterbrate hosts. This may make *C.fasculata* limited in the number of pathways representing potentially druggable targets shared with the pathogenic kinetoplastids. In addition, conducting studies in *C. fasciculata* and then validating them in the actual pathogenic kinetoplastids seem to be a very long process than conducting these studies direct on the kinetoplastid pathogens. However, although this might be the case, studies on the pathogenic kinetoplastids have for been hampered by the need to culture these highly infectious organisms safely in the laboratory. The dedicated containment level 3 (cat 3) facilities are needed for this purpose but these are very expensive to build, maintain and equip as experimental apparatus cannot be moved in and out of the cat 3 lab without rigorous decontamination. The trypanosomes *T. brucei brucei*, the causative organism of liverstock trypanosomiasis and *leishmania tarentolae*, a protozoan parasite of Gecko has been widely used in studies as safer altenatives of their human pathogenic couterparts. However, unlike these models, *C. fasciculata* have a shorter generation time and can beeasily grown to high densities using comparably less expensive media in a standard laboratory, thus reducing the time required to harvest adequate numbers of parasites for some large-scale applications. Nevertheless, *Crithidia* is an excellent example of a parasite that can easily be isolated and cultured outside of its normal host organism. It is an ideal model to study the biology of not only a single kinetoplastid but rather three pathogenic kinetoplastid (*T.brucei, T. cruzi* and *leishmania* species). It is also important to

notice that the *T. brucei brucei,* which was traditionaly known to be human non-infectious organism, has been reported to cause disease in humans (Deborggraeve et al., 2008). Moreover, unlike the trypanomes models, *C. fasciculata* is easly amenable to molecular genetic and biochemical analysis and itscomplete genome has already been determined and is publically available online to facilitate these studies.

In this study, we have confirmed that *C. fasciculata* can be cultivated in high yields (to high cell densities) using our inexpensive serum-free media and can be handled in a standard laboratory without specific bio-safety precautions. By modifying an existing plasmid from Tetaud and his colleagues (Tetaud et al., 2002), we have successfully constructed plasmid pNUS-PTPcH, which can be utilised for expressing and purifying kinetoplastids protein complexes. Protein expressed from pNUS-PTPcH has the PTP tag, a variant of the TAP tag (but with CBP in TAP is replaced by the protein C peptide). The PTP tag overcomes some of the limitations of the conventional TAP method as described elsewhere (Schimanski et al. 2005; Schimanski et al., 2003; Drakes et al., 2005; Palfi et al., 2005). We have shown that *C. fasciculata* can be efficiently transfected with pNUS-PTPcH by electroporation with Amaxa program X-014 (Burcard et al., 2007), and that the encoded PTP tagged proteins can be readily detected by Western blotting. The pNUS-PTPcH plasmid was maintained as a circular extrachromosomal DNA and conferred a hygromycin resistance on *C.fasciculate* parasites. As a proof of concept, we have successfully cloned, expressed and isolated *C. fasciculata* proteins and their interacting partners though TAP. PTP purification from cell lysates expressing RFC3-PTPcH identifies its interacting proteins RFC1, RFC2, RFC4, RFC5 and RAD17, while PTP purification from cell lysates expressing RRP4-PTPcH identifies RRP6, EAP1, RRP45, RRP40, RRP41B, CSL4, EAP2, RRP41A and EAP4 that have been previously isolated in *T.brucei* exosome complex (Estevez et al., 2001).

Since RFC complex has not been characterised in any kinetoplastid organism, the identification of its associated subunits in *C. fasciculate* will provide a basis for future studies on these complexes in other kinetoplastid pathogens. In particular, the identification of Rad17-RFC as the only alternative complex in our immunoprecipitation experiments may suggest that this complex co-exist with the RFC complex in *C. fasciculata* contraly to what have been observed in other organisms such as *S.cerevisiae* (Green et al., 2000). Nevertheless, although Rad 17 and other large RLC subunits Ctf18 and Elg1 have similar sequence to

RFC1 but are considered non-essential genes (reviewed in Kim and MacNeill, 2003), the identification of Rad17 as only RLC subunit in our experiments may also suggest that perharps Rad17 have some essential roles in these specific parasites and should be properly explored as a potential target for new drugs.

Despite the conserved features and components, the exosomes of different eukaryotes are generally not identical. The genes of the six Rnase PH in human exosome complex do not reveal any orthologous in yeast or trypanosomes and there are no homologs for Rrp43p or Mtr3 in *T. brucei* (Estevez et al., 2001). Moreover, the *T. brucei* and yeast exosome complex have the RRP44 that is not present in human exosomes (Estevez et al., 2001). We also did not find *C. fasciculata* homologs of *T. brucei* RRP44 in both our database searches and immunoprecipitation experiments and never has itbeen identified in *Leishmani*a species (Cristodero et al., 2008). This may suggest that kinetoplastid organisms, RRP44 is perharps conserved in *T. brucei*. All components of the yeast and human exosome except Rrp6p are essential for viability. Contraly, depleting RRP6 in trypanosomes caused a loss of both RRP45 and RRP4, suggesting that unlike in yeast or human cells, RRP6 may have an important role in the trypanosomes (Estevez and Clayton, 2010). Depletion of the Rnase PH domain proteins RRP41 and EAP1 disassembled the *T.brucei* exosome complex but had no effect on the humun exosome complex (Estevez and Clayton, 2010). Functionally, the *T. brucei* RRP4 exosome subunit has a processive exonucleolytic activity while its yeast counterpart has a distributative mode of action (Mitchell et al., 1997). The observed uniqueness in the composition and functions of trypanosomes exosomes as compared to yeast and more importantly human's exosomes makes them ideal drug targets. In particular, utilising the RRP44 as a target protein in human trypanosome infection implies that the drug will specifically inhibit the activity of RRP44 in the trypanosomes. Using the trypanosomes exosomes subunits that have homologues in the host (humans) as drug target will result into a drug cross attacking the host essential exosome subunits causing disastrous effects. More studies are therefore, needed to characterise the molecular mechanism of RRP44 subunit to be considered as a drug target and perhaps a potential biomarker to aid in diagnosis of trypanosomes.

Although we have shown that the pNUS-PTPcH plasmid can be utilized to express and isolate kinetoplastids proteins in *C. fasciculata*, a few points need to be critically looked at for its wider utility. For example, western blots of extracts from cell lines expressing the empty pNUS-PTPcH revealed a very weak protein band for a PTP tag. However, the fact that

a protein band though still weak was observed in the immunoblots of its extract after 4 weeks make us speculate that perhaps a few copy numbers of pNUS-PTPcH plasmid are maintained in the parasites. Future work should therefore consider quantifying copies of pNUS-PTPcH maintained in the parasites. Epitope tags and stringency conditions applied in the purification process might interfere with functions of the proteins as shown in different studies elsewhere. Whether the protein subunits we purified in this study are functional or not is still unknown. It is also imperative to point out that although we have demonstrated the successful PTP purification of replication factor C and exosome complexes proteins, we did not quantify the yield of the proteins purified neither did we manage to pull down other novel proteins as initially anticipated. Future work should therefore consider monitoring the purification efficiency by quantifying the yield of the proteins at each step of the purification process. In addition, it will be important to consider optimizing purification conditions such as buffers used for preparation of cell-free extracts for efficient extraction and purification. Since we used a dounce homogenisation to lyse the cells, other cell lysis methods such as sonication should be considered in the future for comparisons. Nonetheless, while a C-terminal tag has the inherent advantage that only fully synthesized proteins carry the tag, some proteins are inactivated by a C-terminal tag. These proteins may accept a tag fusion at the N-terminal and may improve the purification efficiency (Schimanski et al., 2005). Future studies should therefore consider altenative-tagging ways to compare the efficiency of each tagging on purification.

We also did not control our purification experiments to avoid the co-purification of contaminating proteins such as the major cytoskeletal proteins α and β tubulin that bind to the resins non-specifically. Although we used the *C. fasciculata* cell line expressing the empty pNUS-PTPcH as a specificity control, the ideal control experiment was to generate a cell lines which expressed the PTP fused to an unrelated protein, which is preferentially expressed in the same cellular compartment as the protein of interest and then prepare the extract and perform TAP purifications and protein analyses in parallel. In this case, we would have excluded proteins that potentially interact with the TAP tag itself. Since we have cell lines for pNUS-DCC1-PTP construct (DCC1 is a subunit of the alternative Ctf18-Dcc1-Ctf8 replication factor C complex) and pNUS-Tfb4-PTP construct (Tfb4 is a subunit of theTFIIH complex), we plan to make further optimisations in our purification process and conduct more TAP experiments with these cell lines with an anticipation to pull down some novel

proteins which will be further characterised and validated as potential drug targets in the actual pathogenic kinetoplastids.

One promising approach for identifying new compounds for the drug development pipeline for treatment of patients with diseases caused by kinetoplastids is by HTS of compound collections. Simple *in vitro* cell culture systems for axenic growth of pathogenic kinetoplastids has led to the exploration of a various cost effective whole cell assay formats to serve as tools for HTS with the aim of assessing a large set of chemical libraries and prioritize newly synthesised analogues in hit-to-lead and ultimately lead optimisation phases of the drug discovery process (Muskavitch et al., 2008). Considering that *C. fasciculata* shares a variety of biochemical mechanisms such as polyamine synthesis and methionin salvage with the medically and veterinary important pathogenic kinetoplastids, Tanasor and collegues initiated work of utilising a non-pathigenic kinetoplastid *C. fasciculata* to screen medicinal plants that could posses cross activities against the pathogenic kinetoplastids (Tanasor et al., 2006). Extending this work, we have currently developed a simple, robust and reproducible alamar blue reduction--*C. fasciculata* based phenotypic screening assay that can facilitate the process of predicting potential anti-kinetoplastid compounds, which can be later followed up against the pathogenic kinetoplastids. We have shown that the developed assay fulfils the necessary and desirable criteria for a HTS. Although this assay has been developed in a 96-well format, it may be amenable to automated liquid handler and used in the 384-well formats. Utilising the developed assay, we have identified attractive chemical scaffolds in the Open access chemical boxes that will be considered for follow up testing in the actual pathogenic kinetoplastids. In particular, we have identified a Pyrimidin-4-amine chemical scaffold which has derivatives with well known kinase and cytochrome P450 inhibitors (Gunatilleke et al., 2012 and Pena et al., 2016), the quinazoline-2,4-diamine scaffold which are also well referenced in the literature as folate synthase pathway inhibitors in *Leishmania,Ttrypanosoma* and *Plasmodium* (Pez et al.,2003; Khabnadideh et al.,2005; Muller et al.,2013) and the 5-nitrofuran-2-yl derivatives which are substrates for type I nitroreductases of various parasites that metabolise them into nitrile toxic products (Hall et al., 2011) and are also inhibitors of *Mycobacterium tuberculosis* H37RV (Doreswamy and Chanabasayya, 2013). Nevertheless, our screening revealed the potency of compounds harbouring Quinolin-8-ol and 2-pyridinyl moieties previously reported for their antifungal properties (Musiol et al., 2006) and CYP51 inhibitors (Meissner et al., 2013 and Kaiser et al.,

2015), respectively. Weather these compounds are hitting same targets shared between*C. fasciculata* and the pathogenic kinetoplastids remains an open question. However, considering the evolutionary proximity and the number of conserved cellurar pathways between *C. fasciculata* and the pathogenic kinetoplastids, one may agree that these compounds are likely to target the same pathways and therefore compounds with anti-*Crithidial* activities should be more likely to work against the pathogenic kinetoplastids.

To our knowledge, no any fluorochrome viability assay protocol for *C. fasciculata* parasites has been reported. Therefore, it is impossible to make direct comparisons and conclusions that this assay is ideal than any other alternative viability detection methods currently available unless this assay was developed and evaluated in parallel with a similar viability detection method. However, the fact that *C. fasciculata* can be used to predict potential compounds against not only one specific pathogenic kinetoplastids is of high importance. Since the 96-well method may not be suitable for undertaking HTS of larger libraries because of intensive labour requirement and expenses, it will be of value to upgrade the Alamar blue reduction-*Crithidia* assay into a 384-well format.

Although we managed to identify such attractive chemical scaffolds, it attempts to conduct further comprehensive optimisations and analysis of the near neighbour compounds was not successful, mainly due to the cost of purchasing the related compounds and time factors. Future work should therefore consider further structural optimisation and investigation of the identified chemical scaffolds prior to testing them against *T. brucei, T. cruzi, Leishmania* and mammalian cell lines. However, additional assays such as serum shift, time to kill and reversibility of compound effect of the structurally optimised compounds should be considered to provide further criteria for advancing them through hit-to-lead phase of the project.

Responses to the ionizing gamma radiation-induced oxidative stress varies form one organism to another and within the kinetoplastids. Generally, the primary target of gamma radiation in kinetoplastids is the kDNA (Genois et al., 2014). Although the effect of gamma ionising radiation on the kDNA damage and associated repair mechanisms in pathogenic kinetoplastids have been extensively studied, little is known on how*C. fasciculata* responds to such radiations. More importantly, despite being used as model organism to study kDNA replication and repair mechanisms in the pathogenic kinetoplastids previously (Saxowsky et al., 2002; Shapiro and Englund, 1995, Ryan et al., 1988), it is still unclear to wether *C.*

*fasciculata*parasitesbehave more like *trypanosomes* or *leishmania* when it comes to theirresponses to irradiation.In this study, we have demonstrated that compared to culture forms of *T. cruzi,* which undergoes growth arrest for 96 hours after exposed to 500 Gy (Vieira et al., 2014), *C. fasciculata* is able to recover and resume normal growth within 24 hours after being subjected to gamma ray dose as high as 1000 Gy. It is important to notice that the*C. fasciculata* observed post-irradiation growth kinetics might be similar to the observed post-irradiation growth kinetics of a radiation resistant bacterium *D. radiodurans,* which has also a shorter (9-24 hours) post-irradiation cell growth arrestattributed to its robust DNA repair machinery (Liu et al., 2003). This observation may suggest that Crithidia posses very active post-irradiation recovery mechanisms as compared to other kinetoplastids.

However, the effects of gamma irradiation on *C. fasciculata* currently reported should be interpreted with caution mainly because of the weakness of our experimental design. Our main aim was to investigate the response of *C. fasciculata* to ionizing gamma radiation as compared to the other kinetoplastids. Therefore, the ideal experimental design would have to conduct the experiments in parallel with the other kinetoplastids of interests to avoid bias. Future work should therefore aim to conduct a well-designed comparative study of the susceptibility of these organisms to gamma irradiation to provide undoubted data on the responses of these organisms to irradiation. Nevertheless, for detailed assessment of morphological changes, the extent of DNA damage and the repair kinetics at the level of a single cell, future studies should consider utilising more powerful tools like electron microscopy and assays like comet assay aspreviously described in Lolenzo et al. (2013).

5.2 Principal conclusions

The overall aim of this study was to explore the utilization of *C. fasciculata* as a convenient model organism to study the cell biology of the pathogenic kinetoplastidsand its suitability as a drug discovery vehicle. This study has confirmed that *C. fasciculata* parasites can facilitate various important aspects aimed at studying the biology of different pathogenic kinetoplastids, an imperative step towards the discovery of their respective new drugs, new diagnostic approaches as well as preventive mechanisms.

The current study reports the construction of plasmid pNUS-PTPcH that can be utilised to express PTP tagged kinetoplastids proteins in *C. fasciculata* for subsequent purification. As a proof of concept, we have shown that *C. fasciculata* can be efficiently transfected with this

plasmid to facilitate the isolation of two protein complexes: replication factor C and the exosome. We have demonstrated that the expressed PTP tagged-replication factor C subunit 3 (PTP-RFC3) co-purifies with RFC1, RFC2, RFC4, RFC5 and RAD17, and that the PTP tagged exosome subunit RRP4 co-purifies with RRP6, EAP1, RRP45, RRP40, RRP41B, CSL4, EAP2, RRP41A and EAP4. RFC complex has never been characterised in any kinetoplastid organism. Therefore, the identification of its associated subunits in *C. Fasciculate* may provide basis for future studies on these complexes in other kinetoplastid pathogens. In particular, the identification of Rad17-RFC as the only alternative complex in our immunoprecipitation experiments may suggest that this complex co-exist with the RFC complex in *C. fasciculata* contraly to what have been previously observed in other organisms. As a continuation of this project, we are planning to conduct further TAP experiments on various PTP-tagged kinetoplastid proteins with an anticipation to pull down some novel proteins that will be further characterised and validated as potential drug targets in the actual pathogenic kinetoplastids.

This study also reports the development of a simple and robust resazurin-reduction cell viability-screening assay with *C. fasciculata* that can be used to predict compounds with potential activities against the pathogenic kinetoplastids. The developed assay fulfils the necessary and desirable criteria for a HTS and therefore could speed up the process of hit-to-lead and ultimately lead optimisation phases in the drug discovery cascade. Utilising the current developed assay, we repurposed the open access chemical boxes for anti-*crithidial* compounds that have revealed attractive chemical scaffolds that will be followed up against the actual pathogenic kinetoplastids. We are considering developing a *C. fasciculata* cell line resistant to some of the identified scaffolds and use the whole genome sequencing and recombineering techniques to identify specific drug targets in *C. fasciculata*. Plans are also on the way to upgrade the 96-well format Resazurin reduction-*Crithidia* based assay into a 384-well format compatible for large compound libraries.

Nevertheless, the current study has revealed that *C. fasciculata* parasites behave more like *T. cruzi* than *T.brucei* or *leishmania* in terms of their responses to irradiation. However, compared to cultured forms of *T. cruzi* that undergo growth arrest for 96 hours after exposure to 500 Gy of gamma radiation, *C. fasciculata* is able to recover and resume normal growth within 24 hours after being subjected to doses as high as 1000 Gy. These findings form basis in understanding the kDNA repair mechanisms in the kinetoplastid pathogens when exposed to such stressful conditions. Moreover, since work have already been initiated to determine

changes in gene expression during DNA repair and cell recovery mechanisms following ionizing irradiation in *T. cruzi*, it might be very interesting to extend this work to *C. fasciculata* to find out if there is any overlap in the genes up-regulated or down-regulated following exposure to gamma radiation.

In general, we have shown that *C. fasciculata* can be utilised as a covinient and ideal model organism to study the biology and speed up the drug discovery cascade of the pathogenic kinetoplastids. In particular, the constructed protein expression vector, the developed screening assay and the observed responses of *C. fasciculata* to gamma irradiation will form basis for future studies aimed to discover novel drugs, new diagnostic approaches and preventive mechanisms for kinetoplastid diseases.

6. References

1. Ahmed SA, Gogal RM and Walsh JE (1994). A new rapid and simple non-radioactive assay to monitor and determine the proliferation of lymphocytes: an alternative to [3H] thymidine incorporation assay. J. Immunol. Methods.170:211–224.
2. Al-Khodairy F, Fotou E, Sheldrick KS, Griffiths DJ, Lehmann AR and Carr AM (1994). Identification and characterization of new elements involved in checkpoint and feedback controls in fission yeast. Mol Biol. Cell. 2: 147-50
3. Ansbach AB, Noguchi C, Klansek IW, Heidlebaugh M, Nakamura TM and Noguchi E (2008) RFC^{Ctf18} and the Swi1-Swi3 complex function in separate and redundant pathways required for the stabilization of replication forks to facilitate sister chromatid cohesion in *Schizosaccharomyces pombe*. Mol Biol Cell 19: 595–607.
4. Azzam EI, de Toledo SM and Little JB (2003). Oxidative metabolism, gap junctions and the ionizing radiation induced bystander effect. Oncogene. 22:7050–7057.
5. Azzam EI, Jay-Gerin JP and Pain D (2012). Ionizing radiation-induced metabolic oxidative stress and prolonged cell injury. Cancer Lett. 327(0): 48–60.
6. Baker CT and Tenover FC (1996). Evaluation of Alamar colorimetric broth microdilution susceptibility testing method for staphylococci and enterococci. J. Clin. Microbiol.34: 2654–2659.
7. Barr SC, Warner KL, Kornreic BG, Piscitelli J, Wolfe A, Benet L and Mckerrow JH (2005). A cysteine protease inhibitor protects dogs from cardiac damage during infection by trypanosoma cruzi. Antimicrob agents chemother, 49, 5160-1.
8. Bartholomeu DC, de Paiva RM, Mendes TA, DaRocha WD, Teixeira SM (2014). Unveiling the intracellular survival gene kit of trypanosomatid parasites. PLoS Pathog, 10(12).
9. Belinsky M and Jaiswal AK (1993). NAD (P) H: quinone oxidoreductase1DT-diaphorase expression in normal and tumor tissues. Cancer Metastasis Rev. 12:103–117. Chikuba K, Yubisui T, Shirabe K and Takeshita M (1994). Cloning and nucleotide sequence of a cDNA of the human erythrocyte NADPH-flavin reductase. Biochem. Biophys. Res. Commun. 198:1170–1176.
10. Bern C, Adler-Moore J, Berenguer J, Boelaert M, den Boer M, Davidson RN, Figueras C, Gradoni L, Kafetzis DA, Ritmeijer K, Rosenthal E, Royce C, Russo R, Sundar S, Alvar J (2006). Liposomal amphotericin B for the treatment of visceral leishmaniasis. Clin. Infect. Dis. 43:917–924.
11. Biebinger S and Clayton C (1996). A plasmid shuttle vector bearing an rRNA promoter is extrachromosomally maintained in Crithidia fasciculata. Exp Parasitol. 83:252-8.
12. Bowling T, Mercer L, Don R, Jacobs R and Nare B (2012). Application of a resazurin-based high-throughput screening assay for the identification and progression of new treatments for human African trypanosomiasis.Int J Parasitol Drugs Drug Resist.2:262-70.
13. Bowman GD, O'Donnell M and Kuriyan J (2004). Structural analysis of a eukaryotic sliding DNA clamp-clamp loader complex. Nature 429: 724-730.
14. Brener Z (1962). Therapeutic activity and criterion of cure on mice experimentally infected with *Trypanosoma cruzi*. Rev Inst Med Trop Sao Paulo. 4:389-96.

15. Buonanno M, de Toledo SM and Azzam EI (2011). Increased frequency of spontaneous neoplastic transformation in progeny of bystander cells from cultures exposed to densely-ionizing radiation. PLoS One. 6(6):e21540. doi: 10.1371/journal.pone.0021540.
16. Burkard G, Fragoso CM and Roditi I (2007). Highly efficient stable transformation of bloodstream forms of *Trypanosoma brucei*. Mol Biochem Parasitol. 153 (2): 220-223.
17. Burri C and Brun R (2003). Human African trypanosomiasis. In Manson's tropical diseases. G.C. Cook and A.I. Zumla, editors. 21st edition. W.B. Saunders/Elsevier. Edinburgh, United Kingdom. 1303–1323
18. Calderón-Arguedas OCM, Avendaño A and Carvajal MJ (2006). Multiplicative kinetics of *Crithidia fasciculata* (Kinetoplastida: Trypanosomatidae) clones in an in vitro culture system. Parasitol Latinoam 61:32–36.
19. Casero RA Jr, Klayman DL, Childs GE, Scovill JP, Desjardins RE (1980). Activity of 2-acetylpyridine thiosemicarbazones against Trypanosoma rhodesiense in vitro. Antimicrob Agents Chemother.18 (2):317-22.
20. Chen CY, Gherzi R, Ong SE, Chan EL, Raijmakers R, Pruijn GJ, Stoecklin G, Moroni C, Mann M and Karin M (2001). AU binding proteins recruit the exosome to degrade ARE-containing mRNAs. Cell 107: 451–464
21. Chen S, Levin MK, Sakato M, Zhou Y and Hingorani MM (2009). Mechanism of ATP-driven PCNA clamp loading by S. cerevisiae RFC. J Mol Biol.388:431–42.
22. Chiari E, Mansur Neto E and Brener Z (1968).Some effects of gamma-radiation on *Trypanosoma cruzi,* culture and blood forms.Rev Inst Med Trop Sao Paulo. 10(3):131-7.
23. Choi JY, Podust LM and Roush WR (2014). Drug Strategies Targeting CYP51 in Neglected Tropical Diseases Chem. Rev. 114: 11242– 11271.
24. Clayton C and Estevez A (2010). The exosomes of trypanosomes and other protists. Adv Exp Med Biol. 702:39-49.
25. Coburn CM, Otteman KM, McNeely T, Turco SJ and Beverley SM (1991). Stable DNA transfection of a wide range of trypanosomatids. Mol Biochem Parasitol. 46:169-80.
26. Comini M, Menge U, Wissing J and Flohe L (2005). Trypanothione synthesis in *Crithidia* revisited. J Biol Chem 280:6850–6860
27. Cristodero M, Bottcher B, Diepholz M,Scheffzek K and Clayton C (2008).The *leishmanial tarentolae* exosome: Purification and structural analysis by electron microscopy. Molecular & Biochemical parasitol.159:24-29.
28. Cucinotta FA and Chappell LJ (2010). Non-targeted effects and the dose response for heavy ion tumor induction. Mutat Res. 687:49–53.
29. Cusick ME, Klitgord N, Vidal M and Hill DE (2005). Interactome: gateway into systems biology, Hum. Mol. Genet. 14:171–181.
30. de Castro AM, Luquetti AO, Rassi A, Chiari E and Galvao LM (2006). Detection of parasitemia profiles by blood culture after treatment of human chronic *Trypanosoma cruzi* infection. Parasitol. Res.99:379–383.
31. De Muylder G, Ang KK, Arkin MR, Engel JC and McKerrow JH (2011). A screen against Leishmania intracellular amastigotes: Comparison to a promastigote screen and identification of a host cell-specific hit. PLoS Negl Trop Dis 5: e1253.

32. Deborggraeve S, Koffi M, Jamonneau V, Bonsu FA, Queyson R, Simarro PP, Herdewijn P and Büscher P (2008). Molecular analysis of archived blood slides reveals an atypical human Trypanosoma infection. Diagn Microbiol Infect Dis. 61(4):428-33.
33. Di Noia JM, DÂOrso I, SaÂnchez DO and Frasch ACC (2000). AU-rich elements in the 3`-untranslated region of a new mucin-type gene family of *Trypanosoma cruzi* confers mRNA instability and modulates translation efficiency. Biol Chem. 275:10218-27.
34. Diamond LS (1903). Improved method for the monoxenic cultivation of Entamoeba histolytica Schaudinn. J Parasitol 54: 715–719.
35. Doreswamy and Vastrad CM (2013). Predictive Comparative QSAR Analysis Of As 5-Nitofuran-2-YL Derivatives Myco bacterium tuberculosis H37RV Inhibitors Bacterium Tuberculosis H37RV Inhibitors. *CoRR, abs/1312.2841.*
36. Doyle PS, Chen CK, Johnston JB, Hopkins SD, Leung SS, Jacobson MP, Engel JC, McKerrow JH and Podust LM (2010). A nonazole CYP51 inhibitor cures Chagas' disease in a mouse model of acute infection. Antimicrob. Agents Chemother. 54: 2480–2488.
37. Doyle PS, Zhou YM, Engel JC, and McKerrow JH (2007). A cysteine protease inhibitor cures Chagas' disease in an immunodeficient-mouse model of infection.Antimicrob Agents Chemother. 51(11):3932-9.
38. Drakas R, Prisco M and Baserga R (2005). A modified tandem affinity purification tag technique for the purification of protein complexes in mammalian cells. Proteomics. 5:132–137.
39. Drugs for neglected diseases (2012b). Pivotal study of fexinidazole for human african trypanosomiasis in stage 2 [online]. National library of medicine (us): bethesda (md).
40. Eichinger CSand Jentsch S (2011). 9-1-1: PCNA's specialized cousin.Trends Biochem Sci.36(11):563-8.
41. Emmett J (1950). Effect of X-radiation on *Trypanosome cruzi*. J.Parasit.36:45-47.
42. Eric JH and Amato JG (2006). *Radiobiology for the Radiologist,* Lippincott Williams & Wilkins, 7th edition. p. 16.
43. Erzberger JP and Berger JM (2006). Evolutionary relationships and structural mechanisms of AAA+ proteins. Annu Rev Biophys Biomol Struct. 35:93-114.
44. Estevez AM, Kempf T and Clayton C (2001). The exosome of *Trypanosoma brucei*. EMBO J 20: 3831–3839.
45. Estevez AM, Lehner B, Sanderson CM, Ruppert T and Clayton, C. (2003). The roles of intersubunit interactions in exosome stability. J. Biol. Chem. 278, 34943–34951.
46. Field MC, Horn D, Fairlamb AH, Ferguson MA, Gray DW, Read KD, De Rycker M, Torrie LS, Wyatt PG, Wyllie S and Gilbert IH(2017). Anti-trypanosomatid drug discovery: an ongoing challenge and a continuing need.Nat Rev Microbiol. 15(4):217-231.
47. Flanzblau SG, Witzig R, McLaughlin JC, Torres P, Madico G, Hernandez A, Degnan MT, Cook MB, Quenzer VK, Ferguson RM and Gilman RH (1998). Rapid, low-technology MIC determination with clinical *Mycobacterium tuberculosis* isolates by using the microplate Alamar Blue assay. J. Clin. Microbiol. 36:362–366.

48. Fotie J, Kaiser M, Delfin DA, Manley J, Reid CS, Paris JM, Wenzler T, Maes L, Mahasenan KV, Li C and Werbovetz KA (2010). Antitrypanosomal activity of 1,2-dihydroquinolin-6-ols and their ester derivatives. J. Med. Chem. 53, 966−982.
49. Fumarola L, Spinelli R and Brandonisio O (2004b). In vitro assays for evaluation of drug activity against Leishmania spp. Res Microbiol, 155, 224-230.
50. Garg N, Nunes MP and Tarleton RL (1997). Delivery by Trypanosoma cruzi of proteins into the MHC class I antigen processing and presentation pathway. J Immunol 158: 3293–3302.
51. Gavin AC, Aloy P, Grandi P, Krause R, Boesche M, Marzioch M, Rau C, Jensen LJ, Bastuck S, Dumpelfeld B, Edelmann A, Heurtier MA, Hoffman V, Hoefert C, Klein K, Hudak M, Michon AM, Schelder M, Schirle M, Remor M, Rudi T, Hooper S, Bauer A, Bouwmeester T, Casari G, Drewes G, Neubauer G, Rick JM, Kuster B, Bork P, Russell RB and Superti-Furga G (2006). Proteome survey reveals modularity of the yeast cell machinery. Nature. 440: 631–636.
52. Gavin AC, Bösche M, Krause R, Grandi P, Marzioch M, Bauer A, Schultz J, Rick JM, Michon AM, Cruciat CM, Remor M, Höfert C, Schelder M, Brajenovic M, Ruffner H, Merino A, Klein K, Hudak M, Dickson D, Rudi T, Gnau V, Bauch A, Bastuck S, Huhse B, Leutwein C, Heurtier MA, Copley RR, Edelmann A, Querfurth E, Rybin V, Drewes G, Raida M, Bouwmeester T, Bork P, Seraphin B, Kuster B, Neubauer G, and Superti-Furga G (2002). Functional organization of the yeast proteome by systematic analysis of protein complexes. Nature 415**:**141-147.
53. Gellon L, Razidlo DF, Gleeson O, Verra L and Schulz D (2011). New Functions of Ctf18-RFC in Preserving Genome Stability outside Its Role in Sister. *PLoS Genet.*, **7**.
54. Grazú V, Silber AM, Moros M, Asín L, Torres TE, Marquina C, Ibarra MR, and Goya GF (2012). Application of magnetically induced hyperthermia in the model protozoan Crithidia fasciculata as a potential therapy against parasitic infections.Int. J Nanomedicine. 7:5351-60.
55. Green CM, Erdjument-Bromage H, Tempst P, Lowndes NF (2000). A novel Rad24 checkpoint protein complex closely related to replication factor C. Curr Biol. 13; 10(1):39-42.
56. Griffiths DJ, Barbet NC, McCready S, Lehmann AR and Carr AM (1995). Fission yeast rad17: a homologue of budding yeast RAD24 that shares regions of sequence similarity with DNA polymerase accessory proteins. EMBO J. 14:5812-23.
57. Grynberg P, Passos-Silva DG, Mourão Mde M, Hirata R Jr, Macedo AM, Machado CR, Bartholomeu DC, Franco GR (2012). *Trypanosoma cruzi* Gene Expression in Response to Gamma Radiation. PLoS ONE 7(1): e2959
58. Gunatilleke SS, Calvet CM, Johnston JB, Chen CK, Erenburg G, Gut J, Engel JC, Ang KK, Mulvaney J, Chen S, Arkin MR, McKerrow JH, Podust LM (2012). Diverse inhibitor chemotypes targeting *Trypanosoma cruzi* CYP51. PLoS Negl. Trop. Dis. 6(7):e1736. doi: 10.1371/journal.pntd.0001736.
59. Hajduk S and Ochsenreiter T (2010). RNA editing in kinetoplastids. RNA Biol 7:229–236.
60. Halberstaedter L (1938). The effects of X-Rays on Trypanosomes.Brit.J.Radiol.11:267-270.

61. Hall BS, Bot C and Wilkinson SR (2011). Nifurtimox activation by trypanosomal type I nitroreductases generates cytotoxic nitrile metabolites. J. Biol. Chem. 286, 13088–13095.
62. Hansen JM and Shaffer HL (2001). Sterilization and preservation by radiation sterilization. In Disinfection, Sterilization and Preservation, Edited by SS. Block. Philadelphia, PA: Lippincott Williams and Wilkins.729–746.
63. Hargrove TY, Wawrzak Z, Alexander PW, Chaplin JH, Keenan M, Charman SA, Perez CJ, Waterman MR, Chatelain E and Lepesheva GI (2013). Complexes of *Trypanosoma cruzi* sterol 14α-demethylase (CYP51) with two pyridine based drug candidates for Chagas disease: structural basis for pathogen selectivity. J Biol Chem. 288(44):31602-15.
64. Hartshorne T and Toyofuku W (1999). Two 5`-ETS regions implicated in interactions with U3 snoRNA are required for small subunit rRNAmaturation in *Trypanosoma brucei.* Nucleic Acids Res. 27:3300-09
65. Hedglin M, Kumar R and Benkovic SJ (2013). Replication clamps and clamp loaders. Cold Spring Harb Perspect Biol doi: 10.1101/cshperspect.a010165.
66. Hiltensperger G, Jones NG, Niedermeier S, Stich A, Kaiser M, Jung J, Puhl S, Damme A, Braunschweig H, Meinel L, Engstler M and Holzgrabe U (2012). Synthesis and structure−activity relationships of new quinolone-type molecules against *Trypanosoma brucei.* J. Med. Chem. 55, 2538−2548.
67. Horn D and McCulloch R (2010). Molecular mechanisms underlying the control of antigenic variation in African trypanosomes. Curr Opin Microbiol 13: 700–705.
68. Hughes DE and Simpson L (1986). Introduction of plasmid DNA into the trypanosomatid protozoan *Crithidia fasciculata*. Proc Natl Acad Sci U S A. 83(16):6058-62.
69. Inoue H, Nojima H and Okayama H (1990). High efficiency transformation of *Escherichia coli* with plasmids. Gene 96, 23-28.
70. Kainer MA, Linden JV, Whaley DN, Holmes HT, Jarvis WR, Jernigan DB and Archibald LK (2004). Clostridium infections associated with musculoskeletal-tissue allografts. N Engl J Med 350, 2564–2571.
71. Keenan M, Abbott MJ and Alexander PW (2012). Analogues of Fenarimol Are Potent Inhibitors of *Trypanosoma cruzi* and Are Efficacious in a Murine Model of Chagas Disease. J. Med. Chem. 55, 4189–4204.
72. Kennedy PGE (2013). Clinical features, diagnosis and treatment of human African trypanosomiasis (sleeping sickness). Lancet Neurology 12, 186-194.
73. Khabnadideh S, Pez D, Musso A, Brun R, Pérez LM, González-Pacanowska D, Gilbert IH (2005). Design, Synthesis and Evaluation of 2, 4 Diaminoquinazolines as Inhibitors of Trypanosomal and Leishmanial Dihydrofolate Reductase. Bioorgan. Med. Chem. 1, 2637–2649.
74. Khare S, Nagle AS, Biggart A, Lai YH, Liang F, Davis LC, Barnes SW, Mathison CJ, Myburgh E, Gao MY, Gillespie JR, Liu X, Tan JL, Stinson M, Rivera IC, Ballard J, Yeh V, Groessl T, Federe G, Koh HX, Venable JD, Bursulaya B, Shapiro M, Mishra PK, Spraggon G, Brock A, Mottram JC, Buckner FS, Rao SP, Wen BG, Walker JR, Tuntland T, Molteni V, Glynne RJ, Supek F(2016). Proteasome inhibition for treatment of leishmaniasis, Chagas disease and sleeping sickness. Nature. 537:229–33.

75. Khare SA, Trivedi PC, Kesavan and Parasad R (1982). Effect of gamma-radiation on the structure and function of yeast membrane. Int. J. Rad. Biol., 42: 369-383.
76. Kim J and MacNeill SA (2003). Genome stability: a new member of the RFC family. Curr. Biol. 13: R873–R875.
77. Kollien AH and Schaub GA (2000). The development of *Trypanosoma cruzi* in triatominae. Parasitology today 16: 381–387.
78. Kreft S and Kreft M (2009). Quantification of dichromatism: A characteristic of colour in transparent materials. J. Opt. Soc. Am. A. 26:1576–1581.
79. Kryston TB, Georgiev AB, Pissis P and Georgakilas AG (2011). Role of oxidative stress and DNA damage in human carcinogenesis. Mutat Res. 711:193–201.
80. La Greca F and Magez S (2011). Vaccination against trypanosomiasis: can it be done or is the trypanosome truly the ultimate immune destroyer and escape artist? Hum. Vaccin. 7, 1225–1233
81. Lane RP and Crosskey RW (1993). Medical insects and arachnids. Chapman & Hall. London, United Kingdom. 723 pp.
82. LeBowitz JH, Coburn CM, McMahon-Pratt D and Beverley SM (1990). Development of a stable Leishmania expression vector and application to the study of parasite surface antigen genes. Proc Natl Acad Sci USA. 87:9736-40.
83. Lee JA, Uhlik MT, Moxham CM, Tomandl D and Sall DJ (2012). Modern phenotypic drug discovery is a viable, neoclassic pharma strategy. J. Med. Chem. 55, 4527−4538.
84. Lengronne A, McIntyre J, Katou Y, Kanoh Y, Hopfner K.P, Shirahige K and Uhlmann F (2006). Establishment of sister chromatid cohesion at the S. cerevisiae replication fork. Mol. Cell 23: 787–799.
85. Lepesheva GI, Villalta F and Waterman MR (2011). Targeting *Trypanosoma cruzi* Sterol 14α-Demethylase (CYP51). Adv. Parasitol. 75, 65–87.
86. Liu B, Liu Y, Motyka SA, Agbo EE and Englund PT (2005). Fellowship of the rings: the replication of kinetoplast DNA. Trends Parasitol 21: 363–369
87. Liu Y, Zhou J, Omelchenko MV, Beliaev AS, Venkateswaran A, Stair J, Wu L, Thompson DK, Xu D, Rogozin IB, Gaidamakova EK, Zhai M, Makarova KS, Koonin EV, Daly MJ(2003). Transcriptome dynamics of *Deinococcus radiodurans* recovering from ionizing radiation. Proc Natl Acad Sci USA. 100(7):4191–6.
88. Lorentzen E, Basquin J and Conti E (2008a). Structural organization of the RNA-degrading exosome. Curr Opin Struct Biol 18: 709–713.
89. Lukes J, Hines JC, Evans CJ, Avliyakulov NK, Prabhu VP, Chen J and Ray DS(2001). Disruption of the *Crithidia fasciculata* KAP1 gene results in structural rearrangement of the kinetoplast discMol Biochem Parasitol.117(2):179-86.
90. Mach J, Tachezy J and Sutak R (2013). Efficient iron uptake via a reductive mechanism in procyclic *Trypanosoma brucei*. J. Parasitol. 99, 363–364.
91. Mackey ZB, Baca AM, Mallari JP, Apsel B, Shelat A, Hansell EJ, Chiang PK, Wolff B, Guy KR, Williams J, McKerrow JH (2006). Discovery of trypanocidal compounds by whole cell HTS of *Trypanosoma brucei.* Chem Biol Drug Des 67: 355–363.
92. MacNeill SA (2014). Identification of a Candidate Rad1 Subunit for the Kinetoplastid 9-1-1 (Rad9-Hus1-Rad1) Complex. Biology. 3: 922-927.
93. Majka J, Burgers PM (2003). Yeast Rad17/Mec3/Ddc1: A sliding clamp for the DNA damage checkpoint. Proc Natl Acad Sci U S A. 100: 2249–2254.

94. Makino DL and Conti E (2013). Structure determination of an 11-subunit exosome in complex with RNA by molecular replacement.Acta Crystallogr D Biol Crystallogr.69(11):2226-35.
95. Malvy D and Chappuis F (2011). Sleeping sickness. Clinical Microbiology and Infection 17, 986-995.
96. Martinez-Calvillo S, Lopez I and Hernandez R (1997). pRIBOTEX expression vector: a pTEX derivative for a rapid selection of *Trypanosoma cruzi* transfectants. Gene.199:71-6.
97. Matsumoto K, Yamada Y, Takahashi M, Todoroki T, Mizoguchi K, Misaki H and Yuki H (1990). Fluorometric determination of carnitine in serum with immobilized carnitine dehydrogenase and diaphorase. J. Clin. Chem. 36:2072–2076.
98. Maudlin I, Holmes PH and Miles MA (2004). The Trypanosomiases. CABI Publishing. Wallingford, United Kingdom. 632.
99. Mayer ML, Gygi SP, Aebersold R and Hieter P (2001). Identification of RFC (Ctf18p, Ctf8p, and Dcc1p): An alternative RFC complex required for sister chromatid cohesion in S. cerevisiae. Mol. Cell. 7, 959–970.
100. Meissner A, Boshoff HI, Vasan M, Duckworth BP, Barry CE 3rd, Aldrich CC (2013).Structure activity relationships of 2aminothiazoles effective against Mycobacterium tuberculosis Bioorg Med Chem. 21(21):6385-97.
101. Mendonca AF, Romero MG, Lihono MA, Nannapaneni R and Johnson MG (2004). Radiation resistance and virulence of *Listeria monocytogenes* Scott A following starvation in physiological saline. J Food Prot. 67, 470–474.
102. Merschjohann K and Steverding D (2006). *In vitro* growth inhibition of bloodstream forms of *Trypanosoma brucei* and *Trypanosoma congolens* e by iron chelators. Kinetoplastid Biol Dis 5: 3.
103. Mitchell P, Petfalski E, Shevchenko A, Mann M and Tollervey D (1997). The exosome: a conserved eukaryotic RNA processing complex containing multiple 3'-->5' exoribonucleases. Cell. 91(4):457-66.
104. Moon TW and Mommsen TP (2005). Biochemistry and molecular biology of fishes. Environ. Toxicol. 6:51–56.
105. Moraes CB, Giardini MA, Kim H, Franco CH, Araujo-Junior AM, Schenkman S, Chatelain E and Freitas-Junior LH. (2014). Nitroheterocyclic Compounds Are More Efficacious Than CYP51 Inhibitors against Trypanosoma Cruzi: Implications for Chagas Disease Drug Discovery and Development. Sci. Rep. 4, 4703.
106. Moskalev AA, Plyusnina EN and Shaposhnikov MV (2011). Radiation hormesis and radioadaptive response in Drosophila melanogaster flies with different genetic backgrounds: the role of cellular stress-resistance mechanisms. Biogerontology.12 (3): 253–63.
107. Muller IB and Hyde JE (2013). Folate Metabolism in Human Malaria Parasites—75 Years on. Mol. Biochem. Parasitol. 188, 63–77.
108. Musiol R, Jampilek J, Buchta V, Niedbala H, Podeszwa B, Palka A, Majerz-Maniecka K, Oleksyn B, Polanski J (2006). Antifungal properties of new series of quinoline derivatives. Bioorg. Med. Chem. 14, 3592–3598.
109. Muskavitch MA, Barteneva N and Gubbels MJ (2008). Chemogenomics and parasitology: small molecules and cell-based assays to study infectious processes. Comb. Chem. High Throughput Screening.11:624–646.

110. Nare B, Wring S, Bacchi C, Beaudet B, Bowling T, Brun R, Chen D, Ding C, Freund Y, Gaukel E, Hussain A, Jarnagin K, Jenks M, Kaiser M, Mercer L, Mejia E, Noe A, Orr M, Parham R, Plattner J, Randolph R, Rattendi D, Rewerts C, Sligar J, Yarlett N, Don R, Jacobs R (2010). Discovery of novel orally bioavailable oxaborole 6-carboxamides that demonstrate cure in a murine model of late-stage central nervous system African trypanosomiasis. Antimicrob. Agents Chemother. 54:4379–4388.
111. Navarro MVAS, Oliverira CC, Zanchin NIT and Guimarães BG (2008). Insights into the mechanism of progressive RNA degradation by the archaeal exosome. J. Biol. Chem. 283, 14120–14131.
112. O'Brien J, Wilson I, Orton T and Pognan F (2000). Investigation of the Alamar Blue (resazurin) fluorescent dye for the assessment of mammalian cell cytotoxicity" Eur. J. Biochem. 267:5421–5426.
113. Olsen OW (1974). Animal Parasites. The Life Cycles and Ecology. London: University Park Press.9:73-151.
114. Osterholm MT and Norgan AP (2004). The role of irradiation in food safety. N Engl J Med .350, 1898–1901.
115. Page AB, Page AM and Noel C(1993). A new fluorimetric assay for cytotoxicity measurements in vitro. Int. J. Oncol. 3:473–476.
116. Palfi Z, Schimanski B, Günzl A, Lücke S and Bindereif A (2005). U1 small nuclear RNP from *Trypanosoma brucei*: a minimal U1 snRNA with unusual protein components. Nucleic Acids Res. 33:2493-2503.
117. Panigrahi AK, Zíková A, Dalley RA, Acestor N, Ogata Y, Anupama A, Myler PJ and Stuart KD (2008). Mitochondrial complexes in *Trypanosoma brucei*: A novel complex and a unique oxidoreductase complex. Mol. Cell. Proteom.7:534–545.
118. Patterson S and Wyllie S (2014). Nitro drugs for the treatment of trypanosomatid diseases: past, present, and future prospects. Trends Parasitol. 30, 289–98.
119. Peña I, Manzano PM, Cantizani J, Kessler A, Alonso-Padilla J, Bardera AI, Alvarez E, Colmenarejo G, Cotillo I, Roquero I, de Dios-Anton F, Barroso V, Rodriguez A, Gray DW, Navarro M, Kumar V, Sherstnev A, Drewry DH, Brown JR, Fiandor JM, Martin JJ (2016). New Compound Sets Identified from High Throughput Phenotypic Screening Against Three Kinetoplastid Parasites: An Open Resource. Scientific Reports 5:8771. DOI: 10.1038/srep08771.
120. Perales JB, Freeman J, Bacchi CJ, Bowling T, Don R, Gaukel E, Mercer L, Moore JA 3rd, Nare B, Nguyen TM, Noe RA, Randolph R, Rewerts C, Wring SA, Yarlett N and Jacobs RT (2011).SAR of 2-amino and 2,4-diamino pyrimidines with in vivo efficacy against Trypanosoma brucei Bioorg Med Chem Lett.15;21(10):2816-9.
121. Perković I, Butula I, Kralj M, Martin-Kleiner I, Balzarini J, Hadjipavlou-Litina D, Katsori AM and Zorc B (2012). Novel NSAID 1-acyl-4-cycloalkyl/arylsemicarbazides and 1-acyl-5-benzyloxy/hydroxy carbamoylcarbazides as potential anticancer agents and antioxidants. Eur J Med Chem.51:227–238.
122. Petkau A (1987). Role of superoxide dismutase in modification of radiation injury. Br J Cancer Suppl. 8:87–95.
123. Pez D, Leal I, Zuccotto F, Boussard C, Brun R, Croft SL, Yardley V, Ruiz Perez LM, Gonzalez Pacanowska D, Gilbert IH(2003). 2, 4-Diaminopyrimidines as

inhibitors of Leishmanial and Trypanosomal dihydrofolate reductase. Bioorgan. Med. Chem. 3, 4693–4711.

124. Pink R, Hudson A, Mouries MA and Bendig M (2005). Opportunities and challenges in antiparasitic drug discovery. Nat Rev Drug Discov 4: 727–740.

125. Podesta D, Stoppani A and Villamil SF (2003). Inactivation of Trypanosoma cruzi and Crithidia fasciculata topoisomerase I by Fenton systems. Redox Rep 8: 357–363

126. Popp M and Lattorff HM (2011). Quantitative In Vitro Cultivation Technique to Determine Cell Number and Growth Rates in Strains of Crithidia bombi (Trypanosomatidae), a Parasite of Bumblebees. J Eukaryot Microbiol. 58(1):7-10.

127. Preston S, Yaqing J, Abdul J, Sean LM , Benoît L, Paul W, Timothy NCW and Robin BG (2016). Screening of the 'Pathogen Box' identifies an approved pesticide with major anthelmintic activity against the barber's pole worm. International Journal for Parasitology: Drugs and Drug Resistance. (6): 329-334.

128. Prise KM and O'Sullivan JM (2009). Radiation-induced bystander signalling in cancer therapy. Nat RevCancer.9:351–360.

129. Puig O, Caspary F, Rigaut G, Rutz B, Bouveret E, Bragado-Nilsson E, Wilm M and Séraphin B (2001). The Tandem Affinity Purification (TAP) Method: A General Procedure of Protein Complex Purification. METHODS.24:218-29.

130. Rampersad SN (2012). Multiple applications of Alamar Blue as an indicator of metabolic function and cellular health in cell viability bioassays. Sensors (Basel) 12: 12347–12360.

131. Ravanat JL, Douki T and Cadet J (2001). Direct and indirect effects of UV radiation on DNA and its components. J Photochem Photobiol B. 63(1–3): p. 88–102.

132. Räz B, Iten M, Grether-Bühler Y, Kaminsky R and Brun R (1997). The Alamar Blue assay to determine drug sensitivity of African trypanosomes (*T. b. rhodesiense and T. b. gambiense*) in vitro. Acta Trop. 68:139–147.

133. Regis-da-Silva CG, Freitas JM, Passos-Silva DG, Furtado C, Augusto-Pinto L, Pereira MT, DaRocha WD, Franco GR, Macedo AM, Hoffmann JS, Cazaux C, Pena SD, Teixeira SM, Machado CR(2006). Characterization of the *Trypanosoma cruzi* Rad51 gene and its role in recombination events associated with the parasite resistance to ionizing radiation. Mol Biochem Parasitol 149: 191–200.

134. Richard JV and Werbovetz KA (2010). New antileishmanial candidates and lead compounds Curr Opin Chem Biol.14 (4):447-55.

135. Rigaut G, Shevchenko A, Rutz B, Wilm M, Mann M and Seraphin B (1999). A generic protein purification method for protein complex characterization and proteome exploration. Nature Biotechnology. 17:1030-1032.

136. Rojas R, Segovia C, Trombert AN, Santander J and Manque P (2014). The effect of tunicamycin on the glucose uptake, growth, and cellular adhesion in the protozoan parasite Crithidia fasciculata.Curr Microbiol. 69(4):541-8.

137. Sahin A, Lemercier G, Tetaud E, Espiau B, Myler P, Stuart K, Bakalara N, Merlin G. (2004). Trypanosomatid flagellum biogenesis: ARL-3A is involved in several species. Exp Parasitol 108:126–133

138. Sanger F, Nicklen S and Coulson AR (1977). DNA sequencing with chain terminating inhibitors. Proc Natl Acad Sci USA. 74:5463_/7.

139. Saxowsky TT, Matsumoto Y and Englund PT (2002). The mitochondrial DNA polymerase beta from *Crithidia fasciculata* has 5'-deoxyribose phosphate (dRP) lyase activity but is deficient in the release of dRP.J Biol Chem. 277(40):37201-6.
140. Schaub GA (1994). Pathogenicity of trypanosomatids on insects. Parasitol Today 10: 463–468.
141. Schimanski B, Klumpp B, Laufer G, Marho¨fer RJ, Selzer PM and Gu¨nzl A (2003). The second largest subunit of *Trypanosoma brucei*'s multifunctional RNA polymerase I has a unique N-terminal extension domain. Mol.Biochem. Parasitol. 126:193–200.
142. Schimanski B, Nguyen TN and Gu¨nzl A (2005). Highly Efficient Tandem Affinity Purification of Trypanosome Protein Complexes Based on a Novel Epitope Combination. Eukaryotic Cell. 4: 1942–50.
143. Schmidt SL, Pautz AL and Burgers PM, (2001). ATP utilization by yeast replication factor C. IV. RFC ATP binding mutants show defects in DNA replication, DNA repair, and checkpoint regulation. J Biol Chem.276:34792–800.
144. Schnaufer A, Domingo GJ and Stuart K (2002). Natural and induced dyskinetoplastic trypanosomatids: how to live without mitochondrial DNA," International Journal for Parasitology, 32 (9): 1071–1084.
145. Schneider P, Treumann A, Milne KG, McConville MJ, Zitzmann N and Ferguson MA (1996). Structural studies on a lipoarabinogalactan of Crithidia fasciculata. Biochemical Journal, 313 (3): 963-971.
146. Schwikowski B, Uetz P and Fields S (2000). A network of protein-protein interactions in yeast. Nature Biotechnology. 18 (12): 1257–61.
147. Scolaro EJ, Ames RP and Brittingham A (2005). Growth-phase dependent substrate adhesion in *Crithidia fasciculata*.J Eukaryot Microbiol. 52(1):17-22.
148. Seo M, Chun DK, Hong ST and Lee SH (1993). Influence of heat shock, drugs, and radiation on karyotype of *Leishmania major*. The Korean journal of parasitology 31: 277–283.
149. Seymour CB and Mothersill C (2004). Radiation-induced bystander effects—implications for cancer. Nature Reviews Cancer. 4(2):158-64.
150. Shapiro TA and Englund PT (1995). The structure and replication of kinetoplast DNA.Annu Rev Microbiol. 49:117-43.
151. Sharma P, Jha AB, Dubey RS and Pessarakli M (2012). Reactive oxygen species, oxidative damage, and antioxidative defense mechanism in plants under stressful conditions. J. Bot.26. dx.doi.org/10.1155/2012/217037.
152. Shimony O and Jaffe CL (2008). Rapid fluorescent assay for screening drugs on Leishmania amastigotes. J. Microbiol. Methods. 75:196–200.
153. Silva RM, Lopez V, Chiriboga J and Colon JI (1967). Effect of irradiation on Trypanosoma cruzi.Radiat.Res.31:649.
154. Simarro PP, Franco J, Diarra A, Postigo JAR and Jannin J (2012). Update on field use of the available drugs for the chemotherapy of human African trypanosomiasis. Parasitology 139, 842-846.
155. Singh N, Kumar M and Singh RK (2012). Leishmaniasis: current status of available drugs and new potential drug targets. Asian Pac. J. Trop. Med. 5, 485–497.
156. Sinha KM, Hines JC, Downey N and Ray DS (2004). Mitochondrial DNA ligase in *Crithidia fasciculata*. Proc Natl Acad Sci USA 30: 4361–4366

157. Siqueira-Neto JL, Song OR, Oh H, Sohn JH, Yang G, Nam J, Jang J, Cechetto J, Lee CB, Moon S, Genovesio A, Chatelain E, Christophe T, Freitas-Junior LH (2010). Antileishmanial High-Throughput Drug Screening Reveals Drug Candidates with New Scaffolds. PLoS Negl Trop Dis 4: 4(5):e675.
158. Sommer JM, Hua S, Li F, Gottesdiener KM and Wang CC (1996). Cloning by functional complementation in *Trypanosoma brucei*. Mol Biochem Parasitol. 76:83-9.
159. Spitz DR, Azzam EI, Li JJ and Gius D (2004). Metabolic oxidation/reduction reactions and cellular responses to ionizing radiation: a unifying concept in stress response biology. Cancer Metastasis Rev. 23:311–322.
160. Strober W (2001). Trypan Blue Exclusion Test of Cell Viability. Current Protocols in Immunology. Appendix 3: Appendix 3B.doi: 10.1002/0471142735.
161. Stuart K, Brun R, Croft S, Fairlamb A, Gürtler RE, McKerrow J, Reed S and TarletonR (2008). Kinetoplastids: Related protozoan pathogens, different diseases. J Clin Invest. 118(4):1301–10
162. Sundar S, Jha TK, Thakur CP, Sinha PK and Bhattacharya SK (2007). Injectable paromomycin for Visceral leishmaniasis in India. N. Engl. J. Med. 356:2571–2581.
163. Sykes ML and Avery VM (2009). Development of an Alamar BlueTM Viability Assay in 384-Well Format for High Throughput Whole Cell Screening of Trypanosoma brucei brucei Bloodstream Form Strain 427. Am. J. Trop. Med. Hyg. 81:665–674.
164. Sykes ML and Avery VM (2013). Approaches to protozoan drug discovery: phenotypic screening. J Med Chem. 56: 7727–7740.
165. Takeda GK, Campos R, Kieffer J, Moreira AA, Amato Neto V, Castilho VL, Pinto PL and Duarte MI (1986). Effect of gamma rays on blood forms of Trypanosoma cruzi. Experimental study in mice. Rev Inst Med Trop Sao Paulo 28: 15–18.
166. Tasanor O, Engelmeier D, Brem B, Wiedermann-Schmidt U, Greger H and Wernsdorfer WH(2006). Development of a pharmacodynamic screening model with Crithidia fasciculata.Wien Klin Wochenschr.118 (19-20 Suppl 3):42-9.
167. Teixeira SM, El-Sayed NM and Araujo PR (2011). The genome and its implications. Adv Parasitol 75: 209–230.
168. Tetaud E, Lecuix I, Sheldrake T, Baltz T and Fairlamb HA (2002). A new expression vector for Crithidia fasciculata and Leishmania. Mol Biochemical Parasitol. 120: 195-/204.
169. Tiballi RN, He X, Zarins LT, Revankar SG and Kauffman CA (1995). Use of a colorimetric system for yeast susceptibility testing. J. Clin. Microbiol. 8:374–377.
170. Tobin JF, Reiner SL, Hatam F, Zheng S, Leptak CL, Wirth DF and Locksley RM (1993). Transfected *Leishmania* expressing biologically active IFN-γ J Immunol. 150:5059–5069.
171. Tomecki R, Drazkowska K and Dziembowski A (2010). Mechanisms of RNA degradation by the eukaryotic exosome. Chembiochem. 11:938-45.
172. Ueno N and Wilson ME (2012). Receptor-mediated phagocytosis of Leishmania: implications for intracellular survival. Trends Parasitol 28: 335–344.

173. Ullu E, Tschudi C and Gunzl A (1996). Trans-splicing in trypanosomatid protozoa. In Smith DF and Parsons M (eds), Molecular Biology of Parasitic Protozoa. Oxford University Press, New York. 1996; 115-133.
174. Urbina JA (2010). Specific chemotherapy of Chagas disease: relevance, current limitations and new approaches. Acta Trop, 115, 55-68.
175. Vieira HG, Grynberg P, Bitar M, Pires Sda F, Hilário HO, Macedo AM, Machado CR, de Andrade HM, Franco GR (2014). Proteomic Analysis of *Trypanosoma cruzi* Response to Ionizing Radiation Stress. PLoS ONE 9(5): e97526. doi:10.1371/journal.pone.0097526.
176. Viotti R, Vigliano C, Lococo B, Bertocchi G, Petti M, Alvarez MG, Postan M and Armenti A (2006) Long-term cardiac outcomes of treating chronic Chagas disease with benznidazole versus no treatment: a nonrandomized trial. Ann. Intern. Med 144:724–734.
177. Wallace FG (1966). The trypanosomatid parasites of insects and arachnids. Exp Parasitol 18:124–193.
178. Wang K, Yang T, Wu Q, Zhao X, Nice EC and Huang C(2012). Chemistry-based functional proteomics for drug target deconvolution. Expert Rev. Proteomics 9, 293–310.
179. Wirtz E, Leal S, Ochatt C and Cross GAM (1999). A tightly regulated inducible expression system for conditional gene knock-outs and dominant-negative genetics in *Trypanosoma brucei*. Mol Biochem Parasitol. 99:89–101.
180. Yao NY and O'Donnell M (2012). The RFC clamp loader: Structure and function. Subcell. Biochem. 62:259–279.
181. Zanatta N, Amaral SS, Dos Santos JM, de Mello DL, Fernandes Lda S, Bonacorso HG, Martins MA, Andricopulo AD, Borchhardt DM (2008). Convergent synthesis and cruzain inhibitory activity of novel 2-(N'-benzylidenehydrazino)-4-trifluoromethyl-pyrimidines.Bioorg Med Chem. 16(24):10236-43.
182. Zhang JH, Chung TD and Oldenburg KR (1999). A simple statistical parameter for use in evaluation and validation of high throughput screening assays. J Biomol Screen 4: 67–73.

7. Appendices

7.1 **Appendix 1.** The *C. fasciculata* serum free defined growth media recipe.

Ingredient	**In 1 Litre distilled water**
Yeast Extract	5 g
Tryptone	4 g
Sucrose	15 g
Triethanolamine	4.37 g
Tween 80	4.72 mL
Haemin (2.5mg in 1 ml of 50 mM NaOH)	4 mL

The pH of the media was adjusted to 8.0 with either NaOH or HCl before adding Haemin (final concentration of 10µg/ml). The media was filter sterilised using 0.22µm stericups vacuum filters (Merck Millipore) and stored in the cold room.

7.2 **Appendix 2.** Extraction of *C. fasciculata* genomic DNA.

Ingredients	**Stock concentration**	**In 1000 µl**	**Final concentratio**
Tris-HCl	1 M	10 µl	10 mM
NaCl	5 M	20 µl	100 mM
EDTA pH 8.0	0.5 M	50 µl	25 mM
SDS	10%	50 µl	0.5%
Proteinase K	20 mg/ml	5 µl	0.1 mg/ml
Distilled water		865 µl	

A 1ml of media containing *C. fasciculata* cells in log phase was centrifuged at 2000g for 5 minutes. The cell pellet was then suspended in lysis buffer (see table below) to the final volume of 1000 µl. Cells were lysed and incubated at 56^{o}C for at least 3 hours and the gDNA was precipitated with 500 µl of absolute ethanol. The DNA was then spooled on a sterile pipette tip and washed 2 times with 500 µl of 70% ethanol. The ethanol was allowed to air dry off the spooled gDNA and the gDNA was dissolved into 100 µl elution buffer pH 8.5 (from PCR clean up Kit) before storage in a +4^{o}C fridge.

7.3 **Appendix 3**. The designed forward and reverse primers that were used to amplify the ORFs of target subunits.

Protein subunit	**Primers**	**Sequences**	**Descriptions**
RFC3	CfRFC3-5*Nde*	GGTGGTGGTGCATATGGCA ACTTCGAAG	To PCR amplify the RFC3 insert sequence.
	CfRFC3-3*Not*	GGTGGTGGTGGCGGCCGCC AGCGCTGC	To PCR amplify the RFC3 insert sequence.
RRP4	CfRRP4-5*Nde*	GGTGGTGGTGCATATGTCG TCAGGAGTC	To PCR amplify the RRP4 insert sequence.
	CfRRP4-3*Not*	GGTGGTGGTGGCGGCCGCC CTGGCGGC	To PCR amplify the RRP4 insert sequence.
Vector	pC-Seq-F	GCAAGGCGATTAAGTTGGG TAAC	To sequence inserts within PTP vector
	pC-Seq-R	TGTTGTCCACGGCTTCATCG TG	To sequence inserts within PTP vector

The first 10 are random bases followed by a *Nde*I or *Not*I sequence (in yellow) and ORF sequence of a target subunit gene. The primers pC-Seq-F and pC-Seq-R were used to confirm the fidelity of cloning process. Oligonucleotides were ordered from Integrated DNA Technologies (IDT).

7.4 **Appendix 4(a)**. A conventional PCR reaction recipe and cycling conditions using Q5 High-fidelity DNA polymerase enzyme.

Reaction recipe of PCR using Q5 High-fidelity DNA Polymerase			
Component		**50 µl reaction**	**Final concentration**
Template DNA		5 µl	500 ng
5xQ5 Reaction buffer		10 µl	1x
10 mM dNTPs		1 µl	200 uM
Forward primer(100 µM)		0.5 µl	1 mM
Reverse primer (100 µM)		0.5 µl	1 mM
Q5 High fidelity DNA polymerase		0.5 µl	0.02 U/µl
5xQ5 High GC enhancer(**optional)**		10 µl	1x
Nuclease free water		22.5 µl	
Final reaction volume		**50 µl**	
Thermocycling conditions for PCR			
Step		**Temperature (^{0}C)**	**Time**
Initial Denaturation		98	30 sec
30 Cycles	Denaturation	98	10 sec
	Annealing	70	20 sec

	Extension	72	45 sec
Final extension		72	2 min

All reaction components were assembled on ice and the reaction mixture was quickly transferred to a thermocycler preheated to the denaturation temperature (98^{o}C).

7.5 **Appendix 4(b)**. PCR reaction recipe and cycling conditions for a standard My Taq Red MIX.

Component		**20 µl Reaction**	
Template		5 µl	
Primers (4 µM each)		5 µl	
My Taq Red Mix,2x		10 µl	
Final reaction volume		20 µl	
Step	**Temperature**	**Time**	**Cycles**
Initial denaturation	95^{o}C	1 min	1
Denaturation	95^{o}C	15 sec	30
Annealing	65 ^{o}C	15 sec	
Extension	72 ^{o}C	10 sec	

All reaction components were assembled on ice and the reaction mixture was quickly transferred to a thermocycler preheated to the denaturation temperature (95^{o}C).

7.6 **Appendix 5**. Preparative restriction/diagnostic digest and ligation experimental set up.

Component	**Reaction (20 µl)**
Analytical/Preparative digest	
DNA	2 µl (1-20 µg)
Buffer x2	10 µl
Restriction enzymes (*Nde*I and *Not*I)	2 µl (1 µl each)
Sterile water	6 µl
Dephosphorisation	
Antarctic Phosphatase Rxn Buffer (10X)	4 µl
Antarctic Phosphatase	5 µl
Sterile water	11 µl
Ligations (20 µl reaction)	
10 X T4 DNA Ligase Buffer	2 µl
Vector DNA(~4 kb)	50 ng
Insert DNA (~1 kb)	37.5ng
Nuclease-free water	upto 20 µl
T4 DNA Ligase	1 µl

7.7 **Appendix 6.** Recipes for solution and buffers used for PTP purification experiments.

Lysis buffer	10 ml	150 mM sucrose 300 mM potassium chloride 40 mM potassium L-glutamate 3 mM $MgCl_2$ 20 mM HEPES-KOH (pH 7.7) 2 mM dithiothreitol 0.1% Tween 20
TST buffer	50 ml	50 mM Tris-HCL (pH7.7) 150 mM NaCl 0.05% TWEEN
0.5 M glacial acetic acid	50 ml	1.43 mL Acetic acid in 50 mL d H_20
PA-150 buffer	50 ml	20 mM Tris-HCl (pH7.7) 150 mM KCl 3 mM MgCl 0.1% TWEEN 1 mM DTT
TEV buffer	20 ml	150 mM KCl 20 mM Tris-HCl (pH7.7) 3 mM MgCl 0.5 mM EDTA pH8.0 0.1% TWEEN 1 mM DTT
PC-150 buffer	150 ml	150 mM KCl 20 mM Tris-HCl (pH7.7) 3 mM MgCl 1 mM $CaCl_2$ 0.1% Tween
EGTA/EDTA elution buffer	2 ml	5 mM Tris-HCl (pH7.7) 10 M EGTA 5 mM EDTA
Fix	200 ml	50% methanol 7% acetic acid
Wash	100 ml	10% methanol 7% acetic acid

7.8 **Appendix 7 (a).** Protein sequences of RFC complex subunits identified by Mass spectroscopic analysis.

The residues that were found to be identical with the protein residues on database are highlighted in red.

RFC1

```
  1 MSTLSFSTGI  EAMTPVNTQS  SATAAPRLSE  LWADKYKPRS  IAEMCYPSYA
 51 NKLKAWLENF  TPVGSPGDDP  NKHHGVLLSG  SPGVGKTTTV  YVVARELGRT
101 VIEYNASDFR  SRKSLRENVL  DLISNRAFAA  QATSYTRAVL  LMDEVDGCDI
151 GGVGEVVKML  FITKIPILCT  CNDRWHPKLQ  TLVKYVEDMR  FSHPPCNIVA
201 NYLCERVLAR  EGITLSKPLL  QDIIKKSGSD  IRNMLNNLQL  WCLNRRSLEQ
251 RQLAECAAQA  TKDGDAGLFD  SAEYFLLQGT  SRGERHSIAE  MQACYYNSDL
301 IDMFVQENYL  HYNPEPVDGR  DWMTAVAQAA  SSISRADAAQ  RIMYYEQNWS
351 VSRFHVLSSS  IAPCVYTRGK  YETFMTGQQK  FFDLQRPVKF  PQWLGHNSTA
401 GKNRRLLRCV  AMQASHPTRG  ISGNQEDVAA  DYMPNGWERP  LTQPLAEKEK
451 DGIAEVIALM  DQYNLMRDDW  DLVQTLPHFR  HMETPRQQPP  VSITTAVKAA
501 FTREFNKTHR  FDSFAKTTLK  RTDKADEDDG  IDEEEGESQK  EGAGAKAGTK
551 GRVIADGVTA  VTITGSDAAK  PKAKTSAARK  PRAKKSAANA  AAAADDSGET
601 KPARKRAASA  STRKPAKPAG  KASKAAAGGK  ARKRARVESS  SESEVEISSD
651 SSSDSSDSE
```

RFC2

```
  1 MSLSSQPVTK  KAKTEAAASP  AAAATPWIEK  YRPRTLDEVE  AQDEAVSALR
 51 ACLKEGANMP  HFLFHGPPGT  GKTTSILAVA  HELFGPDYIR  SRVRELNASD
101 DRGINVVREK  IKVFAQGAVS  SGGSSVTQSD  GKVYPVPGFK  LIILDEADAL
151 LPDAQGALRR  MMEDFSDVTR  FCILCNYVSR  IIDPIASRCA  KYRFKPLVKT
201 ALYNRIQFVA  NAEGIELSDA  SLQALDSVSG  GDLRLAIMHL  QSAHKASGSD
251 LTREDFVSVS  GSVPADAMQT  YVAALVSRRL  EDVIAVSRQL  VAQGYAAAQV
301 LVQLQRYLVS  AECPLNSAQR  GRMMLKLCQT  ERRLADGGDD  YLQLLDMGSS
351 VCAS
```

RFC3

```
  1 MATSKQAEDA  KAGGSHLPWV  EKYRPDNLDS  VVAHEDILST  LRHLMNSGNM
 51 PHLLLYGPPG  TGKTTTIKAC  AYYLYGKDRV  RANVLEMNAS  DDRGIDVVRQ
101 QIREFSSTSS  IFSMMGPSSS  SGGGGNGGSG  PLASFKLVIL  DEADQMSHDA
151 QAALRRVIEK  YTKNVRFCIL  CNHINKVIPA  LQSRCTRFRF  APVKKSAMMP
201 RLKYVAEQEK  VKYTTEGLAA  AFRLSHGDLR  RCMNTMQSSA  LSADEITEES
251 VYRVTGNPTP  AEVTAIVSDM  LSGDFATSWA  KVEVAVTQKG  ISIADLAREI
301 HPIMMAMDLP  QDCKCFLLMK  LSDMEYYAAG  GAREAAGLGG  LLGAFQLVKE
351 AVTQRKPIKA  VAGDCSA
```

```
  1 MLCLARDLLL  QNTDAATGAD  KAGGKDILKD  AVLELNASDD  RGLDVVREKI
 51 KLFAQTKKTL  PKKFFTTGEG  AETMEQVVHL  HKIVLLDEAD  SMTPAAQQAL
101 RRTMELHSST  TRFAFACNNS  SKIIEPIQSR  CAVVRFKKLS  DADILRRLVF
151 VIQQEKVSYT  DDGLEALLYL  AEGDLRQAMN  SLQATHTGYG  LVNADNVFKV
201 CDQPHPVLVE  NIITACVTKR  NIEEAHKEMN  RLLNRGYAPA  DVIATFFKVV
251 QTNARLFRSE  LQQLEVLKVV  GETTMRIAEG  VGTSLQLAAM  LARMIAAVEN
301 NQS
```

RFC4

RFC5

```
  1 MLWVDRYRPK  TLKEVELYPE  LNDVLGRLAK  AQDLPHLLFY  GPSGSGKKTR
 51 AMAVLHEIYG  PSVYSVRLEH  KSVQVSDSKV  VDIATLSSPH  HIDINPSDAG
101 NYDRVIVMQM  IREIAQTVPL  HTTASSAKAV  PYKVVVLNEV  DKMSRSAQHA
151 LRRTMEKYMK  TCRLVLICNS  TSRLIPPLRS  RCLGIRVAAH  SKDNLALAVQ
201 HVCEGESRPM  PSPAFLNSLA  LRSDGNLRRG  LLMLEASAMT  KVDWSGNGAA
251 IPQADWKLFL  DEISHDILAE  QTPKKLHEVR  LKFYDLLAQC  ISGETILKTL
301 LDSLLLAVPP  KHQAALIQLA  ATYDHNMKLG  TKPILHLEAF  VAGVMKLIKQ
351 Q
```

Rad17

```
  1 MLNEVYAPTT  VADLAWSRQK  IVALSTLVRS  TRSGAQNPRI  LLLYGPPGCG
 51 KLESLKVLLR  EAPPAAASTT  SKSKTPAPAP  QVIEPPTTVS  VFHTCEASST
101 AYSQFLQHVL  SLCSGQLVGS  ALMLTPKDMH  GGRDTPSAPS  DVQHAHIIKL
151 YGEPATHVLH  RATVAFLRQY  EALRLQAIRE  EEQQQHQRRY  LAKVLASPAS
201 PSTTLMDHLR  RNLIFFVHTT  HDSHNDKVDL  GSALPAAVLQ  SAAVELFHCT
251 PVTEINLKKR  LRHILDTEAR  RRANRSAQQR  RADVAEATDV  DDLFGIAPAL
301 SGSSAAPRRV  AARGGAGSSR  GKKGKENAKH  APVTALHIPD  AADVLDSLAL
351 DAIAAGSQGD  IRQALLQVQW  AALVPPGSST  AASLVETVAD  SSDVVWARLQ
401 HRRALAQAFA  SGSSKADESS  LVLSTKSVAP  LAEACAAPQQ  QDSTVAEDDD
451 GVVLLISSSS  SEFDAPLPLS  AAEVTRRQHL  PSRSHEAATR  KRSRSSENDV
501 VDVDDVGTTS  KAAPPSAQAR  ATDMLSLLDS  QMNGAGESRA  AAAASRGAAK
551 KLLRAAPVRR  DGLAAKNNTD  ADDGAAVLPD  HRTVLPTTRD  EYLGLSHATG
601 RLLSQKYSVD  AVLDILNVPP  RKMLDYLTNN  QVRYFSDAQL  PQYLVCAAAA
```

651 SEVDALRTAE FDGGYGGSAA ALRERRQLAD RTTAGESVGN VARLLDVIAL
701 QTFHRRYLVE QTAVQAPPGF TPQEPPPFLR SAYPRVRDVG STTNTTGPYM
751 TQRGEAVLEL LAGVSEHEWM EQFLLRLDSA VSASGAITSF SSIGRRRMPP
801 AASVVSSDAI FSQPALGLTS PSIRLDEVDI LREGLPDLLY RCGCTESVVM
851 DHYALAPYIV LNLPASSQPS AAAVASQPSP AVTPAGISSA ASGDSADAGG
901 APLSVARPRR TVFKFAASTP PPPPPTQLHS QPAPLSLRET HAARLSARRP
951 CTSLQLKILQ RGRDSAAATL RGDHFVLVAT ENIAEEGSMS EKGGVEERPW
1001 MPEGDDIEDD

7.9 **Appendix 7 (b).** Protein sequences of exosome complex subunits identified by Mass spectroscopic analysis.

The residues that were found to be identical with the protein residues on database are highlighted in red.

RRP 41

1 MSRQKEYVSP AGLRLDGRRP LEARRMDIAF STLSGCDGSC DITLGRSKVC
51 ASVFGPRESV HRQEAKHDEV IITCEVAVAA FAGEVRRNPQ RRGRLSEDIS
101 AAVVQVARSV VLLPQYPNSQ IHIYLEVLQQ DGNEKIACIN AACLALVDAN
151 VAMRDAVCCT NVGLLDEHVL VDLTNEELRS QCPVIAAAFT GHDTRNIIWL
201 ETTSRLLPEA AIRLLKAAGQ SAKELFEGTV RGALVEHATQ ILALQS

RRP41B

1 MSSALSGQSA VTLSSSSSSS HPTAAATAGA SYTRRDGRTA LEIRGKEMRL
51 SEMADFDGSS WYAQGQTAVL VTLHGPTLAK NEEYDTCLVR VRVQHAHGLT
101 PSAGGAERAV YEEMKLEMLT RTDALELESL LESTIDAVVM RDRFPRCVLV
151 VDVVVVQDDG SLAAVALNAV MCALLDAGVP CRTTMAAVCV AAVTRAEDAA
201 AGDASRAVGS SLELLLDPTT AEETLGAGNT AAATAAGGEK ARSTVDATMA
251 EKGDLSGAAA AKLSLLRPDA LQGHYRCVST GVFVFSNPAC GGGVLAQLVR
301 RRSGGDSGTG ANTVSVEVYG QMMTLAERAA VVLFDFFRQC NVAE

RRP6

1 MPPKSAEASL PATKAVVSAV FGAVKDYSKL SAQIPADDFE YHLAFAGFRK
51 HIRDDSVGLV EVMDACCQML PKRRRTNLVA EEDPHSGAVH LAETQRNAVM
101 EAIDSLLENV DSLLDEVKGR KLDAQDQLSV TFGSELAVSA HHDASRGGSS
151 ASNAAGVVRL AHVRRPQLSF ETPVDNSAAP FTPTYRDASG VQHTGVAGEH
201 PFHDAIRAFS VPEAQMMPKA EIPPVPLETC PLSFVDTPDA MQAMVAKLLS
251 ASEIAVDLEH HDFYSYQGFT CLMQISTREE DFIVDCLQLR ASMGALAPVF
301 LNPSILKVFH GAREDVRWLQ KDFALYLVNF FDTGVALQTL HMPYSLAFAV
351 DHFCQVKLNK KYQTADWRVR PLPADMVHYA RQDTHFLLYV YDRLKALLLN
401 SEGRASVGNL LVHVYNESKQ LALQVYAKPN VDPAETYKLA LGRSLGGLTA

451 VQEEVAREIF NWRESAARDV DDSPTAVLHL SSVLAIASKL PTTAKDLLRC
501 CSPATAVLRA NVAHLVELVK KAVASSSEDF ENGVSGSGAG RHGKEEGSRH
551 HNYLDGAAEG SLEWAVYRSR CPTGVHRPMT GTLPSLASVV KTVTPAAVSV
601 SEQAALLSHT MPSSWFSAMS ALSRVLASRQ QHHVELPGAD VRAARQAAAA
651 KSLAGTADAA AAAAVAAEEE TAKAEVESVS SASGEGEQKD EEATGDLPAE
701 ADVAEASSVI ALDKKAFSIK QEYGVGAKSR FKKGEKGGAA KKKK

EAP1

1 MSVSAASISL AEVRAVQDGV ANDVREDGRT LLQRRPVYIT PRSSPSAVAA
51 VVGGSDGGDA AGVAQQSYSG SYVEVRASGT VVLAAATPTV VDGCATAAPS
101 PVSAADNADG AKEAAAAAPH DAGRGQLHIT IDAVPHVLDA YAGTVGGRNT
151 HRYRRDYLAF LAATIRAVFG AAQVQVQEQQ GVAEAEVVPE EREGAEDEVG
201 AGTVSSSAVA PAGSGRGDGE TSLASGFPAA DLYIGEGFGF RVHVDVHVLQ
251 CAGGNLFTAI AYAVHAALRS LQLPAVTLHR APGDGAGVSV EVDRSQPYRR
301 PVQWSQLPLL CVLLVSPTGH YVVDPTLREE WALPQQVHVA AGASGQVFYF
351 RYQQLPSRRG NRYQLQEARK ADAEACAAYV APPMALNLLD CWAVLSDAVY
401 VCQAMIHDCE VALQG

RRP45

1 MLLRSAAPVP ADALVQRNVE FARTAWRAGL RPDQREAHQL RMIEIEFPLL
51 ARDTVQVKCG NTIATASVTC DLVEPMPFRP KHGFFEVHAR QLLHERDPLD
101 QPKAVKQLSM YLTRLLSGSV VETEGLCVIP GRRVWSIAAE VLILNNDGNL
151 HDVAQWAVMA ALQHVRRPEL TIRGDDVVVH PPHERDPVPL SLHHIPLSFT
201 FAVCANPQQV QLAARAAALR RASPVSAGAA GQGSSDNAGE KEDGADASAW
251 SDDALQIVAD PSLEEAAAAA CTVSVAVNAE GHVCSLEKAD GCDVSLEHLE
301 QCMQVALQLT PPLLTQMQEA MAAHDVKRKA AVRSQFLWAQ KRLGIQAAGG
351 AGASQTQEEQ AAKKSKTE

RRP40

1 MSTHSPTLKS VSELVPLKGH VCLPGEPVLM VQSSAVVAVG GGLRLLAQPS
51 TATDASQDVA DVFLAEYCAP LQRSSHHLHT HVPRYTVATP ASRRYTPRHA
101 DPVIAVIARK VSQHYYYCYI GGSSLAYLEA IAFDGATKVS RPRLAEGDVV
151 YCYVKPRAAA SYVDGAAASS AAATAAAVSS GGEVELACTA AEVGLPPKDW
201 TSGEAVFGPL LGGRLLTLPL AYVRRLLAPL PATLSGEGPA VKRARVEGGG
251 GEAEEVPASY LLHLLGQRVP FEVAVGMNGL VWVKGLTSEA DATAAARRTV
301 AVSACISEAQ YDATRAEMEA RVESYFPS

RRP4

```
  1 MSSGVVIVGD  SICGGERIQK  LNTSNDEVYL  RGFNTFAGNN  PSDIALVHEG
 51 AGEIVAAING  HIEVTDRVVS  VKGLLPRYQP  EIGDVVVGRI  LEVTGNKWQV
101 DVNSTQTAIM  LLSNVTEPGG  MLRRRGRGDE  LGMRQLFDQE  DLVAAEVQRI
151 SPDGVVSLHT  RAAEKYGRIG  GFGVLVSVRP  SLVKRAKHQF  VELAEHHVRL
201 TIGMNGNIWV  SRKEETADGT  EDKEREAEAR  QNVARVANCV  KALGVAHIQI
251 HPATIEAAVA  ASVEAGFSAF  HVSLEKNRDA  LLVSVHDAIG  VKRRRQ
```

CSL4

```
  1 MPVLVHTGAR  VAPGDALFSS  AAHVPTGTDA  SAATAGDTVS  DSDVIPGEGC
 51 VVHYVEVPSE  STGDSSRVRR  HIVATRQGVA  QWDGRLVSVF  AAGATGTTAQ
101 LQGASTAVRS  AVTGPRPGDT  VHVRITRLSR  LFAFGEITAV  NWQWCSHRSA
151 AGASVSGVFK  GVLRLEDIRP  FRPTRDQLQP  PPPTMAFALG  DVVLAEVISQ
201 SDAHQYQLST  VGEGFGVVES  YVSTAEEHYS  GRERVKLQHL  PGRRDAMLVP
251 ATGAVVPRWC  PLLP
```

EAP2

```
  1 MSLPPNTGSI  ELTAFRAHTS  QLLARGERLD  KRDFTTCRVP  TVVREERAAE
 51 APSSSSSGVV  QTGINMANSG  NLAAVMYTDS  YGACMQCTVQ  GLLGPPRPDR
101 PAAGRLNIHV  EAPFVEQLGG  GAATNYKSFQ  YIISNGNADL  PLRQLEGYIG
151 SVVDGCFDPT  QLSIYDGEAC  WVLNVTVTLL  SFDGGLRAAS  LHAVLAALHQ
201 LRLPRTRLPN  GDVIESRRVR  LSCLPTACTF  GFLAGAQVRL  LADTTAIEEY
251 VADGLLTIAV  SESGEVVGVH  QVGRCPLLAQ  ALTAAVQQWT  EQSASVRKAL
301 YG
```

EAP4

```
  1 MTRLDGRQST  EAVRAIHVAT  NVLANCHSSA  CVEIGQTRVL  CGVRPPQQLV
 51 QEYRGTRGRI  SCQLHRSSAS  SAAATVADNS  ADRDMALALE  GVAEQAVVLE
101 RIPQLLVEVL  IEVLHDDGAV  WDAAATALSA  ALTAGGVEVY  DTFTACSAAV
151 RPDGAIVVDL  TQEEEAAATA  RVVVCGGVSL  GGVYYMCHLG  ACEAATMAQL
201 VQAATKGMQV  RKALLLEQIR  NQ
```

7.10 **Appendix 8**. The full sequence of the constructed pNUS-PTPcH plasmid

AAGCTTACCGACAAGACCAGAATAGCGCTTATGTGTGTGTGTTTGTGTGTGGGTGTGTGTGCCCATGTGTGACAAAGAG
GCCAGTGCTTTCTCTAAAGCAAGAGCGCGAGGTTGCTGGCTAAGGACTCTAAGTCCCTCACAGTGATGGCGTGTTGCAT
TTTCTAAACCGTCAATCCAACACGTCGGTAGCATATCGGTTTTGTAGGCTCTTCTGGATACCTTCCCCAGTAAGACCGC
CACTGCTTCGTGACTGAAGCACTGTAAATATCACTGAAACCGTCGCGTTGCTTTGTCTAATTATCACCGCCTTTGCCAG
CTATCGCCTCAGGCTGCGCTCTTTGACTAATCCACTCACCACTTCTCTGCCTTCTTCCTCCGGTTGTTGTTGTGTCCTG
CGTGTACATGGCGCGTGTCCTTTTCGAGCAAACAGCTGTCTTTTCTTTCACGATAACACACTCATATTAAACGCGAGTA
TTACTCATCAGTCAACGTCACATTCCGCTCTGTCCACTTCGACCTTACACCTCTACTTGTCCAACTATCTTCCACTTGT
CAAGCGAATTCCATATGCTCGAGGATATCGGCGGCCGCGAAGATCAGGTCGATCCTCGTCTTATTGATGGGAAATATGA
TATTCCAACTACTGCTAGCGAGAATTTGTATTTTCAGGGTGAGCTCAAAACCGCGGCTCTTGCGCAACACGATGAAGCC
GTGGACAACAAATTCAACAAAGAACAACAAAACGCGTTCTATGAGATCTTACATTTACCTAACTTAAACGAAGAACAAC
GAAACGCCTTCATCCAAAGTTTAAAAGATGACCCAAGCCAAAGCGCTAACCTTTTAGCAGAAGCTAAAAAGCTAAATGA
TGCTCAGGCGCCGAAAGTAGACAACAAATTCAACAAAGAACAACAAAACGCGTTCTATGAGATCTTACATTTACCTAAC
TTAAACGAAGAACAACGAAACGCCTTCATCCAAAGTTTAAAAGATGACCCAAGCCAAAGCGCTAACCTTTTAGCAGAAG
CTAAAAAGCTAAATGATGCTCAGGCGCCGAAAGTAGACGCGAACTCCGCGGGGAAGTCAACCTGATAATAGGAATTCTG
TATTACGCCGTTTTAAGAGCTCCTTCGACGCCTTTTTGTCCTTCAGCTGCTCCACGGTGACTCGCTTCTCTCTCTTTCC
ACAGTGTCTCTTTTTTCTTTTCACTCTCTATACAAATGTGAGCGACCTCCTTTTCTGTACAACGGCCTTCCGGCGTGTG
CTTTTCTCATCGACCTCTCCTCGCTTCTTGGGCACTCCTTCATCGAGCAAACAAGACGAGGGAGGTGACGCGATTGGTG
AGACCACTACGAGTATGGACGGAGCTGTCTGATACCCCCTGTTTTTTATCTTGTACCCCGCTCTGCAGTGACGGTAGCC
CGCTGCTGTGCTTCGGTATCGCCGCTTCATACGCTTCTCTCTTTTTTCAACGTGCGGCGCTGATTCAAAGGTTACCTCA
ACGCGACCCGCCGCTGCATCCTTTGTTGCTCCTCTTGTCGCAAACAAACAAAAAACGTGCTGTGCTTTTTCCTTTATCG
TGTCTTTTTGCAAAGTCTAGAGTTTACCGACAAGACCAGAATAGCGCTTATGTGTGTGTGTTTGTGTGTGGGTGTGTGT
GCCCATGTGTGACAAAGAGGCCAGTGCTTTCTCTAAAGCAAGAGCGCGAGGTTGCTGGCTAAGGACTCTAAGTCCCTCA
CAGTGATGGCGTGTTGCATTTTCTAAACCGTCAATCCAACACGTCGGTAGCATATCGGTTTTGTAGGCTCTTCTGGATA
CCTTCCCCAGTAAGACCGCCACTGCTTCGTGACTGAAGCACTGTAAATATCACTGAAACCGTCGCGTTGCTTTGTCTAA
TTATCACCGCCTTTGCCAGCTATCGCCTCAGGCTGCGCTCTTTGACTAATCCACTCACCACTTCTCTGCCTTCTTCCTC
CGGTTGTTGTTGTGTCCTGCGTGTACATGGCGCGTGTCCTTTTCGAGCAAACAGCTGTCTTTTCTTTCACGATAACACA
CTCATATTAAACGCGAGTATTACTCATCAGTCAACGTCACATTCCGCTCTGTCCACTTCGACCTTACACCTCTACTTGT
CCAACTATCTTCCACTTGTCAAGCGTCGACATGAAAAAGCCTGAACTCACCGCGACGTCTGTCGAGAAGTTTCTGATCG
GAAAGTTCGACAGCGTCTCCGACCTGATGCAGCTCTCGGAGGGCGAAGAATCTCGTGCTTTCAGCTTCGATGTAGGAGG
GCGTGGATATGTCCTGCGGGTAAATAGCTGCGCCGATGGTTTCTACAAAGATCGTTATGTTTATCGGCACTTTGCATCG
GCCGCGCTCCCGATTCCGGAAGTGCTTGACATTGGGGAGTTCAGCGAGAGCCTGACCTATTGCATCTCCCGCCGTGCAC
AGGGTGTCACGTTGCAAGACCTGCCTGAAACCGAACTGCCCGCTGTTCTTCAGCCGGTCGCGGAGGCCATGGATGCGAT
CGCTGCGGCCGATCTTAGCCAGACGAGCGGGTTCGGCCCATTCGGACCGCAAGGAATCGGTCAATACACTACATGGCGT
GATTTCATTTGCGCGATTGCTGATCCCCATGTGTATCACTGGCAAACTGTGATGGACGACACCGTCAGTGCGTCCGTCG
CGCAGGCTCTCGATGAGCTGATGCTTTGGGCCGAGGACTGCCCCGAAGTCCGGCACCTCGTGCACGCGGATTTCGGCTC
CAACAATGTCCTGACGGACAATGGCCGCATAACAGCGGTCATTGACTGGAGCGAGGCGATGTTCGGGGATTCCCAATAC
GAGGTCGCCAACATCTTCTTCTGGAGGCCGTGGTTGGCTTGTATGGAGCAGCAGACGCGCTACTTCGAGCGGAGGCATC
CGGAGCTTGCAGGATCGCCGCGGCTCCGGGCGTATATGCTCCGCATTGGTCTTGACCAACTCTATCAGAGCTTGGTTGA
CGGCAATTTCGATGATGCAGCTTGGGCGCAGGGTCGATGCGACGCAATCGTCCGATCCGGAGCCGGGACTGTCGGGCGT
ACACAAATCGCCCGCAGAAGCGCGGCCGTCTGGACCGATGGCTGTGTAGAAGTACTCGCCGATAGTGGAAACCGACGCC
TCAGCACTCGTCCGAGGGCAAAGGAATAGGGATCCAGCAGGCGGAGAAAGAGGGAAGTATAAGGCGGACGCATAGGTCG
GAGTATCGAGAAAAAGAGGCAGAGATGGGTGGTGGCGGAGCGCCCCTCTCTGCCCTTCTCTGTTTTACTGTTCCCGCCA
CGTCGCCAACTCCTCTTTTTGTTTGCTCTAATGTCGGTGCTATCCTCTTCCTCTTTTTACTCTCCGTTTTTCTTCCTTC
CGTTTTGTCTTGTTATCACCGTTATTTTTCTTCTTCTTTCTTAGCCGATTTGGGTCTCCTGCCTACGGCAGCGGTGATG
AGTCGCACTTCCGTCCCCCTTTCCTCTCCGTAAGTACTCCCTCGATGCCTCAGGCGCTTCTATTTTGCGGCACTGTGCT
GACCACCTCCCACGTGTGCAGTGAGAGCGCCAGAGACATTCAGGAGAAGAGGGAAGAGGGGAAGTAAATACCAAAGCGA
GGAAGATGTCTTTCTCGCTGCTTCTCATCCTGTTGACCGGTGTGCACGGCGGTGTGTCCTCTCGGCTTCCCTCCTCCTT
CCCTCGCTCCCCTTTTTCTGTGTTTTTTCTTTCTAACATGATTGCGCCTGCTCTTTTTGCCCCGCAGCGTCGCAGTGGG
TGTCACCTGCGACCGCCGTACGTTTTACTATATACATATTTGTTTCTGTGCTGATGCCATTTGTCCGCTACTCCATATC
GTGCGTGTTTGTTTTCCAGTGGTGACGCCTTCCGCATCATTTTAATCAATTCGAGGCGAAAAGGGTGATTTGAGTGTTG
GAGTGGGCTTTTTTATTTATTTGACTCCAAACATCTTTTCTTTTCCCGGTATCTTCGGGTCCGTCACGCAGGTCGGTGG
GTGTGTCCGAGTGCGCTTCTTTACTCACGTGCCGCTGCGCACATACACAGATTTTAAAAGCACGCATACACGATCTGTG
CCTTCAAAACTAATCAACAAAAACAAAAATACAAAAAAGACAAGAATAAGAGGTCAGCAACGCACCCACGGCTCCTTTC
TTCCTGATCCACGTCGTGGCCGCTGTACGCTCTCAAACACGCTTTGGCGCTGATGCGTGCCTTTATACAAAGAACAAAG

AAGAAGCGAAAAACGGGAGCGTGTTGCTTTGGGGATGTATGCGTGCCACAGTTCTGCGGTACAATTCGTAATCATGGTC
ATAGCTGTTTCCTGTGTGAAATTGTTATCCGCTCACAATTCCACACAACATACGAGCCGGAAGCATAAAGTGTAAAGCC
TGGGGTGCCTAATGAGTGAGCTAACTCACATTAATTGCGTTGCGCTCACTGCCCGCTTTCCAGTCGGGAAACCTGTCGT
GCCAGCTGCATTAATGAATCGGCCAACGCGCGGGGAGAGGCGGTTTGCGTATTGGGCGCTCTTCCGCTTCCTCGCTCAC
TGACTCGCTGCGCTCGGTCGTTCGGCTGCGGCGAGCGGTATCAGCTCACTCAAAGGCGGTAATACGGTTATCCACAGAA
TCAGGGGATAACGCAGGAAAGAACATGTGAGCAAAAGGCCAGCAAAAGGCCAGGAACCGTAAAAAGGCCGCGTTGCTGG
CGTTTTTCCATAGGCTCCGCCCCCCTGACGAGCATCACAAAAATCGACGCTCAAGTCAGAGGTGGCGAAACCCGACAGG
ACTATAAAGATACCAGGCGTTTCCCCCTGGAAGCTCCCTCGTGCGCTCTCCTGTTCCGACCCTGCCGCTTACCGGATAC
CTGTCCGCCTTTCTCCCTTCGGGAAGCGTGGCGCTTTCTCAATGCTCACGCTGTAGGTATCTCAGTTCGGTGTAGGTCG
TTCGCTCCAAGCTGGGCTGTGTGCACGAACCCCCCGTTCAGCCCGACCGCTGCGCCTTATCCGGTAACTATCGTCTTGA
GTCCAACCCGGTAAGACACGACTTATCGCCACTGGCAGCAGCCACTGGTAACAGGATTAGCAGAGCGAGGTATGTAGGC
GGTGCTACAGAGTTCTTGAAGTGGTGGCCTAACTACGGCTACACTAGAAGGACAGTATTTGGTATCTGCGCTCTGCTGA
AGCCAGTTACCTTCGGAAAAAGAGTTGGTAGCTCTTGATCCGGCAAACAAACCACCGCTGGTAGCGGTGGTTTTTTTGT
TTGCAAGCAGCAGATTACGCGCAGAAAAAAAGGATCTCAAGAAGATCCTTTGATCTTTTCTACGGGGTCTGACGCTCAG
TGGAACGAAAACTCACGTTAAGGGATTTTGGTCATGAGATTATCAAAAAGGATCTTCACCTAGATCCTTTTAAATTAAA
AATGAAGTTTTAAATCAATCTAAAGTATATATGAGTAAACTTGGTCTGACAGTTACCAATGCTTAATCAGTGAGGCACC
TATCTCAGCGATCTGTCTATTTCGTTCATCCATAGTTGCCTGACTCCCCGTCGTGTAGATAACTACGATACGGGAGGGC
TTACCATCTGGCCCCAGTGCTGCAATGATACCGCGAGACCCACGCTCACCGGCTCCAGATTTATCAGCAATAAACCAGC
CAGCCGGAAGGGCCGAGCGCAGAAGTGGTCCTGCAACTTTATCCGCCTCCATCCAGTCTATTAATTGTTGCCGGGAAGC
TAGAGTAAGTAGTTCGCCAGTTAATAGTTTGCGCAACGTTGTTGCCATTGCTACAGGCATCGTGGTGTCACGCTCGTCG
TTTGGTATGGCTTCATTCAGCTCCGGTTCCCAACGATCAAGGCGAGTTACATGATCCCCCATGTTGTGCAAAAAAGCGG
TTAGCTCCTTCGGTCCTCCGATCGTTGTCAGAAGTAAGTTGGCCGCAGTGTTATCACTCATGGTTATGGCAGCACTGCA
TAATTCTCTTACTGTCATGCCATCCGTAAGATGCTTTTCTGTGACTGGTGAGTACTCAACCAAGTCATTCTGAGAATAG
TGTATGCGGCGACCGAGTTGCTCTTGCCCGGCGTCAATACGGGATAATACCGCGCCACATAGCAGAACTTTAAAAGTGC
TCATCATTGGAAAACGTTCTTCGGGGCGAAAACTCTCAAGGATCTTACCGCTGTTGAGATCCAGTTCGATGTAACCCAC
TCGTGCACCCAACTGATCTTCAGCATCTTTTACTTTCACCAGCGTTTCTGGGTGAGCAAAAACAGGAAGGCAAAATGCC
GCAAAAAAGGGAATAAGGGCGACACGGAAATGTTGAATACTCATACTCTTCCTTTTTCAATATTATTGAAGCATTTATC
AGGGTTATTGTCTCATGAGCGGATACATATTTGAATGTATTTAGAAAAATAAACAAATAGGGGTTCCGCGCACATTTCC
CCGAAAAGTGCCACCTGACGTCTAAGAAACCATTATTATCATGACATTAACCTATAAAAATAGGCGTATCACGAGGCCC
TTTCGTCTCGCGCGTTTCGGTGATGACGGTGAAAACCTCTGACACATGCAGCTCCCGGAGACGGTCACAGCTTGTCTGT
AAGCGGATGCCGGGAGCAGACAAGCCCGTCAGGGCGCGTCAGCGGGTGTTGGCGGGTGTCGGGGCTGGCTTAACTATGC
GGCATCAGAGCAGATTGTACTGAGAGTGCACGATATGCGGTGTGAAATACCGCACAGATGCGTAAGGAGAAAATACCGC
ATCAGGCGCCATTCGCCATTCAGGCTGCGCAACTGTTGGGAAGGGCGATCGGTGCGGGCCTCTTCGCTATTACGCCAGC
TGGCGAAAGGGGGATGTGCTGCAAGGCGATTAAGTTGGGTAACGCCAGGGTTTTCCCAGTCACGACGTTGTAAAACGAC
GGCCAGTGCC

7.11 **Appendix 9**. Profiles and percentage anticrithidial activities of compounds in the MMV pathogen box

Plate barcode	**Position**	**Compound ID**	**Inhibition (%) at 100µM concentration**
PathogenBox_PlateA	A02	MMV010764	92
PathogenBox_PlateA	A03	MMV688472	67
PathogenBox_PlateA	A04	MMV688416	59
PathogenBox_PlateA	A05	MMV689758	87
PathogenBox_PlateA	A06	MMV688796	79
PathogenBox_PlateA	A07	MMV676526	19
PathogenBox_PlateA	A08	MMV688553	28
PathogenBox_PlateA	A09	MMV676501	73
PathogenBox_PlateA	A10	MMV676449	87
PathogenBox_PlateA	A11	MMV676412	94
PathogenBox_PlateA	B02	MMV1110498	90
PathogenBox_PlateA	B03	MMV000907	95

PathogenBox_PlateA	B04	MMV688889	20
PathogenBox_PlateA	B05	MMV688776	75
PathogenBox_PlateA	B06	MMV688934	68
PathogenBox_PlateA	B07	MMV676389	82
PathogenBox_PlateA	B08	MMV676603	70
PathogenBox_PlateA	B09	MMV676401	86
PathogenBox_PlateA	B10	MMV102872	94
PathogenBox_PlateA	B11	MMV676477	72
PathogenBox_PlateA	C02	MMV084603	91
PathogenBox_PlateA	C03	MMV688548	95
PathogenBox_PlateA	C04	MMV688888	90
PathogenBox_PlateA	C05	MMV690028	73
PathogenBox_PlateA	C06	MMV688943	95
PathogenBox_PlateA	C07	MMV053220	73
PathogenBox_PlateA	C08	MMV676584	88
PathogenBox_PlateA	C09	MMV676439	84
PathogenBox_PlateA	C10	MMV676395	70
PathogenBox_PlateA	C11	MMV676379	82
PathogenBox_PlateA	D02	MMV687762	88
PathogenBox_PlateA	D03	MMV1028806	94
PathogenBox_PlateA	D04	MMV661713	17
PathogenBox_PlateA	D05	MMV688793	90
PathogenBox_PlateA	D06	MMV688942	95
PathogenBox_PlateA	D07	MMV688554	72
PathogenBox_PlateA	D08	MMV676555	85
PathogenBox_PlateA	D09	MMV676383	86
PathogenBox_PlateA	D10	MMV676444	77
PathogenBox_PlateA	D11	MMV676409	95
PathogenBox_PlateA	E02	MMV688514	87
PathogenBox_PlateA	E03	MMV676350	72
PathogenBox_PlateA	E04	MMV553002	94
PathogenBox_PlateA	E05	MMV688797	88
PathogenBox_PlateA	E06	MMV688756	70
PathogenBox_PlateA	E07	MMV090930	88
PathogenBox_PlateA	E08	MMV676431	42
PathogenBox_PlateA	E09	MMV676571	76
PathogenBox_PlateA	E10	MMV676445	94
PathogenBox_PlateA	E11	MMV676589	80
PathogenBox_PlateA	F02	MMV026020	91
PathogenBox_PlateA	F03	MMV688471	88
PathogenBox_PlateA	F04	MMV676388	95
PathogenBox_PlateA	F05	MMV202553	76
PathogenBox_PlateA	F06	MMV688936	92
PathogenBox_PlateA	F07	MMV676476	64

PathogenBox_PlateA	F08	MMV676377	95
PathogenBox_PlateA	F09	MMV676406	75
PathogenBox_PlateA	F10	MMV676461	84
PathogenBox_PlateA	F11	MMV676509	76
PathogenBox_PlateA	G02	MMV688470	93
PathogenBox_PlateA	G03	MMV688704	90
PathogenBox_PlateA	G04	MMV188296	60
PathogenBox_PlateA	G05	MMV688958	89
PathogenBox_PlateA	G06	MMV063404	87
PathogenBox_PlateA	G07	MMV676558	73
PathogenBox_PlateA	G08	MMV688555	64
PathogenBox_PlateA	G09	MMV676597	95
PathogenBox_PlateA	G10	MMV676588	96
PathogenBox_PlateA	G11	MMV676554	70
PathogenBox_PlateA	H02	MMV688350	94
PathogenBox_PlateA	H03	MMV688360	95
PathogenBox_PlateA	H04	MMV099637	95
PathogenBox_PlateA	H05	MMV688798	93
PathogenBox_PlateA	H06	MMV676539	95
PathogenBox_PlateA	H07	MMV202458	95
PathogenBox_PlateA	H08	MMV676474	92
PathogenBox_PlateA	H09	MMV461553	94
PathogenBox_PlateA	H10	MMV676520	95
PathogenBox_PlateA	H11	MMV676512	95
PathogenBox_PlateB	A02	MMV676480	52
PathogenBox_PlateB	A03	MMV652003	64
PathogenBox_PlateB	A04	MMV000062	72
PathogenBox_PlateB	A05	MMV006372	40
PathogenBox_PlateB	A06	MMV688854	71
PathogenBox_PlateB	A07	MMV011903	70
PathogenBox_PlateB	A08	MMV020591	46
PathogenBox_PlateB	A09	MMV020623	71
PathogenBox_PlateB	A10	MMV020512	70
PathogenBox_PlateB	A11	MMV688761	75
PathogenBox_PlateB	B02	MMV012074	66
PathogenBox_PlateB	B03	MMV676604	52
PathogenBox_PlateB	B04	MMV002529	68
PathogenBox_PlateB	B05	MMV687776	80
PathogenBox_PlateB	B06	MMV687800	40
PathogenBox_PlateB	B07	MMV020982	60
PathogenBox_PlateB	B08	MMV020120	56
PathogenBox_PlateB	B09	MMV676605	66
PathogenBox_PlateB	B10	MMV007638	56
PathogenBox_PlateB	B11	MMV021057	74

PathogenBox_PlateB	C02	MMV690027	68
PathogenBox_PlateB	C03	MMV676600	63
PathogenBox_PlateB	C04	MMV676382	62
PathogenBox_PlateB	C05	MMV001625	70
PathogenBox_PlateB	C06	MMV001493	41
PathogenBox_PlateB	C07	MMV020136	17
PathogenBox_PlateB	C08	MMV020710	40
PathogenBox_PlateB	C09	MMV020517	52
PathogenBox_PlateB	C10	MMV019721	63
PathogenBox_PlateB	C11	MMV688763	80
PathogenBox_PlateB	D02	MMV020537	50
PathogenBox_PlateB	D03	MMV637953	69
PathogenBox_PlateB	D04	MMV676536	67
PathogenBox_PlateB	D05	MMV000063	54
PathogenBox_PlateB	D06	MMV689255	56
PathogenBox_PlateB	D07	MMV019838	68
PathogenBox_PlateB	D08	MMV020520	51
PathogenBox_PlateB	D09	MMV019234	23
PathogenBox_PlateB	D10	MMV016136	28
PathogenBox_PlateB	D11	MMV688762	29
PathogenBox_PlateB	E02	MMV676386	64
PathogenBox_PlateB	E03	MMV688773	64
PathogenBox_PlateB	E04	MMV000011	59
PathogenBox_PlateB	E05	MMV687775	76
PathogenBox_PlateB	E06	MMV002817	76
PathogenBox_PlateB	E07	MMV676442	40
PathogenBox_PlateB	E08	MMV020152	50
PathogenBox_PlateB	E09	MMV024397	20
PathogenBox_PlateB	E10	MMV019807	65
PathogenBox_PlateB	E11	MMV560185	25
PathogenBox_PlateB	F02	MMV019189	46
PathogenBox_PlateB	F03	MMV688774	78
PathogenBox_PlateB	F04	MMV003270	14
PathogenBox_PlateB	F05	MMV637229	76
PathogenBox_PlateB	F06	MMV688853	82
PathogenBox_PlateB	F07	MMV020321	62
PathogenBox_PlateB	F08	MMV019087	8
PathogenBox_PlateB	F09	MMV676528	62
PathogenBox_PlateB	F10	MMV020320	34
PathogenBox_PlateB	F11	MMV085210	73
PathogenBox_PlateB	G02	MMV069458	68
PathogenBox_PlateB	G03	MMV688991	51
PathogenBox_PlateB	G04	MMV687801	58
PathogenBox_PlateB	G05	MMV689480	78

PathogenBox_PlateB	G06	MMV003152	78
PathogenBox_PlateB	G07	MMV006239	70
PathogenBox_PlateB	G08	MMV000858	21
PathogenBox_PlateB	G09	MMV006741	20
PathogenBox_PlateB	G10	MMV688768	81
PathogenBox_PlateB	G11	MMV000023	70
PathogenBox_PlateB	H02	MMV676602	78
PathogenBox_PlateB	H03	MMV000014	82
PathogenBox_PlateB	H04	MMV687803	14
PathogenBox_PlateB	H05	MMV668727	75
PathogenBox_PlateB	H06	MMV019742	27
PathogenBox_PlateB	H07	MMV009054	73
PathogenBox_PlateB	H08	MMV006901	8
PathogenBox_PlateB	H09	MMV020391	74
PathogenBox_PlateB	H10	MMV676380	76
PathogenBox_PlateB	H11	MMV688994	84
PathogenBox_PlateC	A02	MMV675997	95
PathogenBox_PlateC	A03	MMV676204	95
PathogenBox_PlateC	A04	MMV687239	23
PathogenBox_PlateC	A05	MMV688122	96
PathogenBox_PlateC	A06	MMV688852	95
PathogenBox_PlateC	A07	MMV687145	95
PathogenBox_PlateC	A08	MMV688327	94
PathogenBox_PlateC	A09	MMV008439	96
PathogenBox_PlateC	A10	MMV595321	96
PathogenBox_PlateC	A11	MMV687747	96
PathogenBox_PlateC	B02	MMV020388	89
PathogenBox_PlateC	B03	MMV688547	96
PathogenBox_PlateC	B04	MMV688466	89
PathogenBox_PlateC	B05	MMV687749	94
PathogenBox_PlateC	B06	MMV688846	85
PathogenBox_PlateC	B07	MMV054312	97
PathogenBox_PlateC	B08	MMV689060	74
PathogenBox_PlateC	B09	MMV689061	23
PathogenBox_PlateC	B10	MMV689028	84
PathogenBox_PlateC	B11	MMV688371	95
PathogenBox_PlateC	C02	MMV688508	13
PathogenBox_PlateC	C03	MMV688283	71
PathogenBox_PlateC	C04	MMV687243	91
PathogenBox_PlateC	C05	MMV687730	96
PathogenBox_PlateC	C06	MMV687251	96
PathogenBox_PlateC	C07	MMV687254	96
PathogenBox_PlateC	C08	MMV688509	47
PathogenBox_PlateC	C09	MMV688361	93

PathogenBox_PlateC	C10	MMV689029	62
PathogenBox_PlateC	C11	MMV022236	95
PathogenBox_PlateC	D02	MMV688410	68
PathogenBox_PlateC	D03	MMV676048	96
PathogenBox_PlateC	D04	MMV687703	96
PathogenBox_PlateC	D05	MMV687248	87
PathogenBox_PlateC	D06	MMV688125	89
PathogenBox_PlateC	D07	MMV687188	95
PathogenBox_PlateC	D08	MMV690103	95
PathogenBox_PlateC	D09	MMV688124	16
PathogenBox_PlateC	D10	MMV688845	68
PathogenBox_PlateC	D11	MMV1030799	96
PathogenBox_PlateC	E02	MMV675994	23
PathogenBox_PlateC	E03	MMV676057	37
PathogenBox_PlateC	E04	MMV687699	95
PathogenBox_PlateC	E05	MMV687146	96
PathogenBox_PlateC	E06	MMV687696	50
PathogenBox_PlateC	E07	MMV687170	92
PathogenBox_PlateC	E08	MMV690102	96
PathogenBox_PlateC	E09	MMV689709	96
PathogenBox_PlateC	E10	MMV021375	91
PathogenBox_PlateC	E11	MMV1029203	90
PathogenBox_PlateC	F02	MMV676053	60
PathogenBox_PlateC	F03	MMV688179	96
PathogenBox_PlateC	F04	MMV023969	96
PathogenBox_PlateC	F05	MMV687138	52
PathogenBox_PlateC	F06	MMV688262	96
PathogenBox_PlateC	F07	MMV687189	89
PathogenBox_PlateC	F08	MMV687807	48
PathogenBox_PlateC	F09	MMV676478	87
PathogenBox_PlateC	F10	MMV062221	96
PathogenBox_PlateC	F11	MMV688921	72
PathogenBox_PlateC	G02	MMV676191	45
PathogenBox_PlateC	G03	MMV675993	91
PathogenBox_PlateC	G04	MMV021660	89
PathogenBox_PlateC	G05	MMV688417	91
PathogenBox_PlateC	G06	MMV687273	96
PathogenBox_PlateC	G07	MMV687180	76
PathogenBox_PlateC	G08	MMV1088520	95
PathogenBox_PlateC	G09	MMV688891	28
PathogenBox_PlateC	G10	MMV023370	46
PathogenBox_PlateC	G11	MMV688703	94
PathogenBox_PlateC	H02	MMV675969	80
PathogenBox_PlateC	H03	MMV688313	92

PathogenBox_PlateC	H04	MMV687172	92
PathogenBox_PlateC	H05	MMV688844	85
PathogenBox_PlateC	H06	MMV1198433	40
PathogenBox_PlateC	H07	MMV024311	93
PathogenBox_PlateC	H08	MMV1019989	52
PathogenBox_PlateC	H09	MMV1037162	83
PathogenBox_PlateC	H10	MMV689437	93
PathogenBox_PlateC	H11	MMV688955	67
PathogenBox_PlateD	A02	MMV026468	28
PathogenBox_PlateD	A03	MMV020670	90
PathogenBox_PlateD	A04	MMV023953	67
PathogenBox_PlateD	A05	MMV010576	69
PathogenBox_PlateD	A06	MMV032967	76
PathogenBox_PlateD	A07	MMV031011	79
PathogenBox_PlateD	A08	MMV688178	70
PathogenBox_PlateD	A09	MMV688362	93
PathogenBox_PlateD	A10	MMV687706	68
PathogenBox_PlateD	A11	MMV026356	93
PathogenBox_PlateD	B02	MMV011511	92
PathogenBox_PlateD	B03	MMV007625	64
PathogenBox_PlateD	B04	MMV007471	87
PathogenBox_PlateD	B05	MMV024829	88
PathogenBox_PlateD	B06	MMV045105	73
PathogenBox_PlateD	B07	MMV022029	66
PathogenBox_PlateD	B08	MMV676064	87
PathogenBox_PlateD	B09	MMV688180	92
PathogenBox_PlateD	B10	MMV024035	92
PathogenBox_PlateD	B11	MMV688941	82
PathogenBox_PlateD	C02	MMV020291	64
PathogenBox_PlateD	C03	MMV006833	84
PathogenBox_PlateD	C04	MMV026490	80
PathogenBox_PlateD	C05	MMV687246	67
PathogenBox_PlateD	C06	MMV676162	73
PathogenBox_PlateD	C07	MMV024114	67
PathogenBox_PlateD	C08	MMV688467	46
PathogenBox_PlateD	C09	MMV675998	93
PathogenBox_PlateD	C10	MMV659010	86
PathogenBox_PlateD	C11	MMV676008	64
PathogenBox_PlateD	D02	MMV676269	60
PathogenBox_PlateD	D03	MMV020081	71
PathogenBox_PlateD	D04	MMV026550	62
PathogenBox_PlateD	D05	MMV675995	82
PathogenBox_PlateD	D06	MMV688274	71
PathogenBox_PlateD	D07	MMV023860	75

PathogenBox_PlateD	D08	MMV688407	93
PathogenBox_PlateD	D09	MMV023949	76
PathogenBox_PlateD	D10	MMV676050	78
PathogenBox_PlateD	D11	MMV024406	46
PathogenBox_PlateD	E02	MMV023233	87
PathogenBox_PlateD	E03	MMV085230	86
PathogenBox_PlateD	E04	MMV085071	93
PathogenBox_PlateD	E05	MMV659004	92
PathogenBox_PlateD	E06	MMV676260	85
PathogenBox_PlateD	E07	MMV688364	71
PathogenBox_PlateD	E08	MMV032995	81
PathogenBox_PlateD	E09	MMV688279	66
PathogenBox_PlateD	E10	MMV688271	93
PathogenBox_PlateD	E11	MMV019790	53
PathogenBox_PlateD	F02	MMV009135	90
PathogenBox_PlateD	F03	MMV011765	91
PathogenBox_PlateD	F04	MMV024937	84
PathogenBox_PlateD	F05	MMV085499	75
PathogenBox_PlateD	F06	MMV023985	88
PathogenBox_PlateD	F07	MMV024195	91
PathogenBox_PlateD	F08	MMV676063	31
PathogenBox_PlateD	F09	MMV676186	77
PathogenBox_PlateD	F10	MMV688474	93
PathogenBox_PlateD	F11	MMV687812	42
PathogenBox_PlateD	G02	MMV007803	89
PathogenBox_PlateD	G03	MMV001059	65
PathogenBox_PlateD	G04	MMV011691	49
PathogenBox_PlateD	G05	MMV676877	78
PathogenBox_PlateD	G06	MMV663250	92
PathogenBox_PlateD	G07	MMV407539	79
PathogenBox_PlateD	G08	MMV688372	84
PathogenBox_PlateD	G09	MMV658993	71
PathogenBox_PlateD	G10	MMV676182	92
PathogenBox_PlateD	G11	MMV676411	93
PathogenBox_PlateD	H02	MMV007133	90
PathogenBox_PlateD	H03	MMV022478	92
PathogenBox_PlateD	H04	MMV024101	92
PathogenBox_PlateD	H05	MMV676881	87
PathogenBox_PlateD	H06	MMV024443	93
PathogenBox_PlateD	H07	MMV688469	84
PathogenBox_PlateD	H08	MMV023388	92
PathogenBox_PlateD	H09	MMV675968	94
PathogenBox_PlateD	H10	MMV675996	84
PathogenBox_PlateD	H11	MMV688980	17

PathogenBox_PlateE	A02	MMV011229	93
PathogenBox_PlateE	A03	MMV676468	97
PathogenBox_PlateE	A04	MMV688771	15
PathogenBox_PlateE	A05	MMV687798	77
PathogenBox_PlateE	A06	MMV688775	75
PathogenBox_PlateE	A07	MMV676159	97
PathogenBox_PlateE	A08	MMV393144	11
PathogenBox_PlateE	A09	MMV007920	83
PathogenBox_PlateE	A10	MMV688270	72
PathogenBox_PlateE	A11	MMV019993	84
PathogenBox_PlateE	B02	MMV687794	95
PathogenBox_PlateE	B03	MMV676470	86
PathogenBox_PlateE	B04	MMV688938	97
PathogenBox_PlateE	B05	MMV689000	97
PathogenBox_PlateE	B06	MMV004168	97
PathogenBox_PlateE	B07	MMV676161	78
PathogenBox_PlateE	B08	MMV023183	93
PathogenBox_PlateE	B09	MMV047015	96
PathogenBox_PlateE	B10	MMV688795	96
PathogenBox_PlateE	B11	MMV688352	58
PathogenBox_PlateE	C02	MMV676398	89
PathogenBox_PlateE	C03	MMV676472	89
PathogenBox_PlateE	C04	MMV671636	80
PathogenBox_PlateE	C05	MMV676599	82
PathogenBox_PlateE	C06	MMV689244	97
PathogenBox_PlateE	C07	MMV688411	95
PathogenBox_PlateE	C08	MMV687765	89
PathogenBox_PlateE	C09	MMV020165	57
PathogenBox_PlateE	C10	MMV676524	85
PathogenBox_PlateE	C11	MMV611037	94
PathogenBox_PlateE	D02	MMV688766	9
PathogenBox_PlateE	D03	MMV200748	93
PathogenBox_PlateE	D04	MMV667494	77
PathogenBox_PlateE	D05	MMV028694	91
PathogenBox_PlateE	D06	MMV001499	97
PathogenBox_PlateE	D07	MMV688345	97
PathogenBox_PlateE	D08	MMV010545	89
PathogenBox_PlateE	D09	MMV023227	95
PathogenBox_PlateE	D10	MMV687700	71
PathogenBox_PlateE	D11	MMV676384	94
PathogenBox_PlateE	E02	MMV020289	94
PathogenBox_PlateE	E03	MMV002816	78
PathogenBox_PlateE	E04	MMV634140	85
PathogenBox_PlateE	E05	MMV030734	71

PathogenBox_PlateE	E06	MMV689243	97
PathogenBox_PlateE	E07	MMV676358	84
PathogenBox_PlateE	E08	MMV687729	64
PathogenBox_PlateE	E09	MMV407834	64
PathogenBox_PlateE	E10	MMV687813	49
PathogenBox_PlateE	E11	MMV153413	97
PathogenBox_PlateE	F02	MMV019551	96
PathogenBox_PlateE	F03	MMV688552	92
PathogenBox_PlateE	F04	MMV016838	80
PathogenBox_PlateE	F05	MMV676270	86
PathogenBox_PlateE	F06	MMV688755	97
PathogenBox_PlateE	F07	MMV228911	59
PathogenBox_PlateE	F08	MMV272144	97
PathogenBox_PlateE	F09	MMV026313	97
PathogenBox_PlateE	F10	MMV161996	57
PathogenBox_PlateE	F11	MMV688543	81
PathogenBox_PlateE	G02	MMV146306	96
PathogenBox_PlateE	G03	MMV688557	94
PathogenBox_PlateE	G04	MMV021013	97
PathogenBox_PlateE	G05	MMV392832	85
PathogenBox_PlateE	G06	MMV688754	93
PathogenBox_PlateE	G07	MMV001561	97
PathogenBox_PlateE	G08	MMV658988	97
PathogenBox_PlateE	G09	MMV084864	92
PathogenBox_PlateE	G10	MMV676492	97
PathogenBox_PlateE	G11	MMV688415	76
PathogenBox_PlateE	H02	MMV688330	34
PathogenBox_PlateE	H03	MMV687796	27
PathogenBox_PlateE	H04	MMV688939	78
PathogenBox_PlateE	H05	MMV688978	97
PathogenBox_PlateE	H06	MMV688990	83
PathogenBox_PlateE	H07	MMV688273	29
PathogenBox_PlateE	H08	MMV393995	94
PathogenBox_PlateE	H09	MMV1236379	94
PathogenBox_PlateE	H10	MMV688550	82
PathogenBox_PlateE	H11	MMV495543	84

7.12 **Appendix 10.** Profiles and percentage anticrithidial activities of compounds in the GSK *T.brucei* box.

Plate barcode	Position	Compound ID	Inhibition (%) at 100µM concentration
G20SL2B	A2	TCMDC-143074	100
G20SL2B	G7	TCMDC-143100	46
G20SL2B	B8	TCMDC-143121	53
G20SL2B	H9	TCMDC-143123	44
G20SL2B	A10	TCMDC-143128	53
G20SL2B	A7	TCMDC-143131	52
G20SL2B	E5	TCMDC-143132	57
G20SL2B	C11	TCMDC-143138	91
G20SL2B	D11	TCMDC-143154	49
G20SL2B	A9	TCMDC-143167	31
G20SL2B	E3	TCMDC-143172	84
G20SL2B	A3	TCMDC-143176	74
G20SL2B	H2	TCMDC-143199	63
G20SL2B	H7	TCMDC-143205	55
G20SL2B	B11	TCMDC-143206	21
G20SL2B	C7	TCMDC-143225	50
G20SL2B	E6	TCMDC-143230	40
G20SL2B	G9	TCMDC-143233	97
G20SL2B	E9	TCMDC-143240	65
G20SL2B	B6	TCMDC-143242	82
G20SL2B	F10	TCMDC-143251	71
G20SL2B	A11	TCMDC-143257	48
G20SL2B	F7	TCMDC-143263	100
G20SL2B	C9	TCMDC-143264	45
G20SL2B	G2	TCMDC-143265	73
G20SL2B	E8	TCMDC-143267	78
G20SL2B	C4	TCMDC-143270	78
G20SL2B	H3	TCMDC-143289	59
G20SL2B	H8	TCMDC-143290	32
G20SL2B	E2	TCMDC-143292	100
G20SL2B	E10	TCMDC-143307	72
G20SL2B	G8	TCMDC-143320	63
G20SL2B	B7	TCMDC-143323	89
G20SL2B	B4	TCMDC-143335	74
G20SL2B	B9	TCMDC-143337	59
G20SL2B	F11	TCMDC-143342	67
G20SL2B	G3	TCMDC-143343	52
G20SL2B	A8	TCMDC-143356	88
G20SL2B	D7	TCMDC-143359	73

G20SL2B	D8	TCMDC-143361	68
G20SL2B	D10	TCMDC-143365	50
G20SL2B	D3	TCMDC-143378	74
G20SL2B	G5	TCMDC-143399	58
G20SL2B	H6	TCMDC-143424	67
G20SL2B	D5	TCMDC-143428	100
G20SL2B	F9	TCMDC-143444	80
G20SL2B	D2	TCMDC-143449	94
G20SL2B	C10	TCMDC-143453	59
G20SL2B	C8	TCMDC-143454	66
G20SL2B	G6	TCMDC-143457	94
G20SL2B	B5	TCMDC-143460	100
G20SL2B	F3	TCMDC-143462	90
G20SL2B	H10	TCMDC-143475	56
G20SL2B	G4	TCMDC-143493	60
G20SL2B	H5	TCMDC-143505	50
G20SL2B	F2	TCMDC-143510	76
G20SL2B	H11	TCMDC-143513	40
G20SL2B	C2	TCMDC-143515	99
G20SL2B	F6	TCMDC-143516	61
G20SL2B	A5	TCMDC-143533	97
G20SL2B	D9	TCMDC-143551	51
G20SL2B	D4	TCMDC-143556	62
G20SL2B	F5	TCMDC-143565	76
G20SL2B	A6	TCMDC-143572	76
G20SL2B	C6	TCMDC-143575	54
G20SL2B	E4	TCMDC-143578	72
G20SL2B	D6	TCMDC-143579	65
G20SL2B	C5	TCMDC-143581	36
G20SL2B	B10	TCMDC-143585	69
G20SL2B	G11	TCMDC-143587	77
G20SL2B	E11	TCMDC-143597	88
G20SL2B	A4	TCMDC-143609	98
G20SL2B	H4	TCMDC-143624	67
G20SL2B	G10	TCMDC-143638	77
G20SL2B	F4	TCMDC-143645	59
G20SL2B	B3	TCMDC-143080	95
G20SL2B	C3	TCMDC-143194	81
G20SL2B	B2	TCMDC-143273	68
G20SL2B	F8	TCMDC-143497	51
G20SL2B	E7	TCMDC-143569	84
G20SL2C	H10	TCMDC-142497	94
G20SL2C	A2	TCMDC-143073	99
G20SL2C	A9	TCMDC-143089	27

G20SL2C	A11	TCMDC-143102	87
G20SL2C	E4	TCMDC-143104	89
G20SL2C	D8	TCMDC-143107	55
G20SL2C	G10	TCMDC-143111	89
G20SL2C	G2	TCMDC-143116	70
G20SL2C	G9	TCMDC-143125	100
G20SL2C	B10	TCMDC-143134	43
G20SL2C	D3	TCMDC-143146	68
G20SL2C	D2	TCMDC-143158	80
G20SL2C	E7	TCMDC-143173	69
G20SL2C	B6	TCMDC-143189	45
G20SL2C	C8	TCMDC-143195	10
G20SL2C	F8	TCMDC-143204	78
G20SL2C	F9	TCMDC-143210	80
G20SL2C	C10	TCMDC-143219	100
G20SL2C	B5	TCMDC-143220	91
G20SL2C	A7	TCMDC-143227	10
G20SL2C	A3	TCMDC-143228	16
G20SL2C	C6	TCMDC-143229	15
G20SL2C	C9	TCMDC-143231	58
G20SL2C	B9	TCMDC-143243	100
G20SL2C	A10	TCMDC-143250	85
G20SL2C	G4	TCMDC-143283	30
G20SL2C	E10	TCMDC-143294	49
G20SL2C	G7	TCMDC-143303	15
G20SL2C	F3	TCMDC-143326	67
G20SL2C	H2	TCMDC-143339	87
G20SL2C	D11	TCMDC-143341	46
G20SL2C	H3	TCMDC-143352	77
G20SL2C	C3	TCMDC-143357	56
G20SL2C	C5	TCMDC-143360	100
G20SL2C	D4	TCMDC-143363	100
G20SL2C	H11	TCMDC-143366	76
G20SL2C	H5	TCMDC-143368	23
G20SL2C	G5	TCMDC-143369	74
G20SL2C	A8	TCMDC-143370	90
G20SL2C	G8	TCMDC-143373	19
G20SL2C	C11	TCMDC-143374	88
G20SL2C	G11	TCMDC-143380	83
G20SL2C	E11	TCMDC-143386	80
G20SL2C	H6	TCMDC-143390	44
G20SL2C	D6	TCMDC-143393	65
G20SL2C	E2	TCMDC-143394	84
G20SL2C	D7	TCMDC-143400	28

G20SL2C	B11	TCMDC-143401	90
G20SL2C	H4	TCMDC-143402	90
G20SL2C	F11	TCMDC-143412	12
G20SL2C	H7	TCMDC-143425	86
G20SL2C	F6	TCMDC-143435	87
G20SL2C	A6	TCMDC-143436	50
G20SL2C	E5	TCMDC-143438	50
G20SL2C	F4	TCMDC-143445	68
G20SL2C	E9	TCMDC-143446	79
G20SL2C	D10	TCMDC-143452	25
G20SL2C	G6	TCMDC-143456	62
G20SL2C	C4	TCMDC-143458	66
G20SL2C	B7	TCMDC-143496	61
G20SL2C	D9	TCMDC-143499	56
G20SL2C	E3	TCMDC-143525	72
G20SL2C	E6	TCMDC-143540	58
G20SL2C	E8	TCMDC-143543	88
G20SL2C	B4	TCMDC-143547	81
G20SL2C	A4	TCMDC-143580	12
G20SL2C	F2	TCMDC-143582	88
G20SL2C	C7	TCMDC-143589	63
G20SL2C	D5	TCMDC-143595	80
G20SL2C	G3	TCMDC-143596	82
G20SL2C	B8	TCMDC-143619	83
G20SL2C	H8	TCMDC-143634	12
G20SL2C	C2	TCMDC-143640	58
G20SL2C	F5	TCMDC-143641	93
G20SL2C	B2	TCMDC-143642	76
G20SL2C	B3	TCMDC-143643	80
G20SL2C	F7	TCMDC-143644	72
G20SL2C	F10	TCMDC-143648	57
G20SL2C	A5	TCMDC-143130	65
G20SL2C	H9	TCMDC-143526	94
G211HCO	D2	TCMDC-143226	14
G211HCO	C2	TCMDC-143316	99
G211HCO	F2	TCMDC-143330	20
G211HCO	G2	TCMDC-143377	73
G211HCO	A3	TCMDC-143382	70
G211HCO	H2	TCMDC-143392	92
G211HCO	B2	TCMDC-143468	82
G211HCO	E2	TCMDC-143646	91
G211HCO	A2	TCMDC-143163	29
G211IMU	E2	TCMDC-142716	81
G211IMU	G2	TCMDC-143079	93

G211IMU	A2	TCMDC-143112	100
G211IMU	C2	TCMDC-143192	61
G211IMU	H2	TCMDC-143254	60
G211IMU	A3	TCMDC-143299	92
G211IMU	B2	TCMDC-143318	50
G211IMU	D2	TCMDC-143364	46
G211IMU	C3	TCMDC-143466	54
G211IMU	F2	TCMDC-143469	92
G211IMU	D3	TCMDC-143471	90
G211IMU	B3	TCMDC-143636	58
G211IRO	B2	TCMDC-143312	35
G211IRO	C2	TCMDC-143470	72
G211IRO	E2	TCMDC-143544	51
G211IRO	A2	TCMDC-143583	36
G211IRO	D2	TCMDC-143635	48
G214GU7	B2	TCMDC-143312	28
G214GU7	A2	TCMDC-143583	58

7.13 **Appendix 11**. Profiles and percentage anticrithidial activities of compounds in the GSK *T. cruzi* box.

Plate barcode	**Position**	**Compound ID**	**Inhibition (%) at 100μM concentration**
G20SL2D	H9	TCMDC-143081	70
G20SL2D	E11	TCMDC-143083	95
G20SL2D	E2	TCMDC-143088	100
G20SL2D	G5	TCMDC-143097	21
G20SL2D	C8	TCMDC-143108	55
G20SL2D	H4	TCMDC-143114	87
G20SL2D	G10	TCMDC-143135	91
G20SL2D	A5	TCMDC-143142	100
G20SL2D	G2	TCMDC-143143	57
G20SL2D	A6	TCMDC-143148	14
G20SL2D	A4	TCMDC-143149	100
G20SL2D	H3	TCMDC-143150	87
G20SL2D	A10	TCMDC-143152	100
G20SL2D	B4	TCMDC-143155	96
G20SL2D	G11	TCMDC-143156	68
G20SL2D	F2	TCMDC-143157	13
G20SL2D	H5	TCMDC-143161	67
G20SL2D	B2	TCMDC-143162	93
G20SL2D	E3	TCMDC-143178	74

G20SL2D	A7	TCMDC-143187	37
G20SL2D	F3	TCMDC-143190	67
G20SL2D	C10	TCMDC-143200	67
G20SL2D	B10	TCMDC-143203	97
G20SL2D	E10	TCMDC-143207	96
G20SL2D	C3	TCMDC-143222	99
G20SL2D	H10	TCMDC-143224	70
G20SL2D	E6	TCMDC-143235	100
G20SL2D	F10	TCMDC-143241	10
G20SL2D	B5	TCMDC-143244	76
G20SL2D	E4	TCMDC-143247	89
G20SL2D	A11	TCMDC-143248	46
G20SL2D	B6	TCMDC-143253	94
G20SL2D	A9	TCMDC-143256	54
G20SL2D	D3	TCMDC-143258	26
G20SL2D	F9	TCMDC-143262	100
G20SL2D	G7	TCMDC-143272	94
G20SL2D	B9	TCMDC-143276	96
G20SL2D	D10	TCMDC-143279	96
G20SL2D	C11	TCMDC-143284	65
G20SL2D	B7	TCMDC-143300	68
G20SL2D	A2	TCMDC-143309	76
G20SL2D	H8	TCMDC-143313	14
G20SL2D	F7	TCMDC-143319	20
G20SL2D	H11	TCMDC-143324	84
G20SL2D	D9	TCMDC-143328	73
G20SL2D	B8	TCMDC-143329	100
G20SL2D	G4	TCMDC-143332	55
G20SL2D	D6	TCMDC-143346	68
G20SL2D	C2	TCMDC-143362	42
G20SL2D	D2	TCMDC-143384	26
G20SL2D	G6	TCMDC-143387	81
G20SL2D	E8	TCMDC-143405	80
G20SL2D	H7	TCMDC-143408	65
G20SL2D	D7	TCMDC-143409	95
G20SL2D	D8	TCMDC-143411	68
G20SL2D	C4	TCMDC-143415	100
G20SL2D	E7	TCMDC-143421	90
G20SL2D	G3	TCMDC-143434	18
G20SL2D	C5	TCMDC-143439	90
G20SL2D	D11	TCMDC-143461	100
G20SL2D	A3	TCMDC-143504	66
G20SL2D	D4	TCMDC-143507	47
G20SL2D	B11	TCMDC-143527	33

G20SL2D	F8	TCMDC-143529	100
G20SL2D	A8	TCMDC-143535	55
G20SL2D	D5	TCMDC-143537	65
G20SL2D	F6	TCMDC-143541	100
G20SL2D	E9	TCMDC-143552	69
G20SL2D	F11	TCMDC-143555	93
G20SL2D	G9	TCMDC-143561	41
G20SL2D	C9	TCMDC-143598	54
G20SL2D	E5	TCMDC-143602	100
G20SL2D	G8	TCMDC-143605	8
G20SL2D	C7	TCMDC-143608	100
G20SL2D	H6	TCMDC-143611	84
G20SL2D	H2	TCMDC-143616	18
G20SL2D	B3	TCMDC-143617	35
G20SL2D	C6	TCMDC-143620	86
G20SL2D	F4	TCMDC-143632	87
G20SL2D	F5	TCMDC-143637	42
G211GWY	B2	TCMDC-143080	89
G211GWY	C5	TCMDC-143087	100
G211GWY	A7	TCMDC-143109	100
G211GWY	E2	TCMDC-143130	74
G211GWY	G5	TCMDC-143137	70
G211GWY	G3	TCMDC-143160	95
G211GWY	A3	TCMDC-143163	52
G211GWY	B3	TCMDC-143164	69
G211GWY	E6	TCMDC-143186	99
G211GWY	A6	TCMDC-143193	71
G211GWY	C2	TCMDC-143194	81
G211GWY	C3	TCMDC-143197	80
G211GWY	A2	TCMDC-143273	57
G211GWY	A4	TCMDC-143308	100
G211GWY	D3	TCMDC-143315	100
G211GWY	D6	TCMDC-143325	100
G211GWY	F4	TCMDC-143331	97
G211GWY	F6	TCMDC-143371	94
G211GWY	F3	TCMDC-143414	74
G211GWY	C4	TCMDC-143430	100
G211GWY	F2	TCMDC-143446	67
G211GWY	C6	TCMDC-143455	100
G211GWY	D4	TCMDC-143464	100
G211GWY	G4	TCMDC-143477	100
G211GWY	E4	TCMDC-143481	100
G211GWY	A5	TCMDC-143492	100
G211GWY	B6	TCMDC-143494	100

G211GWY	D2	TCMDC-143497	85
G211GWY	H5	TCMDC-143498	100
G211GWY	G6	TCMDC-143506	100
G211GWY	G2	TCMDC-143526	75
G211GWY	E3	TCMDC-143539	100
G211GWY	D5	TCMDC-143542	100
G211GWY	H6	TCMDC-143550	100
G211GWY	E5	TCMDC-143562	100
G211GWY	H2	TCMDC-143569	63
G211GWY	H4	TCMDC-143590	100
G211GWY	B5	TCMDC-143593	100
G211GWY	H3	TCMDC-143599	96
G211GWY	B4	TCMDC-143601	100
G211GWY	F5	TCMDC-143614	100
G211GWZ	B2	TCMDC-123621	100
G211GWZ	G2	TCMDC-125222	100
G211GWZ	F2	TCMDC-139489	22
G211GWZ	E2	TCMDC-140766	33
G211GWZ	A3	TCMDC-143071	53
G211GWZ	F8	TCMDC-143082	68
G211GWZ	C9	TCMDC-143084	61
G211GWZ	A10	TCMDC-143103	22
G211GWZ	E6	TCMDC-143105	56
G211GWZ	E9	TCMDC-143120	71
G211GWZ	A9	TCMDC-143126	96
G211GWZ	C2	TCMDC-143127	100
G211GWZ	B10	TCMDC-143151	100
G211GWZ	G6	TCMDC-143153	44
G211GWZ	G9	TCMDC-143159	100
G211GWZ	C11	TCMDC-143179	18
G211GWZ	C6	TCMDC-143182	71
G211GWZ	H10	TCMDC-143191	62
G211GWZ	C3	TCMDC-143209	22
G211GWZ	H5	TCMDC-143232	67
G211GWZ	H8	TCMDC-143275	70
G211GWZ	G8	TCMDC-143282	57
G211GWZ	A4	TCMDC-143286	100
G211GWZ	F7	TCMDC-143288	39
G211GWZ	B3	TCMDC-143291	32
G211GWZ	D2	TCMDC-143298	13
G211GWZ	A6	TCMDC-143301	69
G211GWZ	H4	TCMDC-143302	56
G211GWZ	A11	TCMDC-143304	100
G211GWZ	E3	TCMDC-143310	100

G211GWZ	B5	TCMDC-143311	33
G211GWZ	A2	TCMDC-143314	10
G211GWZ	D7	TCMDC-143317	45
G211GWZ	F10	TCMDC-143333	59
G211GWZ	B6	TCMDC-143334	60
G211GWZ	D3	TCMDC-143336	48
G211GWZ	B11	TCMDC-143338	17
G211GWZ	G11	TCMDC-143354	71
G211GWZ	C10	TCMDC-143372	76
G211GWZ	H11	TCMDC-143389	82
G211GWZ	E7	TCMDC-143403	44
G211GWZ	D4	TCMDC-143410	79
G211GWZ	G7	TCMDC-143416	100
G211GWZ	H2	TCMDC-143417	35
G211GWZ	F4	TCMDC-143422	100
G211GWZ	D6	TCMDC-143423	67
G211GWZ	F11	TCMDC-143426	85
G211GWZ	F3	TCMDC-143432	100
G211GWZ	D8	TCMDC-143437	88
G211GWZ	E8	TCMDC-143440	100
G211GWZ	A5	TCMDC-143463	69
G211GWZ	H9	TCMDC-143465	50
G211GWZ	H6	TCMDC-143467	95
G211GWZ	C7	TCMDC-143474	74
G211GWZ	E4	TCMDC-143476	79
G211GWZ	G5	TCMDC-143479	73
G211GWZ	F5	TCMDC-143484	45
G211GWZ	E5	TCMDC-143490	79
G211GWZ	A8	TCMDC-143495	100
G211GWZ	C4	TCMDC-143502	100
G211GWZ	B4	TCMDC-143511	100
G211GWZ	G10	TCMDC-143519	56
G211GWZ	A7	TCMDC-143520	95
G211GWZ	G3	TCMDC-143528	44
G211GWZ	D11	TCMDC-143530	67
G211GWZ	F9	TCMDC-143545	51
G211GWZ	C8	TCMDC-143546	61
G211GWZ	H7	TCMDC-143548	48
G211GWZ	E11	TCMDC-143549	93
G211GWZ	F6	TCMDC-143553	89
G211GWZ	E10	TCMDC-143559	76
G211GWZ	B9	TCMDC-143564	38
G211GWZ	C5	TCMDC-143588	52
G211GWZ	D10	TCMDC-143592	88

G211GWZ	D5	TCMDC-143604	91
G211GWZ	D9	TCMDC-143613	58
G211GWZ	B7	TCMDC-143615	14
G211GWZ	H3	TCMDC-143623	81
G211GWZ	B8	TCMDC-143626	25
G211GWZ	G4	TCMDC-143631	73
G211IMQ	D2	TCMDC-143221	71
G211IMQ	C3	TCMDC-143293	89
G211IMQ	G2	TCMDC-143376	75
G211IMQ	B3	TCMDC-143379	90
G211IMQ	C2	TCMDC-143381	60
G211IMQ	B2	TCMDC-143385	60
G211IMQ	E3	TCMDC-143413	66
G211IMQ	E2	TCMDC-143433	57
G211IMQ	F3	TCMDC-143466	60
G211IMQ	H2	TCMDC-143606	98
G211IMQ	F2	TCMDC-143610	95
G211IMQ	D3	TCMDC-143612	100
G211IMQ	A3	TCMDC-143622	100
G211IMQ	A2	TCMDC-143625	100
Q203FAM	C2	TCMDC-143085	47
Q203FAM	A2	TCMDC-143118	44
Q203FAM	B2	TCMDC-143185	86
Q203FAM	D2	TCMDC-143500	77

7.14 **Appendix 12**. Profiles and percentage anticrithidial activities of compounds in the GSK *Leishmania* box

Plate barcode	**Position**	**Compound ID**	**Inhibition (%) at 100µM concentration**
G211IMR	B8	TCMDC-125387	83
G211IMR	C8	TCMDC-142900	100
G211IMR	B7	TCMDC-143075	96
G211IMR	F7	TCMDC-143098	82
G211IMR	E5	TCMDC-143099	82
G211IMR	F6	TCMDC-143101	84
G211IMR	B2	TCMDC-143129	100
G211IMR	E8	TCMDC-143133	75
G211IMR	E4	TCMDC-143139	81

G211IMR	D5	TCMDC-143140	70
G211IMR	C5	TCMDC-143144	84
G211IMR	H6	TCMDC-143170	95
G211IMR	H3	TCMDC-143171	81
G211IMR	C4	TCMDC-143184	91
G211IMR	A7	TCMDC-143188	100
G211IMR	C2	TCMDC-143201	95
G211IMR	D3	TCMDC-143202	100
G211IMR	F8	TCMDC-143218	100
G211IMR	G7	TCMDC-143236	92
G211IMR	A8	TCMDC-143237	98
G211IMR	E2	TCMDC-143245	85
G211IMR	F4	TCMDC-143246	80
G211IMR	G2	TCMDC-143252	98
G211IMR	E3	TCMDC-143266	92
G211IMR	B6	TCMDC-143268	100
G211IMR	H4	TCMDC-143278	100
G211IMR	D7	TCMDC-143287	92
G211IMR	E7	TCMDC-143306	100
G211IMR	B4	TCMDC-143340	84
G211IMR	C7	TCMDC-143345	68
G211IMR	G6	TCMDC-143347	72
G211IMR	A4	TCMDC-143353	74
G211IMR	H7	TCMDC-143375	100
G211IMR	D8	TCMDC-143404	94
G211IMR	E6	TCMDC-143407	82
G211IMR	C3	TCMDC-143418	77
G211IMR	A5	TCMDC-143419	100
G211IMR	F2	TCMDC-143427	90
G211IMR	F3	TCMDC-143431	94
G211IMR	G4	TCMDC-143443	100
G211IMR	A6	TCMDC-143491	78
G211IMR	G5	TCMDC-143508	100
G211IMR	B3	TCMDC-143514	81
G211IMR	F5	TCMDC-143523	73
G211IMR	G3	TCMDC-143536	67
G211IMR	A2	TCMDC-143538	79
G211IMR	H2	TCMDC-143557	87
G211IMR	H5	TCMDC-143558	80
G211IMR	A3	TCMDC-143570	90
G211IMR	D2	TCMDC-143573	97
G211IMR	D4	TCMDC-143574	100
G211IMR	H8	TCMDC-143576	95
G211IMR	B5	TCMDC-143577	75

G211IMR	C6	TCMDC-143591	92
G211IMR	G8	TCMDC-143600	100
G211IMR	B9	TCMDC-125387	69
G211IMS	D4	TCMDC-143163	66
G211IMS	A9	TCMDC-143164	75
G211IMS	C5	TCMDC-143197	77
G211IMS	H11	TCMDC-143315	98
G211IMS	D2	TCMDC-125160	89
G211IMS	G5	TCMDC-125826	100
G211IMS	A5	TCMDC-143086	57
G211IMS	A8	TCMDC-143094	100
G211IMS	G7	TCMDC-143106	96
G211IMS	B9	TCMDC-143110	99
G211IMS	F2	TCMDC-143113	100
G211IMS	E3	TCMDC-143115	98
G211IMS	B5	TCMDC-143119	71
G211IMS	H10	TCMDC-143124	72
G211IMS	B4	TCMDC-143136	100
G211IMS	C6	TCMDC-143141	76
G211IMS	H9	TCMDC-143145	100
G211IMS	A3	TCMDC-143147	96
G211IMS	F8	TCMDC-143165	100
G211IMS	F7	TCMDC-143166	100
G211IMS	E8	TCMDC-143168	76
G211IMS	B8	TCMDC-143169	73
G211IMS	A6	TCMDC-143174	97
G211IMS	G8	TCMDC-143175	93
G211IMS	H5	TCMDC-143181	56
G211IMS	A10	TCMDC-143196	82
G211IMS	D8	TCMDC-143208	91
G211IMS	D7	TCMDC-143214	74
G211IMS	A11	TCMDC-143223	92
G211IMS	D3	TCMDC-143239	100
G211IMS	C4	TCMDC-143249	74
G211IMS	B6	TCMDC-143255	94
G211IMS	D9	TCMDC-143259	78
G211IMS	D6	TCMDC-143261	78
G211IMS	D11	TCMDC-143269	59
G211IMS	F6	TCMDC-143271	100
G211IMS	D5	TCMDC-143274	100
G211IMS	F10	TCMDC-143277	99
G211IMS	H2	TCMDC-143280	93
G211IMS	C7	TCMDC-143281	99
G211IMS	G2	TCMDC-143295	92

G211IMS	C8	TCMDC-143297	100
G211IMS	F5	TCMDC-143305	85
G211IMS	G3	TCMDC-143327	65
G211IMS	C10	TCMDC-143344	75
G211IMS	E11	TCMDC-143351	72
G211IMS	B2	TCMDC-143355	74
G211IMS	H7	TCMDC-143358	95
G211IMS	G4	TCMDC-143367	74
G211IMS	H8	TCMDC-143383	76
G211IMS	C9	TCMDC-143388	71
G211IMS	B10	TCMDC-143391	71
G211IMS	E10	TCMDC-143396	63
G211IMS	H6	TCMDC-143398	97
G211IMS	E2	TCMDC-143406	96
G211IMS	C3	TCMDC-143442	100
G211IMS	E5	TCMDC-143447	100
G211IMS	H4	TCMDC-143451	75
G211IMS	A2	TCMDC-143473	78
G211IMS	F4	TCMDC-143483	74
G211IMS	G6	TCMDC-143501	88
G211IMS	G9	TCMDC-143509	100
G211IMS	B11	TCMDC-143518	96
G211IMS	C11	TCMDC-143522	78
G211IMS	A7	TCMDC-143524	84
G211IMS	F3	TCMDC-143531	63
G211IMS	G10	TCMDC-143534	91
G211IMS	G11	TCMDC-143554	100
G211IMS	H3	TCMDC-143563	66
G211IMS	C2	TCMDC-143566	72
G211IMS	E7	TCMDC-143567	91
G211IMS	E9	TCMDC-143571	100
G211IMS	F9	TCMDC-143584	78
G211IMS	B7	TCMDC-143586	100
G211IMS	A4	TCMDC-143603	100
G211IMS	E4	TCMDC-143607	99
G211IMS	B3	TCMDC-143618	66
G211IMS	D10	TCMDC-143621	94
G211IMS	F11	TCMDC-143628	72
G211IMS	E6	TCMDC-143629	90
G211IMT	G4	TCMDC-124508	60
G211IMT	C3	TCMDC-142704	100
G211IMT	B3	TCMDC-143072	82
G211IMT	C5	TCMDC-143076	70
G211IMT	B5	TCMDC-143077	96

G211IMT	E4	TCMDC-143078	80
G211IMT	C2	TCMDC-143117	65
G211IMT	A5	TCMDC-143211	79
G211IMT	A4	TCMDC-143212	100
G211IMT	C4	TCMDC-143213	82
G211IMT	D4	TCMDC-143215	77
G211IMT	B4	TCMDC-143216	96
G211IMT	D5	TCMDC-143217	89
G211IMT	H4	TCMDC-143285	100
G211IMT	A3	TCMDC-143296	96
G211IMT	H3	TCMDC-143350	66
G211IMT	E2	TCMDC-143397	100
G211IMT	F3	TCMDC-143429	66
G211IMT	G2	TCMDC-143448	94
G211IMT	D3	TCMDC-143478	74
G211IMT	D2	TCMDC-143480	66
G211IMT	H2	TCMDC-143482	70
G211IMT	E5	TCMDC-143488	100
G211IMT	F2	TCMDC-143517	100
G211IMT	F5	TCMDC-143521	90
G211IMT	A2	TCMDC-143532	74
G211IMT	F4	TCMDC-143568	100
G211IMT	B2	TCMDC-143594	81
G211IMT	G3	TCMDC-143633	78
G211IMT	E3	TCMDC-143647	100
Q203FAN	A4	TCMDC-134026	97
Q203FAN	D2	TCMDC-143090	98
Q203FAN	H2	TCMDC-143091	95
Q203FAN	A3	TCMDC-143092	93
Q203FAN	A2	TCMDC-143093	98
Q203FAN	B3	TCMDC-143095	91
Q203FAN	E2	TCMDC-143096	98
Q203FAN	F2	TCMDC-143238	97
Q203FAN	D3	TCMDC-143260	75
Q203FAN	G2	TCMDC-143348	90
Q203FAN	C3	TCMDC-143349	75
Q203FAN	G3	TCMDC-143459	69
Q203FAN	B2	TCMDC-143486	80
Q203FAN	F3	TCMDC-143487	97
Q203FAN	C2	TCMDC-143503	100
Q203FAN	H3	TCMDC-143512	66
Q203FAN	E3	TCMDC-143630	83